

# Petrologic and Geochemical Composition of the AND-2A Core, ANDRILL Southern McMurdo Sound Project, Antarctica

K.S. PANTER<sup>1\*</sup>, F.M. TALARICO<sup>2\*</sup>, K. BASSETT<sup>3</sup>, P. DEL CARLO<sup>4</sup>, B. FIELD<sup>5</sup>, T. FRANK<sup>6</sup>,  
S. HOFFMANN<sup>7</sup>, G. KUHN<sup>8</sup>, L. REICHEL<sup>7</sup>, S. SANDRONI<sup>2</sup>, M. TAVIANI<sup>9</sup>, L. BRACCIALI<sup>10</sup>,  
G. CORNAMUSINI<sup>2,11</sup>, H. VON EYNATTEN<sup>7</sup>, S. ROCCHI<sup>10</sup>  
& THE ANDRILL-SMS SCIENCE TEAM<sup>12</sup>

<sup>1</sup>Dept. of Geology, Bowling Green State University, Bowling Green, OH, 43403 – USA

<sup>2</sup>Dipt. di Scienze della Terra, Università di Siena, Via Laterina 8, 53100 Siena – Italy

<sup>3</sup>Dept. of Geological Science, University of Canterbury, Private Bag 4800, Christchurch – New Zealand

<sup>4</sup>Istituto Nazionale di Geofisica e Vulcanologia, Sezione di Pisa, via della Faggiola 32, 56126 Pisa – Italy

<sup>5</sup>GNS Science, 1 Fairway Ave, Lower Hutt – New Zealand

<sup>6</sup>Dept. of Geosciences, University of Nebraska-Lincoln, Lincoln, NE 68588 – USA

<sup>7</sup>Dept. of Sedimentology & Environ., Geology, Geoscience Center Göttingen (GZG), Goldschmidtstr. 3,  
37077 Göttingen – Germany

<sup>8</sup>Alfred Wegener Institute for Polar and Marine Research, 27568 Bremerhaven – Germany

<sup>9</sup>ISMAR-CNR, via Gobetti 101, 40129, Bologna – Italy

<sup>10</sup>Dipt. di Scienze della Terra, Università di Pisa, Via S. Maria, 53, 56126 Pisa – Italy

<sup>11</sup>Centro di Geotecnologie, Università di Siena, San Giovanni Val d'Arno, Arezzo – Italy

<sup>12</sup><http://sms.andrill.org/projects/sms/team/html>

\*Corresponding authors (kpanter@bgsu.edu; talarico@unisi.it)

**Abstract** – The compositional record of the AND-2A drillcore is examined using petrological, sedimentological, volcanological and geochemical analysis of clasts, sediments and pore waters. Preliminary investigations of basement clasts (granitoids and metasediments) indicate both local and distal sources corresponding to variable ice-volume and ice-flow directions. Low abundance of sedimentary clasts (e.g., arkose, litharenite) suggests reduced contributions from sedimentary covers while intraclasts (e.g., diamictite, conglomerate) attest to intrabasinal reworking. Volcanic material includes pyroclasts (e.g., pumice, scoria), sediments and lava. Primary and reworked tephra layers occur within the Early Miocene interval (1093 to 640 metres below sea floor). The compositions of volcanic clasts reveal a diversity of alkaline types derived from the McMurdo Volcanic Group. Finer-grained sediments (e.g., sandstone, siltstone) show increases in biogenic silica and volcanic glass from 230 to 780 mbsf and higher proportions of terrigenous material ca. 350 to 750 mbsf and below 970 mbsf. Basement clast assemblages suggest a dominant provenance from the Skelton Glacier - Darwin Glacier area and from the Ferrar Glacier - Koettlitz Glacier area. Provenance of sand grains is consistent with clast sources. Thirteen Geochemical Units are established based on compositional trends derived from continuous XRF scanning. High values of Fe and Ti indicate terrigenous and volcanic sources, whereas high Ca values signify either biogenic or diagenic sources. Highly alkaline and saline pore waters were produced by chemical exchange with glass at moderately elevated temperatures.

## INTRODUCTION

Data are presented following the subdivision into 14 lithostratigraphic units (LSUs) on the basis of major changes in lithology recognised during core description by Fielding and others (this volume). Following a multi-disciplinary approach, this chapter comprises a summary of compositional data that were provided by investigations involving sedimentological, petrological and geochemical methodologies and techniques, including:

- (a) logging of all clasts with diameter larger than 2 millimetres (mm) and preliminary description of basement clasts (S. Sandroni, F. Talarico);
- (b) preliminary petrographical analysis of sedimentary clasts larger than 2 mm (G. Cornamusini);

- (c) logging and petrographical analysis of volcanic and dolerite clasts (P. Del Carlo, K. Panter);
- (d) sand petrology (K. Bassett) and smear slide analysis (B. Field);
- (e) compositional characterisation of bulk sediments by continuous XRF core scanning (G. Kuhn, S. Hoffmann, H. von Eynatten, L. Reichelt); and
- (f) composition of volcanic clasts by XRF measurements on fused single whole-rock samples (L. Bracciali, S. Rocchi).

These key letters (a) through (f) in the above list of investigations are inserted within the text (at the beginning of the pertinent paragraph) to enhance immediate identifications of specific contributions and analytical approach. Data are presented in order of successive Lithostratigraphic Units (LSU), but following

a subdivision of the above cores, in order to provide a detailed and integrated description of the various compositional features observed at different grain size and with different analytical techniques.

The second part of this contribution includes a report on the geochemical analysis of interstitial water (T. Frank) and the results of diagenesis of allochems (M. Taviani and T. Frank). The methodology for the collection of high-resolution colour reflectance data (G. Kuhn, S. Hoffmann, L. Reichelt) and porewater geochemistry (T. Frank) is presented in the *Explanatory Notes* (this volume).

Each section in this report includes an introduction that provides a general overview of the performed investigations and their specific analytical procedures. Additional information on the objectives, roles, operations and procedures of the ANDRILL Southern McMurdo Sound (SMS) Geochemistry and Petrology team are described in the *Explanatory Notes* (this volume). Summary tables of basement, sedimentary and volcanic clasts are compiled in Appendix 1, as supplementary tables and figures, available for this volume on-line at the *Terra Antartica* website [www.mna.it/english/Publications/TAP/terranta.html](http://www.mna.it/english/Publications/TAP/terranta.html) and at the ANDRILL data site [www.andrill.org/data](http://www.andrill.org/data). Please refer to the list of appendices at the end of this contribution.

All of these data on the composition of the AND-2A drillcore will contribute to: (1) inferences regarding paleoclimatic information; (2) understanding provenance history of terrigenous and volcanoclastic components in the AND-2A core; (3) recording changes in depositional environment; (4) providing spatial and temporal evolution of the Cenozoic volcanic activity in the McMurdo Sound area; and (5) documenting rock-water interactions during sedimentation, diagenesis and possible later episodes of hydrothermal alteration linked to volcanic processes.

## **CORE COMPOSITION CLAST AND SAND PETROLOGY, VOLCANOLOGY AND GEOCHEMISTRY**

### **Overview of Procedures and Analytical Methods**

This summary is a compilation of initial macroscopic observations of the core and geochemical data provided by high-resolution X-ray fluorescence (XRF) core scanning. Samples were taken from representative facies within each LSU for preliminary microscopic analysis of smear slides and thin sections on-ice (K. Bassett, P. Del Carlo, B. Field), as well as for off-ice geochemistry (S. Rocchi, H. von Eynatten, L. Bracciali), calibration of the XRF core scanner data (G. Kuhn, S. Hoffmann, H. von Eynatten) and  $^{40}\text{Ar}/^{39}\text{Ar}$  dating (G. Di Vincenzo, see Acton et al., this volume).

The primary objectives of the on-ice team during the Core-Characterisation Phase were to provide preliminary data on clast distribution patterns (based on the logging of all clasts from granule to boulder

size), petrography of volcanic and basement clasts (intrusive, sub-volcanic, metamorphic and sedimentary rocks), the petrographic and textural characterisation of volcanic layers and sandstones (including the sand fraction in the sandy siltstones and in diamictite). A preliminary geochemical characterisation of all lithologies in the core was provided by continuous measurements on the archive halves of the core using a non-destructive, transportable, XRF core scanner. Measurements for the elements Si, Cl, K, Ca, Ti, Fe and Ba were processed from the XRF raw data set on-ice and were used to divide the AND-2A core into 13 Geochemical Units (GUs). A detailed description of each GU in correspondence to a LSU is presented in the *Results* section, and a summary table with the top and bottom depths of each GU will follow in the *Discussion* section.

## **PETROLOGICAL INVESTIGATIONS**

(a) Clast logging was performed following the same procedure adopted for the Cape Roberts Project (CRP)-2/2A core (Cape Roberts Science Team, 1999). Total number of clasts per 1 metre (m) and per 10 centimetre (cm) intervals are presented in a graphical form (using a logarithmic scale) and integrated by means of *PSICAT* (Palaeontological-Stratigraphic Interval & Construction Analysis Tool) in the summary lithological logs (see Fielding et al., this volume). Within the uppermost 200 m, clasts larger than 1 cm were also logged by means of *Corelyzer* software; for each clast, information such as dimension, shape and lithology were collected and included in the AND-2A database. Sampling, macroscopic observations, and preliminary petrographical analyses of basement clasts were performed following the same procedure and sample management adopted for the CRP-1 core (Cape Roberts Science Team, 1998). A list of all basement clast samples is given in Appendix 1\_Table\_A1\_1.

(b) A partial and preliminary set (27 samples) of sedimentary clasts larger than 2 mm, including diamictite extraformational clasts, have been preliminarily characterised through microscopical analyses (Appendix 1\_Table\_A1\_2). Samples were taken from the top of recovered section to 985 mbsf, with variable spacing. Petrographical analyses were performed through thin-section qualitative estimates by optical microscopy, taking into account the mineralogical constituents and petrographical-textural features. This allowed the recognizing of some lithological groups or petrofacies, according to previous procedures (Cape Roberts Science Team, 2000; Settini et al., 2005). Lithological groups also include diamictite clasts that may be extraformational or intraformational in origin; however, we consider them intraclasts due to intrabasinal reworking. Intraclasts also include conglomerates and coarse sandstones with evidences of intrabasinal reworking. In contrast, the other lithological groups are almost entirely of extrabasinal and extraformational origin, indicating a recycling of oldest well-lithified rocks.

Furthermore, lithological groups of clasts have been related to the sedimentary facies of the beds containing the samples, in order to detect relationships between petrofacies and sedimentary facies.

(c) Macroscopic observations of volcanic and dolerite clasts were made during core logging and 140 representative samples were selected for thin sections (Appendix 1\_Table\_A1.3). Volcanic clasts were taken from all LSUs except 3 and 14. The composition of volcanic clasts is based on the mineral assemblage recognised in thin section using standard petrographic techniques: mafic (basaltic) compositions are characterised by phenocrysts of clinopyroxene (Mg-rich), olivine and plagioclase; intermediate compositions consist of plagioclase, clinopyroxene (Fe-rich)  $\pm$  amphibole; felsic (phonolitic, trachytic) compositions contain phenocrysts of K-feldspar, clinopyroxene (aegirine)  $\pm$  amphibole. A limited number of volcanic clasts that appear relatively fresh in thin section are classified using whole-rock geochemistry (see XRF Single Sample Analysis below). A full description of volcanic lithofacies is provided in the report by Fielding et al. (this volume).

(d) Smear slide samples were taken at 1 m spacings below 229 mbsf and at similar or wider spacings above 229 mbsf. Additional samples were taken where lithologies appeared likely to provide dateable material. Smear slide estimates are semi-quantitative only and will be particularly inaccurate in a small proportion of slides where smeared sediment was dilute (less than 50% coverage). Trends in percentages of components are more reliable than absolute percentages from single slides. Some biogenic carbonate might have been powdered during sampling and smearing of hard lithologies and been recorded as non-biogenic carbonate but most carbonate (apart from horizons with serpulid macrofossils) is probably secondary. The 'terrigenous' component comprises all sediment not included as biogenic, fresh volcanic glass or non-biogenic carbonate, and therefore includes altered volcanic glass and any volcanic rock fragments.

(d) Sandstones and the matrix of diamictites were targeted and sampled at fairly regular intervals and to cover the variation within each identified LSU. Many fine-grained units were not examined since minerals are difficult to resolve with microscopic techniques and are better characterised by XRF. Thin section analysis contributed detailed mineral identification of framework grains, matrix composition and texture, diagenetic alterations of framework grains and matrix, and cement composition.

#### HIGH RESOLUTION X-RAY FLUORESCENCE (XRF) CORE SCANNING

(e) X-ray fluorescence core scanning is a low-cost, quick and non-destructive technique for the analysis of chemical elements directly on the split-core sediment surface. Continuous XRF scanning provides a high-resolution geochemical dataset, and has been used in several case studies for rapid paleoclimate changes

in low and high latitudes on various time scales (e.g., Adegbe et al., 2003; Grützner et al., 2005; Haug et al., 2001; Helmke et al., 2005; Westerhold et al., 2005). In order to obtain a high-resolution geochemical dataset to identify rapid changes in the Antarctic cryosphere recorded in the AND-2A sediment core, an Avaatech XRF core scanner ([www.avaatech.com](http://www.avaatech.com)) of the 2<sup>nd</sup> generation was set up directly in McMurdo Station. This core scanner measures the variation in elements of atomic mass range from Al (atomic no. 13) to U (atomic no. 92) (Richter et al., 2006). The continuous XRF measurements began on 16 Oct. 2007 and ended on 7 Dec. 2007. During the on-ice period the measurements were carried out with the same settings as used in the previous ANDRILL McMurdo Ice Shelf (MIS) Project (Pompilio et al., 2007). Immediately after core splitting the continuous XRF scanning was done on the archive half of the core. Depending on the rate of drilling advance, and the available time for core scanning, the measurement point resolution varied over the whole core between 1 and 10 centimetres.

The technical details of the Avaatech XRF Core Scanner are summarised in Appendix 2\_Table\_A2\_1. Inside the scanner the X-ray-source, the detector and the He-flushed prism are oriented as a triangle over the sediment surface (Appendix 2\_Fig.\_A2\_1). The generated radiation from the X-ray source travels through the He-flushed prism and hits the sediment surface under a 45° angle. For background optimization different filters can be moved inside the beam. The detector for the outgoing fluorescence radiation is also oriented in an angle of 45°. To minimize absorption of fluorescence radiation by air, the prism between X-ray source and detector is flushed with helium. During scanning, the surface of the sediment core was covered with a 4  $\mu$ m thin SPEXCerti Prep Ultralene® foil to avoid contamination of the prism, since the prism touches the surface of the core at every measurement point (Appendix 2\_Fig.\_A2\_1). All air bubbles and water beneath the foil were squeezed out and the sediment surface was smoothed if possible.

The measuring spot size (irradiated sample length) was constant at 1 x 1cm over the whole measuring period. This is the highest possible setting on the XRF core scanner and should be large enough to minimise inhomogeneities. Furthermore, every specific core section was checked by hand to prevent measurements on big clasts, fractures or veins.

The measurements were carried out on the whole core with 10 kV and 50 kV (Appendix 3\_Table\_A3\_2), but some particular sections were measured with 30 kV. To suppress the background radiation a copper filter was put in the beam at 50 kV and a thick lead filter at 30 kV. Only with the 10 kV setting was no filter used. These instrumental settings are recommended to achieve reliable results (Richter et al., 2006). A count time of 30 s was used for the 10 kV and 30 kV setting and 40 s for the 50 kV setting. To achieve a dead-time below 40% the count time is respectively

prolonged for each measurement point.

The raw spectra of all approx. 22 000 measurement points were saved on a computer connected to the XRF scanner. Before the spectra for every measurement could be processed with the Canberra WinAxil and WinAxilBatch ([www.canberra.com](http://www.canberra.com)) software, a processing model was arranged to obtain counts for each element. On the basis of the processed model, the software calculated the element counts as peak integrals and applied background subtraction. The quality of every single spectra and peak integral can be easily checked with a  $\chi^2$  value.

Regular instrumental tests during the XRF scanning are essential for accurate measurements with stable conditions downcore: standard material measurements provide an easy way to estimate the instrumental drift (see Appendix 3; and *Explanatory Notes*, this volume). Another useful indicator for the X-ray source stability is the measurement of the target material Rh. During the measuring period of the AND-2A core the Rh counts stay fairly constant over the upper 1 040.28 metres. Below this point the

Rh counts drop exactly at the boundary of LSU 13 to 14 of about 30% and stays constant at a lower level until the bottom of the core (see description of LSU 14 below). Repeated measurements indicate that the reason for this drop is probably not related to the source, but rather to the changes in the lithologies and associated rock behaviour of these LSUs. Further data correction procedures can be found in Appendix 3 (*Ar correction*) and *Explanatory Notes* (this volume).

#### GEOCHEMICAL AND MINERALOGICAL DISCRETE SAMPLE ANALYSIS

(e) Rock samples from almost every metre of the core were taken on-ice for further geochemical analysis. All samples were freeze-dried, crushed and clasts greater than 2mm were removed by hand. The water content of each sample can be calculated by weighing before and after freeze-drying (Fig. 1). At the top of the AND-2A core the water content reaches a maximum of 45% and decreased continuously with increasing depth to about 8% at the bottom of the core. After grinding the samples to an analytical powder they will be analysed by conventional XRF for correction and calibration of the XRF core scanner data. ICP-MS, CNS, biogenic opal, dry bulk density and XRD measurements will also be carried out to expand the existing geochemical data set.

#### X-RAY FLUORESCENCE (XRF) SINGLE SAMPLE ANALYSIS

(f) Whole-rock major elements were determined on glass beads by X-Ray Fluorescence (XRF, ARL 9400 XP spectrometer) at Dipartimento di Scienze della Terra, University of Pisa, following the procedure of Tamponi et al. (2003). Loss on Ignition (LOI) was determined gravimetrically on preheated powders (110°C) after 1 hour ignition at 1000°C in a microwave furnace.

#### RESULTS

##### **Lithostratigraphic Unit 1.1 (0.00 – 10.22 mbsf)**

(a) LSU 1.1 comprises minimally reworked basaltic volcanic material. It includes sandy volcanic breccia and ripple cross-laminated volcanic sandstone. Clasts within LSU 1.1 are almost entirely represented by volcanic rocks, with minor intraclasts (siltstone and sandstone) and rare altered plagioclase, likely derived from granitoid rocks. This unit has a content of c. 41 clasts per metre and includes granule- to pebble-grain sizes.

(c, d) Due to poor recovery and induration, only the ripple cross-laminated volcanic sandstone was sampled for thin sections (9.40 mbsf). This comprises >90 vol.% volcanic glass composed of Fe-rich cusped shards that are a mixture of fresh glass, altered to zeolite, or altered to some Fe-rich mineral such as limonite or hematite. Basaltic lithics make up 2 vol.%, euhedral plagioclase, clinopyroxene, and olivine, and amphibole make up 3%, whereas only 2% is composed of quartz. The lighter colour lining

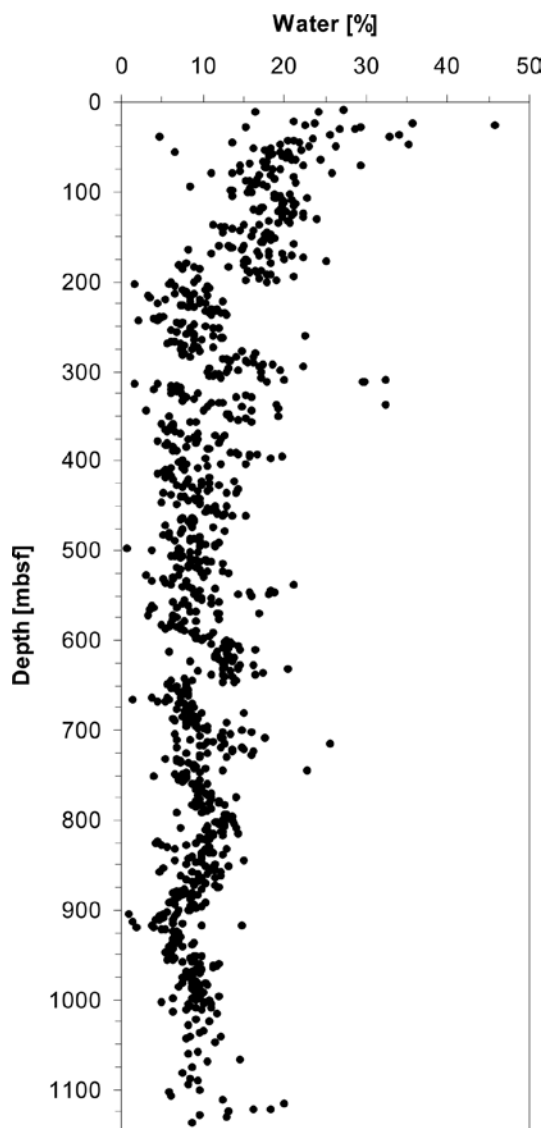


Fig. 1 – Water content of 1 010 samples from the AND-2A core versus depth beneath seafloor.

the foresets is from the finer glass shards altering to clays. The cusped shape of the glass shards indicates the sediment source was from a subaerial basaltic eruption. The dominance of primary basaltic material indicates sediment derivation from a local vent with only the quartz derived from a more distal terrigenous sediment source. This suggests that the sediment has been minimally reworked and transported only a short distance from source, otherwise more mixing with terrigenous material would have occurred. Traces of biogenic silica (including diatoms) occur in the smear slides.

(e) **Geochemical Unit 1.1** (0.00 – 10.22 mbsf): (see LSU 1.3 for Geochemical Unit description).

(f) One sample (AND-2A 8.80 mbsf) was analysed for whole-rock chemistry. It is a porphyritic lava clast characterised by medium- to coarse-grained anhedral anorthoclase phenocrysts, subhedral medium-grained phenocrysts of pale-green clinopyroxene and minor olivine set in an almost opaque vesiculated groundmass. Flattened vesicles and elongated phenocrysts define a flowage texture. According to XRF major element data, this sample plots in the phonolite field in the TAS diagram (Fig. 2).

**Lithostratigraphic Unit 1.2** (10.22–20.57 mbsf)

(c) LSU 1.2 consists of monomictic volcanoclastic breccia and basaltic lava. The monomictic basaltic breccia occurs in the interval between 11.19 and 12.20 mbsf. Features such as the reddish scoriaceous edge of some lava blocks and their angular shape most likely indicate deposition of this deposit in a subaerial environment by non-explosive fragmentation of flowing lava (*i.e.* autoclastic breccia). Petrographic

and textural analyses of sample AND-2A 11.94 indicate that the autoclastic breccia is a mafic porphyritic basalt with phenocrysts of clinopyroxene and olivine in a glassy groundmass that includes microlites of clinopyroxene and olivine as well as plagioclase, amphibole and magnetite.

(c) The lower portion of LSU 1.2 is composed of vesicular basaltic lavas identified in bagged samples between 12.30 and 18.70 mbsf. The thickness and number of lava flows within this interval are unknown due to the poor core recovery. Sample AND-2A 18.03 mbsf has the same mineralogy and glassy groundmass as lava within the autoclastic breccia with only minor variation in the volume percent of olivine.

(e) **Geochemical Unit 1.2** (10.22 – 20.57 mbsf): (see LSU 1.3 for Geochemical Unit description).

(f) Two lava clasts (from the autoclastic breccia) and two samples of the lava flows from LSU 1.2 were analysed for major element composition by XRF. All four samples straddle the boundary between the hawaiite and tephrite-basanite fields of the TAS diagram (Fig. 2). The two lava clasts (AND-2A 10.24 and 12.23 mbsf) have high normative *olivine* content (12.6–15.0%). The two lava flow samples (AND-2A 18.03 and 18.69 mbsf) show lower normative *olivine* content, around 7%.

**Lithostratigraphic Unit 1.3** (20.57–37.07 mbsf)

(c, d) LSU 1.3 is composed of minimally reworked basaltic volcanic material. LSU 1.3 includes sandy volcanic breccia and ripple cross-laminated volcanic sandstone. The examination of sample AND-2A 24.98 mbsf collected from a black stratified volcanic sandstone (24.94–25.26 mbsf) reveals that 70% of the

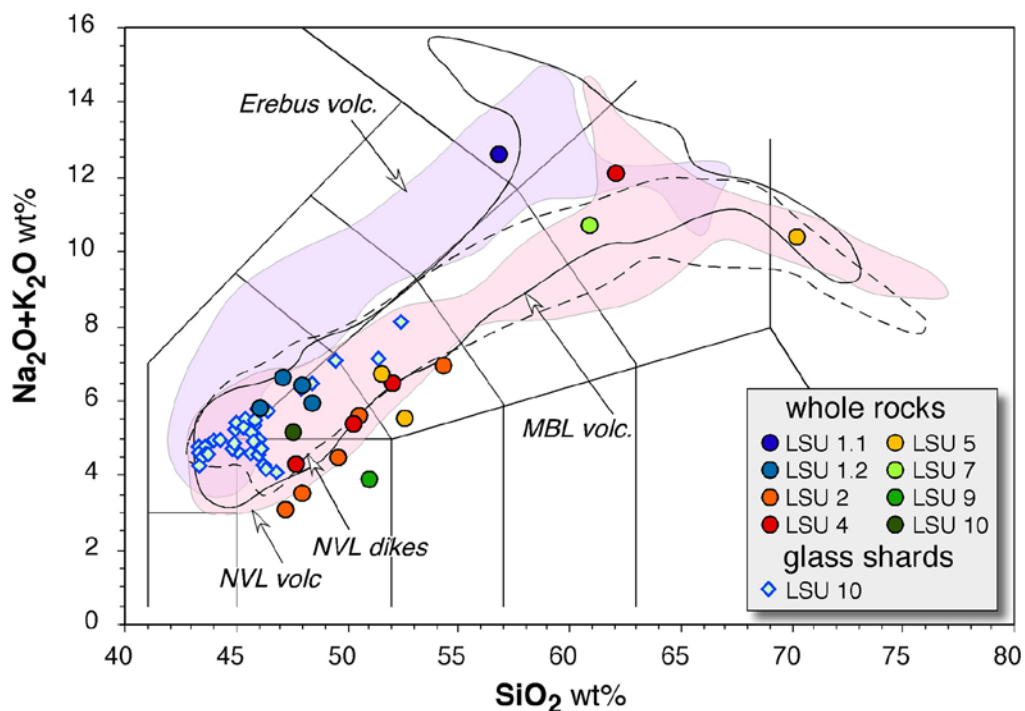


Fig. 2 – Plot of total alkalis versus silica content (wt.%) for lavas and clasts (circles) and brown glass in tephra horizons at c. 709 mbsf (diamonds) in AND-2A. Data sources for comparative compositional fields: Erebus volcanics: LeMasurier & Thomson (1990), Kyle et al. (1992); Marie Byrd Land (MBL) volcanics: LeMasurier & Thomson (1990), Rocchi et al. (2006); Northern Victoria Land (NVL) volcanics and dikes: LeMasurier & Thomson (1990), Armienti et al. (1991), Rocchi et al. (2002).

grains consist of glassy, vesiculated clasts (transparent sideromelane and opaque tachylyte) containing very fine microlites of plagioclase and clinopyroxene. Other fragments include altered lavas and loose crystals of clinopyroxene, plagioclase, amphibole and quartz. The clasts have a rounded to sub-rounded shape indicating that they were reworked by currents in a shallow water setting. The glassy grains were originally formed by magmatic explosive eruptions in a subaerial environment from a vent probably located within a few kilometres (km) of the drillsite.

(c) Downcore samples of volcanoclastic sandy breccia (23.70, 26.33, 27.30 and 29.95 mbsf) were sampled and examined petrographically. Clasts within the breccia consist of angular lava blocks supported within a matrix of volcanic sand. Clast sample AND-2A 27.39 mbsf is a porphyritic basalt lava with phenocrysts of clinopyroxene and olivine in a glassy groundmass that includes phenocrysts of plagioclase, clinopyroxene and magnetite. It is different from the other two lava samples, having a greater percentage of larger phenocrysts (up to 0.5 mm). Overall the clasts of lava are more evolved than in the other samples of lava.

(d) The matrix of the sandy volcanic breccia is also dominated by volcanic glass shards (64-67%), but includes a higher percent of volcanic lithics (25-30%) of both basaltic microlites and scoria. Euhedral crystals of plagioclase, pyroxene and amphibole (2-3%) are locally derived leaving only 0-2% quartz, indicating exotic terrigenous derivation.

(d) At the base of LSU 1.3, close to the contact with underlying diamictite deposits (LSU 2), is a black and whitish fine-grained, ripple cross-laminated sandstone (36.38-36.85 mbsf). Rippled volcanic sandstones were sampled at 35.02 and 36.32 mbsf. They are dominantly comprised of basaltic volcanic glass (97-80%) in the form of cusped shards (<0.1 mm) or vesiculated sideromelane grains that are variably fresh to altered to palagonite. The lithics (0-10%) are scoria with plagioclase crystals and large vesicles. Probable volcanic-derived crystals (2-6%) include euhedral plagioclase, olivine, clinopyroxene and amphibole. Quartz makes up c. 2% and indicates an exotic source. This is supported by trace amounts of biotite, chlorite, muscovite and a single possible granitoid lithic. There are also trace amounts of sponge spicules in the deposit. The texture and composition indicate derivation primarily from a local volcanic vent with minor to trace inputs of exotic terrigenous material.

(a, d) Volcanic rock clasts dominate, followed by intraformational clasts (siltstones and sandstones) and very minor granules of quartz and granitoids. Clast content is c. 143 per metre. Volcanic rocks and intraclasts usually occur as granules and pebbles, but minor cobbles are also present. Traces of biogenic silica occur in some of the smear slides.

(e) Geochemical Unit 1.3 (20.57 – 37.07 mbsf): XRF measurements show that high Fe and Ti counts are notable for the volcanic lithologies of LSU 1. The

total core maxima for both elements are reached in LSU 1.3 (Fig. 3). Cl has low values in LSU 1.1 and increases within LSU 1.3 to higher levels as can be seen in LSU 2 (see Geochemical Unit description of LSU 2). The values of Si, Ca and K are low in all of LSU 1. Ba shows medium high values.

### **Lithostratigraphic Unit 2 (37.07 – 98.47 mbsf)**

LSU 2 is composed of glacial diamictite rarely interbedded with siltstone, sandstone, and granule conglomerate. Recovery was significantly higher, as was lithification.

(a) This unit is characterised by a high clast content (183 clasts per metre) and by a wide variety of clast lithologies, mostly consisting of granitoids, intraclasts (sandstone and siltstone) and volcanic rocks (varying from mafic to felsic composition), with minor metamorphic rocks, quartz, sedimentary rocks and dolerites. Granitoid and metamorphic rock percentages have an increasing trend downcore, whereas volcanic rock content decreases downcore. Sedimentary rock clasts comprise siltstone, sandstone (including quartz-arenites) and diamictite. Clasts mostly occur as granules and pebbles, but cobbles of granitoid, dolerite and metamorphic rock are also present.

(a) Granitoid clasts mainly include foliated or unfoliated grey and pink biotite ±hornblende monzogranite and tonalite, with subordinate biotite leucomonzogranite, biotite Ca-amphibole syenogranite and rare porphyry and quartz-diorite. Preliminary petrographical analyses show granitoids are usually medium- to coarse-grained, with a texture ranging from hypidiomorphic/allotriomorphic to porphyritic, sometimes associated with solid-state deformational microstructures (foliated varieties).

(a) Clasts of metamorphic rocks consist of biotite orthogneiss of granitic composition, biotite gneiss, Ca-amphibole gneiss/granofels, Ca-amphibole schist, marble, amphibolite and low-grade metasediments. Gneisses are medium- to fine-grained, granolepidoblastic, sometimes characterised by a mineralogical layering; the mineral assemblages are usually represented by biotite, ±white mica, cordierite, clinozoisite or Ca-amphibole, whereas the Ca-amphibole bearing variety (±clinopyroxene) is more common below c. 74 mbsf. Marble clasts are granoblastic, fine- to medium-grained, consisting of calcite with minor Ca-amphibole, clinopyroxene or white mica (Fig. 4e). Metasediment clasts include biotite metasandstone, biotite-calcite metasiltstone and metalimestone, with mineral assemblages indicative of low-grade metamorphic conditions.

(c) Clasts of gabbro and dolerite are fine- to medium-grained, showing a texture ranging from hypidiomorphic to allotriomorphic. They are composed of plagioclase, clinopyroxene, ±orthopyroxene, ±potassium feldspar, ±quartz, ±biotite, ±amphibole and Fe-Ti oxide.

(b) Diamictite clast (sample AND-2A 64.01 mbsf) with low sphericity (subprismoidal) and medium-

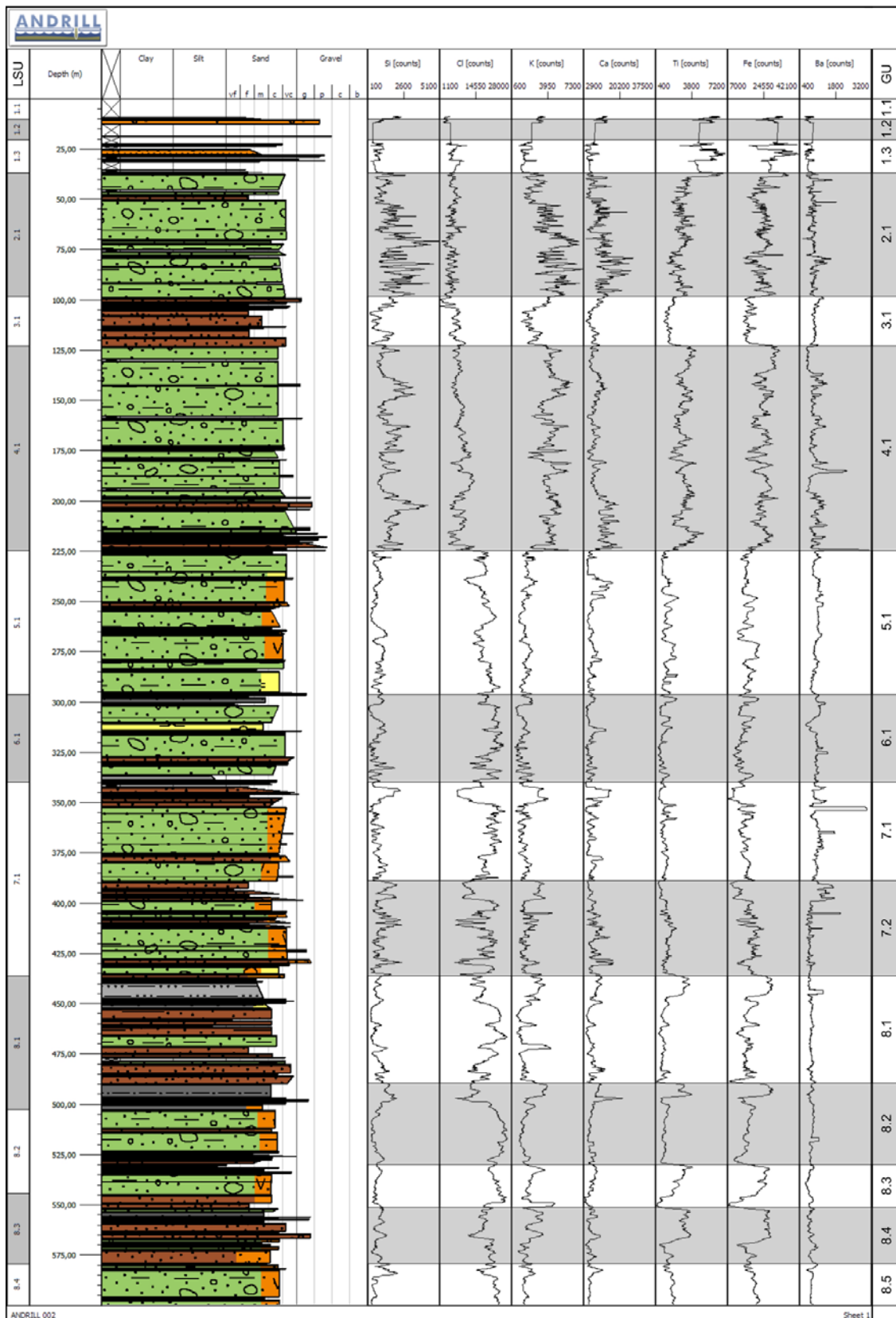


Fig. 3 – Lithostratigraphic Units (LSU; left margin), lithologic log and Geochemical Units (GU; right margin) with selected element counts from the XRF Core scanner for the interval 0 – 600 mbsf of the AND-2A core.

high roundness (rounded) occurs within massive diamictite (e.g., Fig. 5). The internal clast texture is matrix-supported (very poorly sorted), with clasts up to 8 mm in size, from rounded to very angular in roundness. The matrix is mainly shaly, so to define the rock as pebbly mudstone. Clasts consist of grains

of intrusive rock (plagioclase+quartz), quartz, basalt, plagioclase and calcite.

(c) Preliminary petrographic examination of volcanic clasts in LSU 2 shows a wide variety of lithologies based on mineral type. Mafic volcanic clasts occur throughout the unit and consist of porphyritic

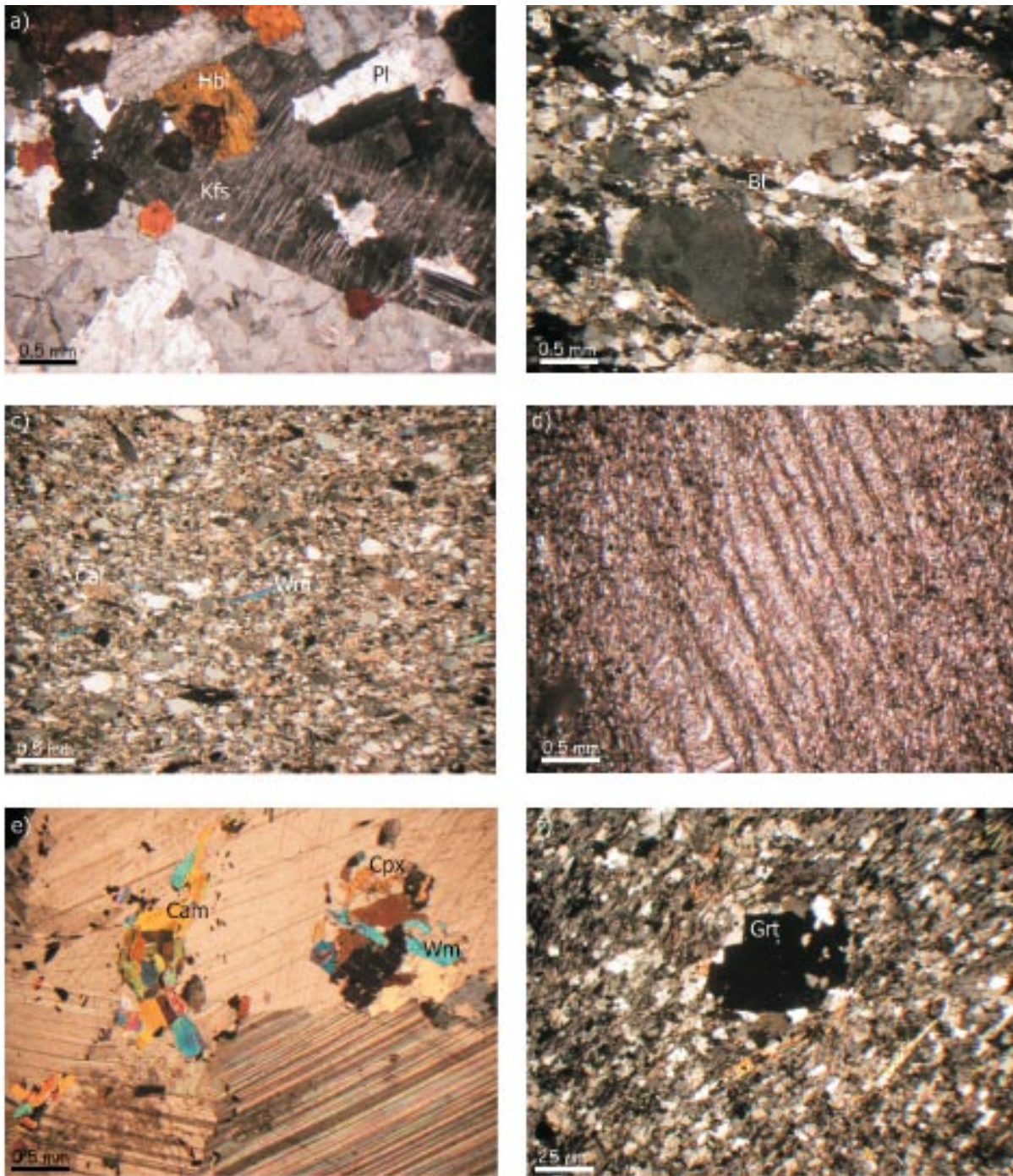


Fig. 4 – Photomicrographs of representative basement rock samples in AND-2A core. (a) Grey hornblende-biotite granodiorite (AND-2A 647.95 mbsf, crossed polarizers), showing a medium-grained hypidiomorphic texture, with mm-sized perthitic K-feldspar carrying smaller inclusions of plagioclase and hornblende. (b) Biotite monzogranitic orthogneiss (AND-2A 673.47 mbsf, crossed polarizers), characterised by a mylonitic texture with porphyroclasts of feldspars set within a granolepidoblastic fine-grained matrix. (c) Calcite-white mica metasandstone (AND-2A 683.96 mbsf, crossed polarizers). (d) White mica-biotite phyllite (AND-2A 868.68 mbsf, crossed polarizers), with flakes of detrital white mica. (e) Ca-amphibole-clinopyroxene-white mica marble (AND-2A 87.75 mbsf, crossed polarizers), with a medium-grained granoblastic texture. (f) Biotite-white mica-garnet schist (AND-2A 363.62 mbsf, crossed polarizers), characterised by subidioblastic porphyroblasts of garnet set within a fine-grained granolepidoblastic matrix. Mineral abbreviations after Kretz (1983), with the addition of Wm to indicate white micas.

basalts with phenocrysts dominated by clinopyroxene with lesser amounts of olivine, magnetite and plagioclase. Groundmass shows interstitial textures with glass and microlites of clinopyroxene, plagioclase and magnetite. Intermediate and felsic lava clasts occur together along with mafic lava clasts near the bottom of the unit. Intermediate lava clasts are characterised by having more plagioclase as phenocrysts and in the groundmass. Amphibole

occurs as rare microphenocrysts in sample AND-2A 50.50 mbsf. Felsic volcanic clasts contain phenocrysts of potassium feldspar in a pilotaxitic groundmass with microlites of plagioclase, potassium feldspar and magnetite (e.g., AND-2A 53.22 and 57.33 mbsf). Other volcanic material includes the intermittent occurrence of light grey to golden brown pumaceous lapilli (Fig. 6B) ( $n = 21$ , 86.70-93.10 mbsf), which are typically less than 1x1 centimetre in dimension.

The examination by smear slide indicates that pumice (AND-2A 86.70 mbsf) contains small (<500  $\mu\text{m}$ ) crystals of sanidine, suitable for dating by the  $^{40}\text{Ar}/^{39}\text{Ar}$  method (see Acton et al., this volume).

(c, d) It is important to note that the alteration of volcanic clasts becomes more pronounced within this unit at depths greater than 60 mbsf. In some instances, the alteration is visible in hand specimen forming a lighter coloured outer rim on clasts. Petrographic examination shows that the most common alteration minerals consist of calcite, chlorite, palagonite (a mineraloid mixture of clays), zeolite and hematite.

In some cases these minerals partially or totally replaced the original crystal (e.g., pseudomorphs of olivine and clinopyroxene).

(d) The sand-sized matrix of the diamictite indicates the same range of composition as shown by the clast compositions. Diamictite lithofacies include massive, stratified and deformed varieties. Representative samples were taken from each lithofacies and described. Matrix ranges from 20 to 80% and is composed of a mixture of clays and altered glass; calcite cement also infills pore spaces within the matrix. The amount of glass varies considerably but seems

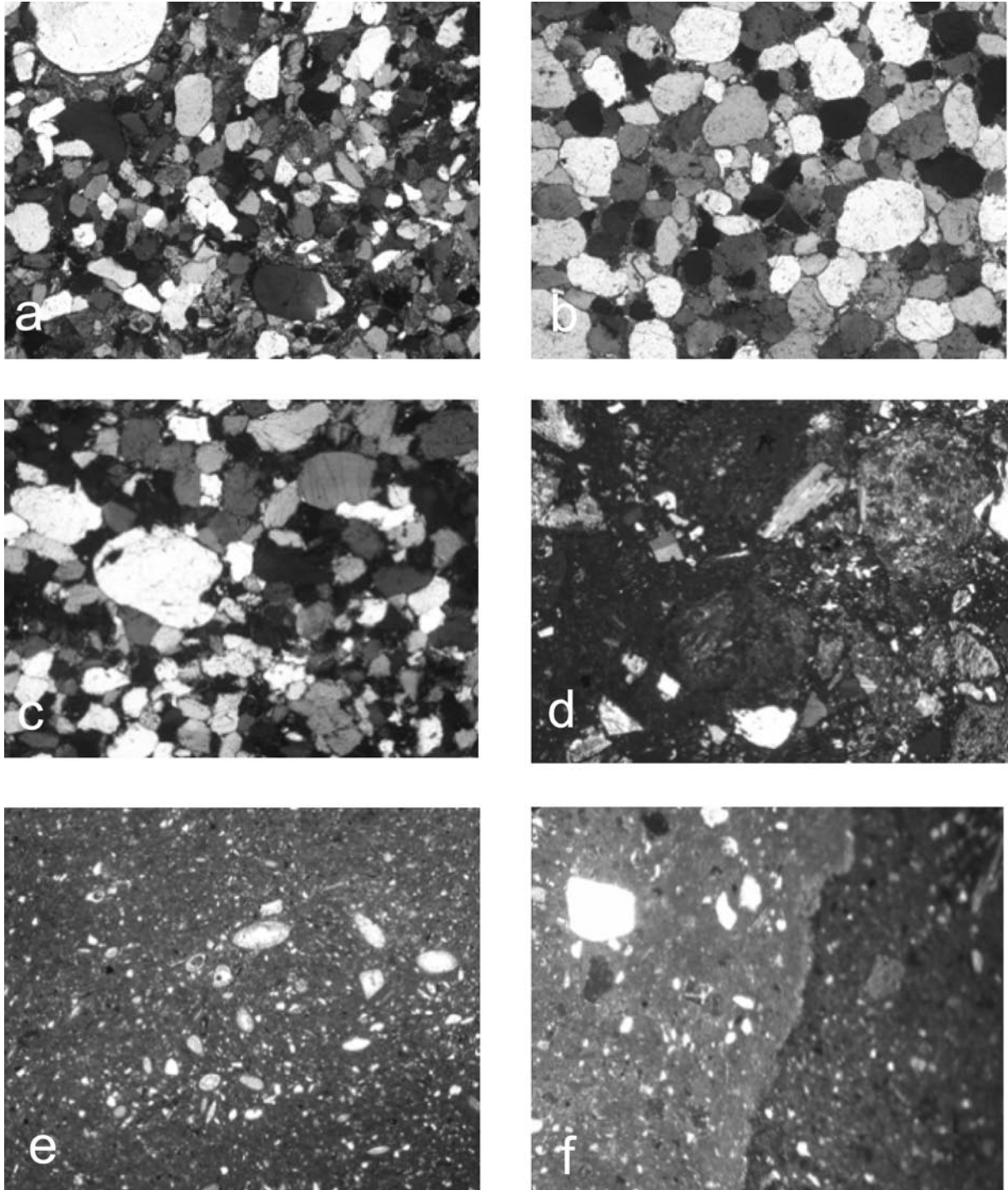


Fig. 5 – Microphotographs of the examined sedimentary clasts; magnification is 40x, cross-polarized light, except for e. (a) arkose, petrofacies A; (b) quartz arenite, petrofacies B; (c) subarkose, petrofacies D; (d) volcanic litharenite, petrofacies Q; (e) biomicrite, petrofacies E; (f) diamictite intraclast enclosed in the matrix (the clast is on the right), petrofacies K.

to be greatest in the stratified/laminated diamictite where it reaches c. 50% of the matrix. Lithic clasts include scoria, basalt, phyllite, metasediment, schist, granite, marble, dolerite and vein quartz indicating a mixture of local and distal sources. Single crystal grains include quartz, plagioclase, olivine, muscovite, biotite, pyroxene, chlorite, amphibole and opaque grains, again indicating a mixture of local volcanic sources and distal basement rock sources. The diamictites also occasionally contain biogenic materials visible in thin section.

(d) Interbedded dark sandstone is dominated by basaltic volcanic material. Q = 2-20%, F = 2-10%, L = 10-85%, devitrified glass = 10-40%, other minerals (muscovite, biotite, pyroxene, amphibole, olivine) = 2-5%. Lithics are primarily composed of basalt, scoria and altered glass grains (to hydrated glass to palagonite), but include rare marble and granite. Sandstone beds and laminations within the diamictite are volcanic-rich and seem to indicate possible episodic local eruptions.

(d) Smear slides were taken at irregular spacings in this LSU but there appears to be very little fresh volcanic glass. Biogenic silica increases in the top c. 12 m and traces of biogenic silica at c. 60 and 81 mbsf indicate at least two of the diamictite facies lower in the LSU accumulated in a marine setting (Fig. 7). A fish scale was noted at 46.47 mbsf. Grain size estimates from the smear slides suggest the diamictites have a generally muddy matrix.

(e) Geochemical Unit 2 (37.07 – 98.47 mbsf): the XRF data show that the geochemical pattern of this LSU is comparable to that of LSU 4 (see corresponding Geochemical Unit description below). In these two LSUs (2 and 4) the counts of all elements fluctuate more strongly than in all other LSUs (Fig. 3). Iron (Fe) has moderately high values and shows a cyclically stacked, saw-tooth pattern with decreasing counts. Thus, values increase steeply up core close to 85.10, 78.30 and 76.40 mbsf. The top part of this LSU has a more variable pattern with many variations of higher frequency. Above 78.30 mbsf Fe and Cl peaks are often anti-correlated whereas below 78.30 mbsf they seem more correlated. Chlorine (Cl) values remain low in this LSU. Silica (Si) and Ca have high values and gradually decrease upwards. Two curve patterns are obvious. Parts with highly variable data are intercalated with smaller sections of levelled and lower values. These minimum parts are at 94.70, 93.00, 89.90, 86.50, 83.60, 81.00, 74.60 mbsf, a broader part from 66.10 to 64.10 mbsf and one at 61.40 mbsf. They are mainly related to matrix-rich diamictite with fewer clasts and related to sand and mudstone intercalations. Elemental concentrations are largely scattered in clast-rich diamictite. In LSU 2, K has the strongest amplitude fluctuation and highest values of the total core. Similar to Si and Ca, K gradually decreases from the base of the unit to the top and has the same pattern of alternating parts with highly variable and less variable data. Both elements (Si and Ca) have corresponding trends.

Barium (Ba) is different; it also has highest total core values in this LSU, but is strongly scattered and does not show a general pattern. The exceptions are three faint minimum counts at 85.30-84.40, 78.20-77.50 and 65.60-63.60 mbsf, whereas Ca, Si and K show maximum counts.

(f) Five centimetre-sized (all subrounded but one, subangular) volcanic clasts from the glacial diamictite were selected from LSU 2 for geochemical whole rock analysis (Fig. 2). They are porphyritic rocks with compositions trending from basalt (AND-2A 43.58, 60.40, 61.73 mbsf) through trachybasalt (AND-2A 84.96 mbsf) to basaltic trachyandesite (AND-2A 69.13 mbsf).

### **Lithostratigraphic Unit 3** (98.47–122.86 mbsf)

LSU 3 is composed of flat-laminated fine to coarse sandstones and minor conglomerate.

(d) Petrographic examination shows that the sand compositions are litharenites (Q = 7-20%, F = 8-25%, L = 45-80%, other = tr-5%, matrix = 5-10%). Lithics are dominated by diamictite grains indicating that they were lithified sufficiently to survive transport and re-deposition into a beach environment. The fine-grained material is a mixture of clay-matrix and carbonate cement, and probably is over-estimated due to its similarity to diamictite grains, or it may even be composed of squashed diamictite grains. The remaining lithics include basalt, scoria, devitrified glass, granite, marble and schist. All volcanic clasts are probably epiclastic (none pyroclastic) based on rounded grain shapes. Mineral fragments include muscovite, biotite, amphibole, pyroxene and olivine. Both the remaining lithics and the other minerals indicate a mixture of volcanic and basement rock sources.

(a) Clasts up to cobble-grain size are mostly concentrated within the conglomerate at the top of the unit, whereas only dispersed granules are present elsewhere; the average clast content is c. 48 per metre. Intraformational clasts, granitoids, quartz and metamorphic rocks dominate over volcanic rocks, with only minor occurrences of sedimentary rocks and dolerites.

(a) Granitoid clasts consist of foliated or unfoliated grey and pink biotite ± hornblende monzogranite and minor biotite leucomonzogranite, similar to those present in LSU 2. Metamorphic rocks include biotite orthogneiss of granitic composition, and possible low-grade metasediment.

(c) Volcanic rocks in LSU 3 include rare mafic, intermediate and felsic lava clasts. Black coarse ash to lapilli sized scoria are found within the sandy conglomerate at the base of the unit (122.66-122.86 mbsf). The glassy appearance and angular margins of the scoria suggest slight reworking of primary material derived from explosive magmatic eruptions.

(d) No fresh volcanic glass or biogenic silica were noted in smear slides from this LSU. Carbonate percentages are around 10%.

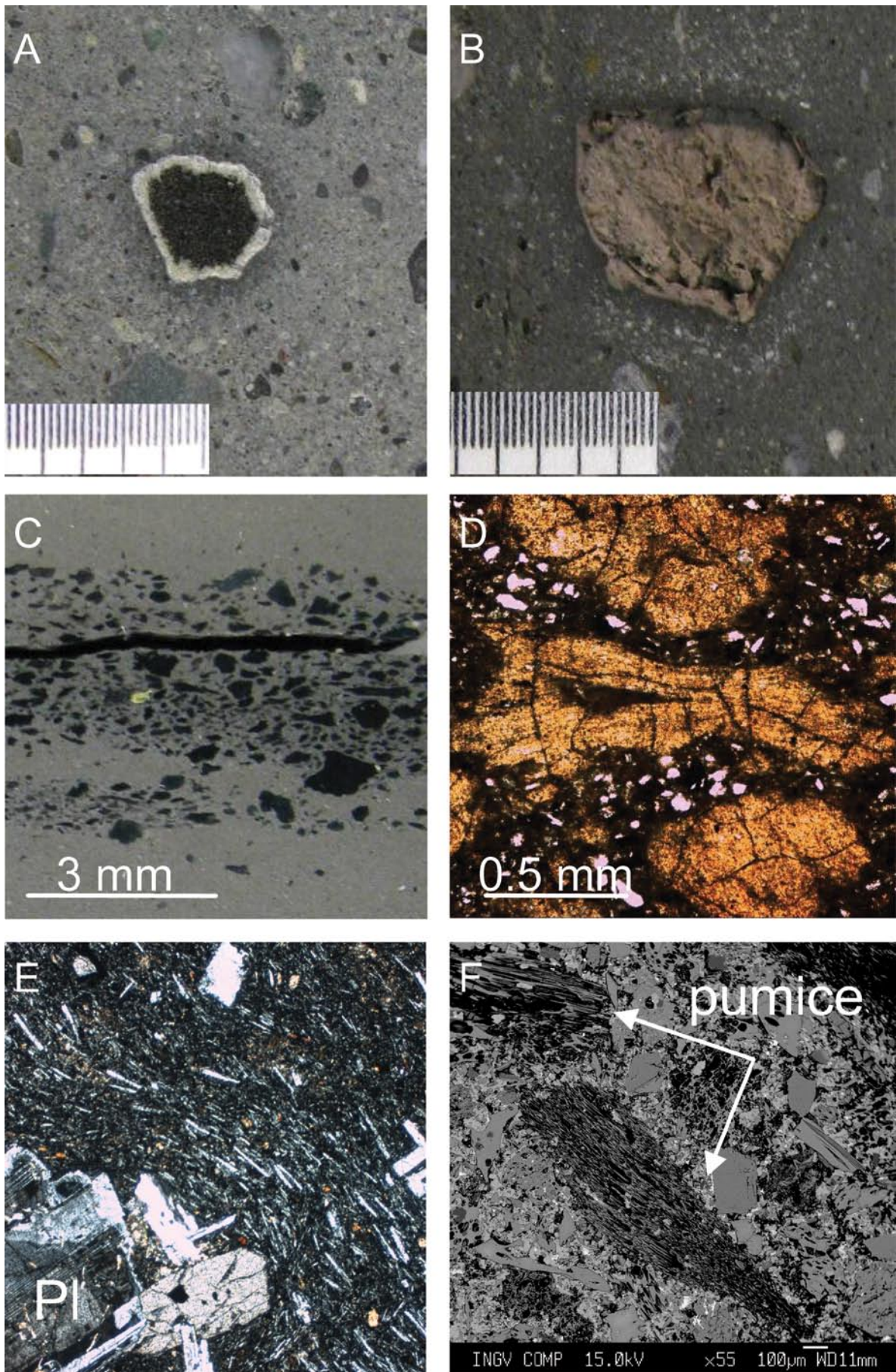


Fig. 6 – Representative volcanic clasts. (a) Photograph of 'armored lapilli' clast in diamictite at 531.02 mbsf. Scale bar is segmented in millimetre increments. (b) Photograph of pumice clast in diamictite at 86.70 mbsf. (c) Dispersed altered pumice clasts in muddy fine sandstone at 954.02 mbsf. (d) Photomicrograph (PPL) of altered pumice at 954.02 mbsf. (e) Porphyritic lava clast showing pilotaxitic texture (FOV = 2 mm). (f) Backscatter electron image of pumice in tephra layer at 640 mbsf.

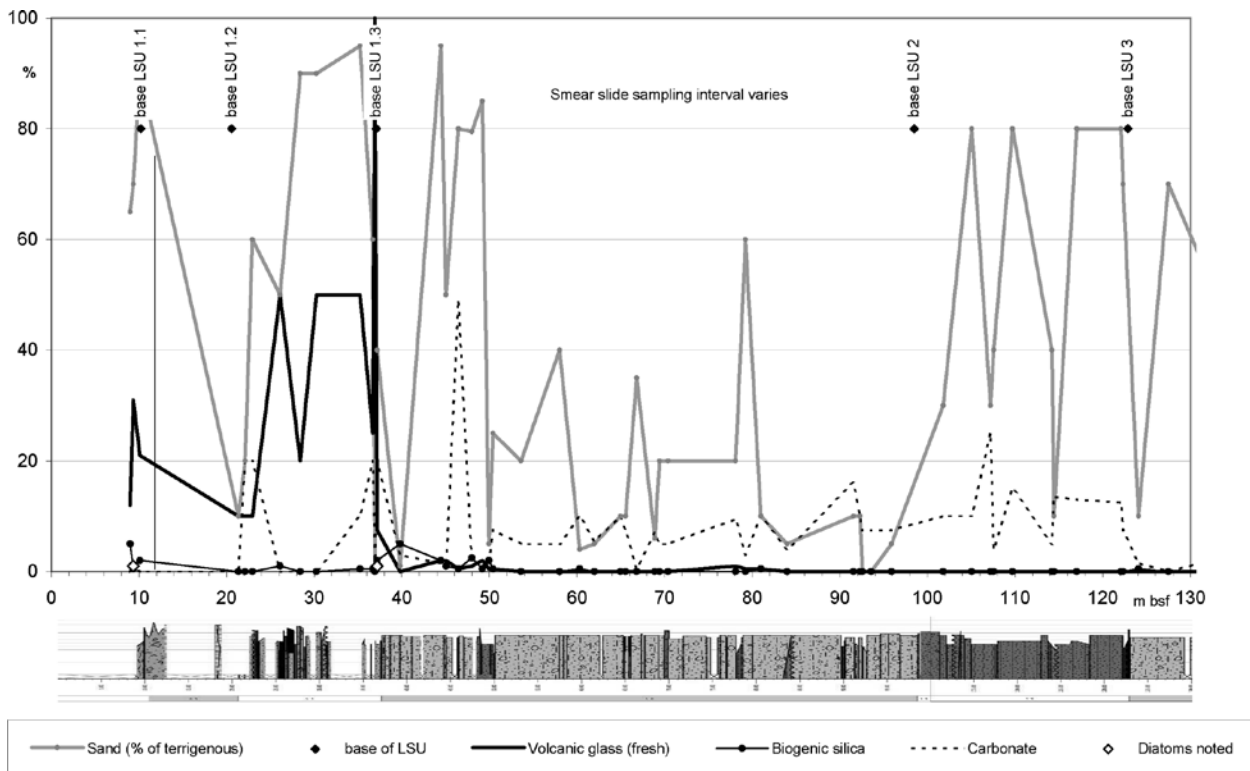


Fig. 7 – Core compositional features in LSUs 1 to 3 based on smear slides.

(e) **Geochemical Unit 3** (98.47 – 122.86 mbsf): there is an increase in mean CI values from LSU 2 to LSU 3. Iron (Fe) has very low values and it is difficult to recognize any variation. Mean values are comparable to those in LSU 5 and 6 (Fig. 3). Silica (Si), Ca and K have minima in the middle of this LSU and increasing values towards the boundaries. The concentration gradient to LSU 2 is steeper than in LSU 4. The cyclic pattern as observed in LSU 4 (Fig. 3) continues in LSU 3. Barium (Ba) values are high and decrease sharply at the boundary with underlying LSU 4.

#### **Lithostratigraphic Unit 4** (122.86–224.82 mbsf)

LSU 4 is composed of diamictite with subordinate conglomerate, sandstone and siltstone.

(a) Clasts in the gravel fraction are mostly represented by volcanic rocks, followed by intrusive rocks, quartz, metamorphic rocks and minor intraformational clasts, dolerites and sedimentary rocks. The average clast content is c. 205 per metre, showing a down-core increasing trend. Specifically, granitoid abundance increases down-core while volcanic rock and quartz decrease down-core. The trend in volcanic clast abundance is smooth relative to the other clast types. Clast size commonly ranges from granule to pebble, but cobbles of intrusive rocks, dolerites and metamorphic and volcanic rocks are also present.

(a) Clasts of igneous intrusive rocks are foliated or unfoliated biotite ± hornblende monzogranite, hornblende-biotite quartz-diorite and clinopyroxene-hornblende-biotite gabbros/diorite, with minor occurrences of leucomonzogranite and foliated porphyry. Monzogranite is typically grey in colour, but

pink to red varieties are also present, mostly from c. 206 mbsf to the bottom of the unit; pink to red monzogranite is usually characterised by a stronger alteration compared to the grey variety. Quartz-diorite is fine- to medium-grained, hypidiomorphic, sometimes characterised by a primary layering, and consist of euhedral/subhedral crystals of zoned plagioclase, brown to green hornblende and biotite associated with minor interstitial quartz and K-feldspar; some samples also show aggregates of green hornblende probably replacing primary clinopyroxene. Gabbro/diorite are medium- to coarse-grained, subophitic, consisting of euhedral clinopyroxenes associated to laths of zoned plagioclase, biotite lamellae, brown hornblende and minor interstitial quartz; green hornblende is usually present replacing clinopyroxene.

(a) Clasts of metamorphic rocks consist of biotite monzogranitic orthogneiss (usually leucocratic), marble, gneiss, granofels, schist, low-grade metasediment and rare metaporphry. Marble is similar to those reported within LSU 2. Gneiss is commonly characterised by the Ca-amphibole-clinopyroxene ± biotite mineral assemblage, with minor occurrences of Ca-amphibole-biotite and biotite ± white mica paragenesis; they are fine- to medium-grained, granonematoblastic to granolepidoblastic in texture. Granofels are fine- to medium-grained, granoblastic, consisting of clinopyroxene and plagioclase associated with minor quartz and sometimes biotite or Ca-amphibole. Schist is fine-grained, granonematoblastic, composed by isoriented Ca-amphibole and interlobate quartz and plagioclase aggregates, sometimes associated with biotite flakes or with a fine grained

opaque minerals. Metasediments include white mica  $\pm$ biotite, Ca-amphibole metasandstone, biotite  $\pm$ white mica, Ca-amphibole phyllites and metalimestone. Metaporphry is cataclastic to mylonitic in texture, sometimes foliated, with mm-sized porphyroclasts of quartz and feldspar set within a very fine grained groundmass, consisting of quartz, feldspar and neoblastic flakes of biotite and white mica, aligned along the foliation.

(b) Sedimentary clasts consist mainly of diamictite and subordinately of quartz arenite and volcanic litharenite (e.g., Fig. 5). Clasts are all included in massive diamictite deposits, with the exception of the lowest (AND-2A 198.81 mbsf), which is inside stratified diamictite. Diamictite clasts (AND-2A 146.78, 152.16, 198.81 mbsf) with medium- to high-grade in roundness are very poorly sorted pebbly mudstone, supported by muddy matrix darker than the enclosing diamicton, with grains ranging in size up to 2.5 mm and with sharp rims. The grain assemblage is formed almost exclusively by basalt and plagioclase (AND-2A 146.78, 152.16 mbsf), or also with the occurrence of subordinate grains of intrusive rock (Kfs+Plg+Qtz), plagioclase, K-feldspar, quartz, muscovite, calcite and others (AND-2A 198.81 mbsf).

(b) Quartz arenite clast (AND-2A 183.48 mbsf) is subrounded and subprismoidal in sphericity, with coarse-grain size and well sorted, clast-supported internal texture. The grain assemblage is composed of rounded to subangular quartz grains, which are almost exclusively monocrystalline, with a slight undulose extinction (grains extinguish between 1 and 5 degrees of stage rotation) and few inclusions organized in rows; rarely, quartz grains are made of composite polycrystalline quartz. The packing is of high grade, with very frequent interpenetrated grain contacts. The cement is formed by quartz overgrowths, marked by thin layer of inclusions; locally clay mineral cement occurs. A crude sedimentary fabric is observable, due to grains organization in laminae or traction carpets. Volcanic litharenite clast (AND-2A 132.82) is well-rounded, blade in shape. Matrix is absent, whereas interstitial spaces have been filled by microcrystalline and sparry calcite cement. Grains, medium to very coarse in grain size, from angular to subrounded, are composed of dominant well-rounded basalt clasts, subordinately by well-rounded to subangular clasts of plagioclase, pyroxene, monocrystalline slightly undulose quartz, K-feldspar, calcite and opaque minerals.

(c) Volcanic clasts in LSU 4 consist of mafic, intermediate and felsic compositions that are similar in their mineralogical makeup to the clasts found near the base of LSU 2 (e.g., AND-2A 129.08 and 139.51). The three fundamental compositions occur together throughout the unit. Light grey to golden brown pumaceous lapilli occur in LSU 4 ( $n = 147$ , 127.51-219.59mbsf) and are similar to the ones identified near the base of LSU 2. Intermediate and felsic lava clasts often exhibit porphyritic and pilotaxitic textures (e.g., Fig. 6E).

(c) A distinctive type of volcanic clast occurs intermittently between intervals 156 and 215 mbsf in LSU 4. This clast type ( $n = 32$ ) ranges in size from 0.5 to 2 cm, has black lava cores surrounded by light grey to grey punky material, and is referred to informally (without reference to their genesis) as 'armored lapilli'. Petrographic examination has revealed that the inner core consists of basaltic lavas with different texture. Sample AND-2A 181.53 mbsf contains phenocrysts of clinopyroxene with subordinate plagioclase in an intersertal groundmass containing microlites of plagioclase, clinopyroxene and magnetite. In contrast, the core of armored lapilli (sample AND-2A 182.69 mbsf) is not porphyritic but has the same groundmass phases as sample AND-2A 181.53 mbsf. The grey rinds on these clasts vary in thickness (1 to 6 mm) and are part of the same rock, but finer-grained with a hydrated and devitrified groundmass.

(c, d) Alteration is particularly pronounced in volcanic clasts with glassy groundmass and in some cases vesicles are partially or completely filled with secondary minerals. Sample AND-2A 133.66 mbsf exhibits parallel bands of palagonite and chlorite extending away from the rim with calcite filling the centre of the vesicle (i.e. amygdale). In addition, many dark brown intermediate to felsic volcanic clasts show prominent light coloured rims (up to 1 cm on a 4 cm diameter clast) that may be a result of diagenesis or surface weathering prior to deposition.

(d) The matrix of the diamictites varies from 40 to 70% and is composed by clays, and volcanic glass altering to and being replaced by zeolite and chlorite; secondary microcrystalline carbonate cement is also present. The reactivity of volcanic glass grains enhances both matrix alteration to zeolite and chlorite and calcite cement precipitation around the grains. Deformed diamictite matrix has more carbonate cement in the shear planes surrounding enclaves of undeformed matrix. Quartz and feldspar single crystal grains make up 10 to 30% of the diamictite matrix. Quartz makes up 5 to 15% and is mostly monocrystalline with a few polycrystalline grains. Feldspars make up 5 to 15% and include plagioclase (most unaltered, some zoned, some altered to sericite) and K-feldspar (most altered to sericite). Heavy minerals generally vary between 1 and 2% and include pyroxene, olivine, amphibole, biotite and muscovite. There are trace to 1% bioclasts, including sponge spicules, shell fragments, foraminifera and serpulid tubes. Lithics (15-20%) are a mixture of basement, epiclastic volcanic and primary volcanic glass. Basement lithics (c. 50%) include metasandstone, biotite to chlorite schist, marble, monzogranite and dolerite. Feldspar in the granites is often altered to sericite. Granite is probably the source of the big single crystal quartz and feldspar grains. Volcanic lithics (c. 50%) include felsic and mafic lavas, black scoria and brown glass. The more mafic compositions range from unaltered to variably altered to Fe-oxide, zeolite, chlorite and possibly glauconite. Brown glass grains are commonly spherulitic altering to zeolite.

Rare diamictite grains are also present.

(d) Minor interbedded sandstones are poorly- to- moderately-sorted with matrix ranging from 5 to 25%. Calcite cement is common but generally microcrystalline. Framework grain composition is much the same as in the diamictite but is more likely to contain fresh unaltered glass (<7%). Glass types include Fe-rich brown glass to clear long-tube pumice. Quartz makes up 15 to 35% of the sandstones, still mostly monocrystalline with few polycrystalline. Feldspars make up 15 to 30% and are composed of altered and unaltered plagioclase and K-feldspar. Heavy minerals are a significant component (5 to 8%) and include the same assemblage as the diamictite matrix (pyroxene, olivine, amphibole, biotite and muscovite). Lithics include the same mix of basement and epiclastic volcanic grains variably altered to zeolite, chlorite (and glauconite?) and opaque oxides.

(d) Fresh volcanic glass is rare in smear slides from this LSU except for the interval c. 174-198 mbsf (Fig. 8). Biogenic silica is also rare, though there is a small peak around 175 mbsf; however no diatoms were recorded. Fish scales were noted around 163 to 175 mbsf. Smear slides are irregularly spaced, but suggest that diamictite near the base and top of the LSU has a sand-rich matrix.

(e) Geochemical Unit 4 (122.86 – 224.82 mbsf): geochemically this LSU shows a cyclically stacked pattern in all elements. Five cycles with an average thickness of 20 m are obvious. Mean Cl values increase gradually down to 195.30 mbsf and return to lower levels as in the upper part of this LSU. Mean Fe, Si, K, Ba and Ca have no general trend. Calcium (Ca) values are higher below 195.30 mbsf (Fig. 3). This boundary can also be observed in some trace elements like Zr and Nb.

(f) Four volcanic clasts from the glacial diamictite were analysed for major elements. Three of them have a rather mafic composition (Fig. 2), roughly trending from basalt (AND-2A 197.86 mbsf) through trachybasalt (AND-2A 221.19 mbsf) to basaltic trachyandesite (AND-2A 128.55 mbsf). The fourth sample is separated from the former by a large chemical gap, having peralkaline trachyte composition of comenditic type (AND-2A 129.08 mbsf).

#### **Lithostratigraphic Unit 5** (224.82–296.34 mbsf)

LSU 5 consists of diamictite with sandstone and minor siltstone.

(a) The average clast content is 87 per metre, the highest concentration located within the volcanic-bearing clast-rich sandy diamictite (238.89 – 249.83 mbsf). Clasts, ranging in size from granule to cobble, are dominated by intrusive, volcanic and metamorphic rocks with minor occurrences of dolerite and rare quartz and intraformational clasts. Metamorphic rock percentage and total number of clasts show a down-core decreasing trend (smoother for metamorphic clasts), whereas volcanic rock content increases down-core and intrusive rocks are almost constant;

nevertheless, fluctuation of the within-unit trends are common.

(a) Clasts of igneous intrusive rocks include foliated and unfoliated biotite  $\pm$ hornblende monzogranite (pink and grey varieties), foliated and unfoliated hornblende-biotite quartz-diorites, gabbro and minor alkali feldspar syenite, tonalite and quartz-monzodiorite. Monzogranite and quartz-diorite are comparable to those described previously. Gabbros are similar to those present in LSU 4, but occasionally the mineral assemblage is also characterised by the presence of euhedral/subhedral orthopyroxene or olivine. Tonalite is medium- to coarse-grained, consisting of subhedral plagioclases associated with biotite lamellae, interstitial quartz and occasionally clinopyroxene, partially to completely replaced by Ca-amphibole. The tonalites are usually characterised by solid-state deformational microstructures and by a strong alteration. Quartz-monzodiorite is medium-grained, ophitic, composed of euhedral plagioclase, biotite and hornblende included within anhedral K-feldspar and quartz.

(a) Clasts of metamorphic rocks consist of biotite monzogranitic orthogneiss (usually leucocratic and sometimes showing mylonitic texture), marble, gneiss, schist, low-grade metasediment and rare quartzite and metaporphry. Gneiss is fine- to medium-grained, granolepidoblastic, consisting of interlobate quartz and plagioclase associated with isoriated flakes of biotite or white mica; mylonitic and porphyroclastic textures are also common. Schist is similar to that present in LSU 4. Quartzite is fine-grained, granoblastic, composed of subpolygonal quartz aggregates sometimes associated with idiomorphic clinozoisite and chlorite. Low-grade metasediments include biotite metasiltsstones/phyllites, biotite-white mica metasandstone, white mica-biotite metaconglomerate and white mica-biotite metacalcarenite. Metaporphry is similar to those present in LSU 4.

(c) Gabbro and dolerite clasts are common in this unit and their grain size varies from fine- to medium-grained, showing a texture ranging from hypidiomorphic to allotriomorphic (e.g., AND-2A 270.46 and 279.56 mbsf). They are composed of plagioclase, clinopyroxene,  $\pm$ orthopyroxene,  $\pm$ potassium feldspar,  $\pm$ quartz,  $\pm$ biotite,  $\pm$ amphibole and opaque oxides.

(c) Volcanic clasts in LSU 5 are dominated by porphyritic, poorly-vesiculated lava with lesser amounts of highly vesiculated to scoriaceous lapilli and rare pumice. The appearance of scoria and the scarcity of pumice and 'armored lapilli' distinguish LSU 5 from LSU 4. Compositionally, the lavas consist mostly of mafic, followed by intermediate and felsic, varieties that are similar in their mineralogical assemblage as the clasts noted in the previous lithostratigraphic units. Intermediate lava clasts are characterised by having plagioclase and minor clinopyroxene as phenocrysts within an interstitial hypohyaline groundmass with microlites of plagioclase, clinopyroxene and magnetite in glass (e.g., AND-2A 241.63, 287.00 mbsf). Felsic

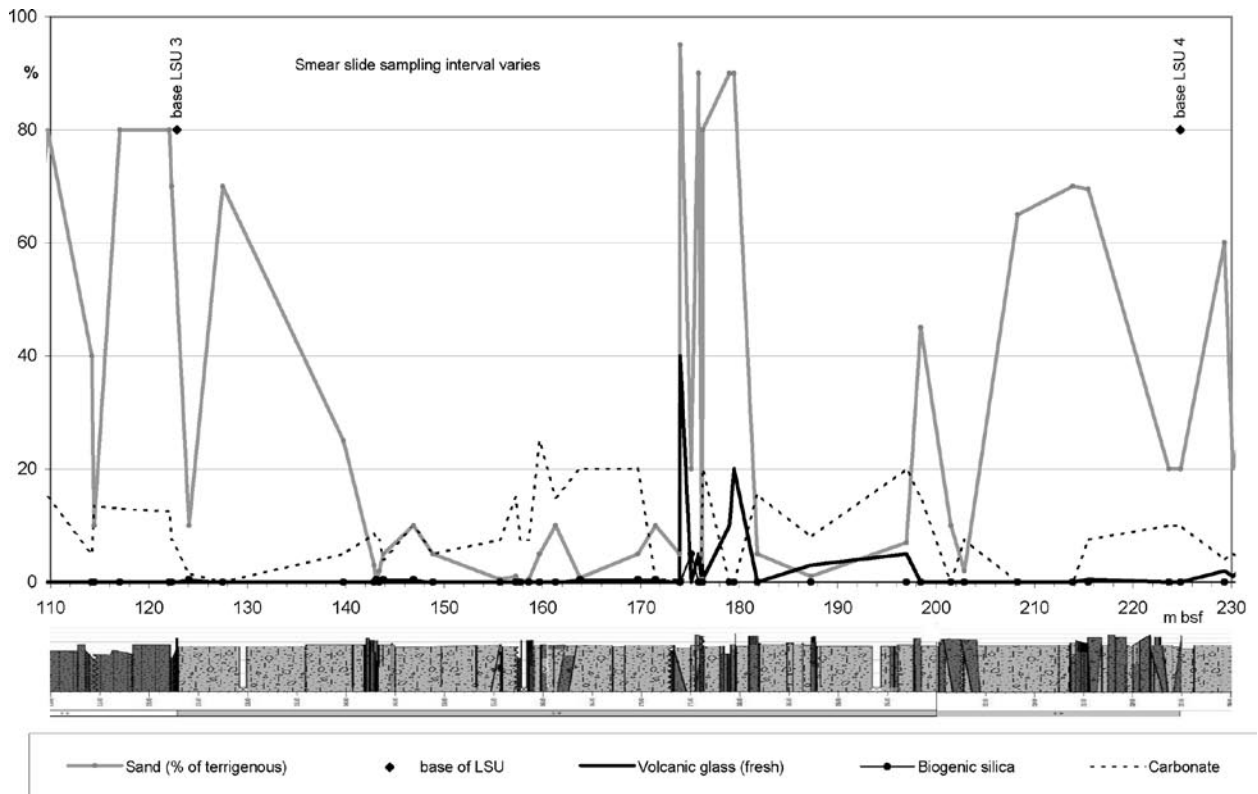


Fig. 8 – Core compositional features in LSU 4 based on smear slides.

lava clasts show a pilotaxitic texture, containing few K-feldspar phenocrysts in a hypocrySTALLINE groundmass composed of K-feldspar and clinopyroxene microlites (e.g., AND-2A 227.76 mbsf).

(c) A different type of volcanic clast occurs at 249.73 mbsf; it is a round-shaped lapilli tuff composed of 1 to 2 mm-sized vesiculated grains made of altered glass and microphenocrysts of plagioclase cemented by an ash matrix. Vesicles are filled by calcite. Numerous ( $n > 100$ ), small ( $< 1$  cm) subrounded to angular clasts of scoriaceous lapilli and ash occur within the interval 248 to 285 mbsf, predominantly in sandy diamictite, and three small ( $\leq 1$  cm) clasts of volcanic breccia are found at 235.585, 285.11 and 285.24 mbsf. The breccia contains intraclasts of black and red scoria supported within a fine-grained matrix.

(c, d) The alteration of crystals and glass within volcanic clasts is similar to that previously described for LSU 4. In some cases vesicles are partially or completely filled with secondary minerals (i.e. amygdaloidal). The most frequent alteration mineral is calcite, followed by chlorite and clay minerals (i.e. palagonite). Calcite occurs in the fractures and forms pseudomorphs of primary minerals (e.g., lava sample AND-2A 227.76).

(d) The fine groundmass of the diamictite is a combination of a matrix of clay and carbonate cement and ranges from 15 to 60% of the rock. Carbonate cement is ubiquitous, often coarsely crystalline and may occur in veins. Deformation structures are often more highly cemented than the adjacent clay-rich enclaves. Carbonate shell fragments and foraminifera are present in 1/3 of the samples. Quartz grains (12-50%) are dominantly monocrystalline and can

make up as much as 50% of the sandy stratified diamictite. Feldspar (8-15%) occurs as single crystal grains and includes both plagioclase and K-feldspar. The K-feldspar is generally heavily altered to sericite, whereas the plagioclase varies from unaltered- to altered- to sericite or calcite. In some samples, the alteration is so complete that it can be difficult to distinguish altered plagioclase from marble or spar. Heavy minerals include pyroxene, amphibole, biotite and chlorite. Lithics continue from above as a mixture of basement and epiclastic volcanic including marble, granite, schist, dolerite, metasandstone, metagranite, basalt and brown glass. In one sample the biotite and chlorite are interfoliated (e.g., AND-2A 270.41 mbsf) and it is common to have either biotite or chlorite in the metagranite. The glass and microcrystalline basalt ranges from unaltered (1-10%) to hydrated to variably devitrified to opaques, zeolite, limonite/hematite, or chlorite/glaucanite.

(d) Fresh volcanic glass and biogenic silica are present in smear slides throughout most of this LSU (Fig. 9). Four main peaks in biogenic silica occur, all within diamictite units, and diatoms are present in nearly all diamictites except near the top of this LSU. The peaks in biogenic silica are not spikes but rather show incremental buildup and decline in abundance. The two largest peaks coincide with intervals of lower and more constant interval velocity and of less sandy matrix. There appears to be an increase in sand up-section in diamictite matrix from 277 to 265 mbsf. Carbonate is generally less than 5%.

(e) Geochemical Unit 5 (224.82 – 296.34 mbsf): the boundary between LSU 4 and 5 is very pronounced for most of the elements. Chlorine (Cl) values increase

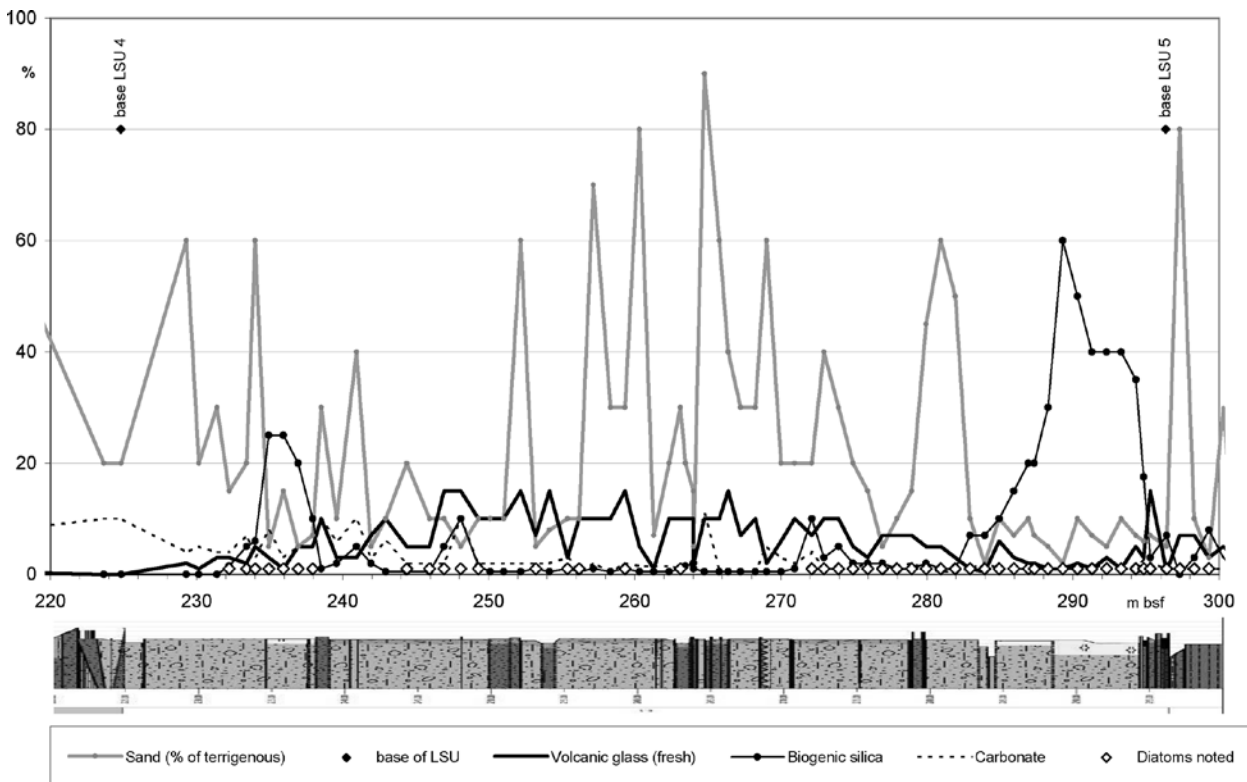


Fig. 9 – Core compositional features in LSU 5 based on smear slides.

whereas Fe, Si, Ca and K decrease to lower values. All of these elements show moderate variations down core. Barium (Ba) remains high at this boundary and shows a minimum directly below the boundary. A second minimum is obvious directly at the boundary with LSU 6.1 (Fig. 3).

(f) The occurrence of both intermediate and felsic compositions in lava clasts from the diamictite observed petrographically is confirmed by XRF major element analyses. Two out of the three analysed lava clasts have basaltic trachyandesite composition (AND-2A 278.69 and 287.00 mbsf), whereas one is a peralkaline rhyolite of comendite type at 227.76 mbsf (Fig. 2).

#### **Lithostratigraphic Unit 6 (296.34–339.92 mbsf)**

LSU 6 is composed of diamictite, diatomite, conglomerate, fine-grained sandstone, siltstone and claystone.

(a) The average clast content is c. 63 per metre. The gravel fraction is dominated by intrusive and volcanic rock, followed by intraformational clasts, metamorphic rock and minor quartz and dolerite. Total number of clasts increases down-core. Quartz is randomly present throughout the unit, whereas all other lithological groups show fluctuating trends, usually smoothly decreasing down-core. Clasts range from granule to pebble grain size, with only one cobble from intrusive rock present.

(a) Clasts of igneous intrusive rocks mainly consist of grey and pink biotite monzogranite (foliated and unfoliated varieties), with minor gabbro and rare tonalite, similar to those previously described. Metamorphic rocks include biotite monzogranitic

orthogneiss (occasionally mylonitic), gneiss, biotite schist, granofels, quartzite, marble and sporadic low-grade metasediment. One orthogneiss is characterised by the presence of clinopyroxene relics. Gneisses are usually biotite-rich, sometimes showing garnet idioblasts or Ca-amphibole and clinopyroxene in the mineral association. Granofels are similar to those present in LSU 4, but one sample is also characterised by the occurrence of garnet subidioblasts.

(c) Clasts of dolerite, as in the previous units, are fine- to medium-grained, showing textures ranging from hypidiomorphic to allotriomorphic (e.g., AND-2A 330.09 and 338.98 mbsf). Dolerite is composed of plagioclase, clinopyroxene,  $\pm$ orthopyroxene,  $\pm$ potassium feldspar,  $\pm$ quartz,  $\pm$ biotite,  $\pm$ amphibole and opaque oxides.

(c) The compositional distribution of volcanic clasts in LSU 6 is similar to LSU 5, consisting primarily of moderately vesicular porphyritic mafic lavas and subordinate intermediate compositions. Felsic lavas are rare. Scoria clasts, which were prominent in LSU 5, are rare in LSU 6 and seven lapilli-sized clasts are found within sandy diamictite at a depth of 331.30 to 331.90 mbsf. One pumice lapilli clast was identified at 309.91 mbsf within the same lithology. Petrographic examination of mafic porphyritic lava clasts (e.g., AND-2A 329.71 mbsf) shows interstitial textures with phenocrysts of clinopyroxene and plagioclase. The groundmass is formed by clinopyroxene, plagioclase, glass and oxides. Intermediate lava clasts show interstitial textures with rare plagioclase and clinopyroxene phenocrysts (e.g., AND-2A 341.00 mbsf). Felsic lava clasts have pilotaxitic textures and contain K-

feldspar phenocrysts in a hypocrystalline groundmass composed of K-feldspar and clinopyroxene microlites (e.g., AND-2A 307.90 mbsf). Felsic lava (AND-2A 307.06 mbsf) shows colour-banding and has a hyalopilitic texture with K-feldspar and clinopyroxene phenocrysts.

(c, d) The alteration of volcanic clasts in LSU 6 is similar to what has been observed in the previous units and consists of primary phases being replaced by secondary minerals, most frequently calcite, and as in-fillings of vesicles and fractures. Other alteration minerals include zeolite, chlorite and clay minerals (i.e. palagonite).

(d) Smear slide data on sandstone, siltstone and claystone lithologies show an up-section increase in biogenic silica (spicules and marine diatoms) from less than 5% to over 90% from c. 312 to c. 310 mbsf (Fig. 10). Less biogenic silica was noted in mudstone around 337 mbsf than in those near the top of the LSU, suggesting differing sedimentation rates or degrees of biosiliceous productivity between the lower and upper parts of the LSU (Fig. 10). There is a rapid increase of diatom abundance from c. 313 to 311 mbsf, just above the peak in fresh volcanic glass. Volcanic glass content reaches over 10% near the base of LSU 6 but decreases gradually up-section in the lower third of the unit. Sandy diamictite in this LSU coincide with zones of higher interval velocities. Carbonate content from smear slides is generally less than 5% and is lower than that recorded in thin sections from this LSU.

(d) Sandy diamictite has a microcrystalline calcite cement ranging from 10 to 20% vol. Unaltered glass is present in all samples (c. 1%) and includes both brown and clear varieties, rounded to cusped and vesicular.

Trace amounts of shell fragments are also present. Quartz makes up c. 25 to 40% of the framework grains. It is dominantly monocrystalline but may contain some large polycrystalline grains. The monocrystalline grains may be either subangular-subrounded or very well rounded with remnant quartz overgrowths. Feldspar includes both K-feldspar and plagioclase (30-43%) and is generally altered to sericite although some plagioclase is unaltered. Heavy minerals include pyroxene, biotite, amphibole, olivine(?) and chlorite with pyroxene dominant (3-4%). Pyroxene is large and clear to slightly pleochroic green/brown. Lithics make up only a minor proportion of the framework grains (5-15%) and include biotite granite, dolerite, schist, metasandstone, marble and basalt with dolerite and granite dominant. The proportion of volcanic lithics decreased significantly from overlying LSUs, and quartz increases.

(d) Interbedded sandstone contains 40% quartz (many monocrystalline and well-rounded with overgrowths), 30% K-feldspar, 20% plagioclase and only 3% lithics of basalt and brown glass altered to zeolite and chlorite/glaucanite. Unaltered cusped brown volcanic glass makes up >2%. Pyroxene, amphibole, chlorite and biotite make up 3% with pyroxene dominant. There are trace amounts of foraminifera. Cement is again secondary microcrystalline calcite and opaques.

(d) The diatomite (80% matrix) with dispersed grains contains up to 7% unaltered brown glass, often cusped and vesicular. Dispersed grains include quartz (5%), feldspars (3%), heavy minerals (1%), lithics of primarily basalt (3%) with trace of granite, metasediment and schist.

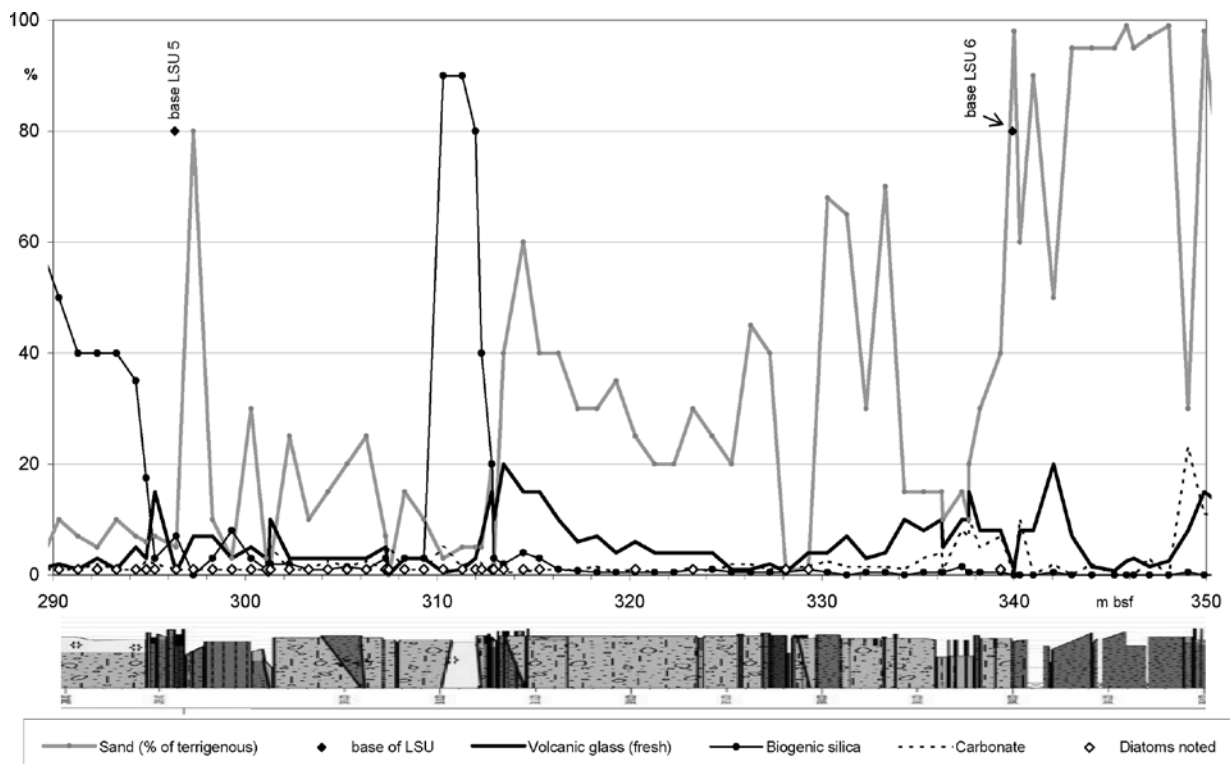


Fig. 10 – Core compositional features in LSU 6 based on smear slides.

(e) **Geochemical Unit 6** (296.34 – 339.92 mbsf): Chlorine (Cl) reaches maximum values in this LSU. The mean levels and the fluctuation pattern of Fe, Si, Ca and K are similar to LSU 5 (Fig. 3). Barium (Ba) values drop to a distinct minimum in the diatomite at 312.30 mbsf, but remain high elsewhere in this LSU.

**Lithostratigraphic Unit 7** (339.92–436.18 mbsf)

LSU 7 consists of volcanic-bearing diamictite and sandstone.

(a) LSU 7 has an average clast content of 122 per metre, with the total number of clasts significantly increasing down-core. Clasts are mostly represented by volcanic rocks, followed by intrusive rocks and minor dolerites, quartz, metamorphic rocks, sedimentary rocks and intraclasts. Both intrusive and metamorphic rock contents are characterised by a down-core decreasing trend, whereas dolerite increases down-core and volcanic rock is almost constant. Gravel fraction includes granules, pebbles, with only minor cobbles of dolerite, intrusive and metamorphic rock.

(a) Clasts of igneous intrusive rocks include grey and pink biotite monzogranite (foliated and not, sometimes carrying K-feldspar megacrysts), biotite-hornblende granodiorite (foliated and not), clinopyroxene gabbro and minor porphyry and biotite syenogranite. Both felsic and intermediate porphyry occurs, with porphyritic texture characterised by up to mm-sized subhedral phenocrysts set within a fine-grained groundmass. Felsic porphyry has monzogranitic composition, with biotite, quartz and feldspar phenocrysts, whereas mafic varieties are monzonitic, with phenocrysts of hornblende, biotite, clinopyroxene and plagioclase. Metamorphic rocks consist of biotite ± white mica orthogneiss (syenogranitic to monzogranitic in composition, sometimes leucocratic and with mylonitic texture), gneiss/granofels, schist, marble, low-grade metasedimentary rock and minor mylonitic felsic metaporphyry and quartzite. Gneiss is similar to those present in LSU 6, whereas schist includes either biotitic (Fig. 4f) or amphibolic varieties. Low-grade metasediment consists of white mica-biotite-calcite metasiltstone, biotite metasandstone and metalimestone.

(b) Sedimentary clasts are comprehensive of conglomerate intraclasts, quartz arenite and subarkose (e.g., Fig. 5). They are all enclosed in stratified diamictite facies beds. A conglomerate intraclast (AND-2A 382.56 mbsf) has irregular shape and not well defined rims. Texturally, the clast is subdivided in two matrix-supported portions, a smaller one richer in muddy matrix and a wider one richer in clasts. These last range from 0.4 to 6.5 mm in size and are well-rounded to angular. Matrix is composed of clay minerals and microcrystalline calcite. Locally, microcrystalline calcite cement may dominate the interstitial spaces. Clast assemblage includes monocrystalline and polycrystalline undulose and non-undulose quartz, K-feldspar, plagioclase, intrusive rock, basalt, metamorphic rock, pyroxene

and calcite. Well-rounded quartz grains often preserve remains of quartz overgrowths.

(b) Clasts of sandstone are quartz arenite (AND-2A 399.16 mbsf) and subarkose (AND-2A 404.86 mbsf). They are subangular in roundness. The texture is characterised by a moderate- to well-sorting, lacking of matrix; cement is formed by quartz overgrowths. Grain size corresponds to medium-coarse sandstone. Grains are lightly oriented, with tangential and partially interpenetrated contacts, with high grade of packing; sometimes a light grading is present. Compositional assemblage includes dominant well-rounded undulose quartz grains, with well developed overgrowths and very subordinate altered grains; locally clay minerals cement is present. Subarkose is characterised by quartz and subordinate altered feldspar.

(c) Volcanic clasts in LSU 7 include lava and scoria with minor amounts of pumice and volcanic breccia. The dominant type of volcanic clasts in this unit are small (c. <5mm), highly vesicular (scoriaceous) coarse ash and lapilli that occur throughout the unit but are more highly concentrated within two depth intervals: between 354 and 358 mbsf and between 415 and 425 mbsf (c. 14 scoria clasts per metre). Both intervals of higher scoria concentration occur in sandy diamictite. Lava clasts within LSU 7 are up to 6 cm in longest dimension but most are less than 2 cm. Texturally the lavas range from non-vesicular to vesicular and amygdaloidal with aphanitic to moderately porphyritic (feldspar- and pyroxene-phyric) grain sizes. Compositionally the lavas consist of mafic, intermediate and felsic varieties. The greater proportions of felsic and intermediate compositions, as well as the high abundance of scoria, distinguish this unit from LSU 6. One dark greenish-grey (mafic?) lava clast (AND-2A 409.18 mbsf) is banded with black zones that exhibit crenulated margins, suggesting magma comingling (Fig. 6). Intermediate lava clasts (e.g., AND-2A 358.11 mbsf) have pilotaxitic textures with rare plagioclase phenocrysts. Felsic lava clasts show pilotaxitic textures with plagioclase ± clinopyroxene microphenocrysts. Scoria lapilli and ash are composed of highly vesiculated light brown glass with rare microphenocrysts of feldspar (e.g., AND-2A 356.28, 377.71 and 420.38 mbsf). Many of the scoria clasts have very irregular shapes, which indicate minimal reworking. Pumice clasts are less frequent (e.g., AND-2A 339.59 mbsf) and show a light glassy groundmass characterised by long tube vesicles and rare K-feldspar crystals (e.g., AND-2A 399.57 mbsf). The intensity and type of alteration appear to be the same as observed in previous units.

(d) Biogenic silica content in smear slides of fine-grained sized fractions is generally low in LSU 7 except near the base (where it reaches 20% within a 6 m interval) and intermittently at c. 25 m spacings up-section where it locally reaches c. 5 to 10% (Fig. 11). Biogenic silica is present at background levels through most of the unit, though diatoms occur more commonly in the lower half. Biogenic silica increases up-section in the lower half of the

diamictite centred on 422 mbsf, then decreases in the upper half of the unit. Percent sand varies greatly within the unit but there are three intervals in which the amount of sand matrix within diamictites appears to have trends up-section. Fresh volcanic glass is present throughout the unit but abundances trail off up-section in the lower part. There is a peak in fresh glass around 354 mbsf. The carbonate content is variable but generally up to 20%.

(d) The diamictite sampled is a sandy diamictite with only 13% matrix of clays and altered feldspars, overprinted with a microcrystalline calcite cement. Calcite veins are also present. There are trace amounts of shell fragments. Unaltered vesicular brown glass makes up 1%. Quartz (35%) is mostly monocrystalline, some subangular and some well-rounded with quartz overgrowths. Feldspar (40%) includes both K-feldspar and plagioclase, both mostly altered to sericite. Heavy minerals (3%) are dominated by large clear pyroxene with minor olivine and chlorite. Opaques, with some identifiable hematite, make up 3% of the rock. Lithics make up only 5% of the total and include altered basalt, biotite granite, schist, dolerite and metasandstone.

(d) The sandstone is moderately well-sorted and dominated by quartz-feldspar (feldsarenite). Cement ranges from blocky calcite to non-existent in highly porous sandstone. Unaltered vesicular brown to clear glass is c. 1 to 2%. Quartz is monocrystalline and either well rounded with overgrowths or subangular. Feldspar (25-30%) is primarily plagioclase, some unaltered and some sericitized. Heavy minerals (2-20%) are dominated by large clear pyroxene with minor amphibole, olivine and biotite. The sample with 20% heavy minerals is enriched in pyroxene.

Lithics make up 8-20% and are dominated by basalt and dolerite with minor metasandstone.

(d) The fossiliferous mudstone is 80% matrix composed of clays and altered brown glass. Bioclasts (3%) include bryozoans and foraminifera. Large unaltered brown glass (5%) is non-vesicular. Quartz (5%) is half monocrystalline and half polycrystalline. The plagioclase (3%) is altered to sericite. Lithics are dominated by brown glass altering to zeolite, followed by basalt, dolerite and granite lithics. Heavy minerals (1%) are an even mix of pyroxene and biotite.

(e) Geochemical Unit 7 (339.92 – 436.18 mbsf): LSU 7 is divided into two geochemical subunits that are characterised by two repeating cycles of geochemical pattern, which are typical for this LSU: Geochemical Unit 7.1 (339.92–389.03 mbsf) and Geochemical Unit 7.2 (389.03 – 436.18 mbsf). The lower cycle (GU 7.2) extends from the base of the unit up to the base of a diamictite at 389.03 mbsf. It has high Cl and moderately high Fe values that drop to minima at 398.25 mbsf at a boundary of a diamictite to coarse sandstone. A comparable Fe minimum is observed at the top of this LSU from 349 mbsf upwards (Fig. 3). Calcium (Ca) values are highly variable in the whole LSU and partially show high frequency stacked cyclicity. A clear difference between the sandstone and diamictite lithologies is missing. Silica (Si) and especially K counts are clearly increased in the sandstones at the top of each of these two cycles. Barium (Ba) values differ from these patterns. They show the biggest gradient at 398.25 mbsf at the base of the lower sandstone, where they increase from mean medium high levels to mean high levels above. This change is very pronounced and the values above and below remain for more than 100 m. Therefore,

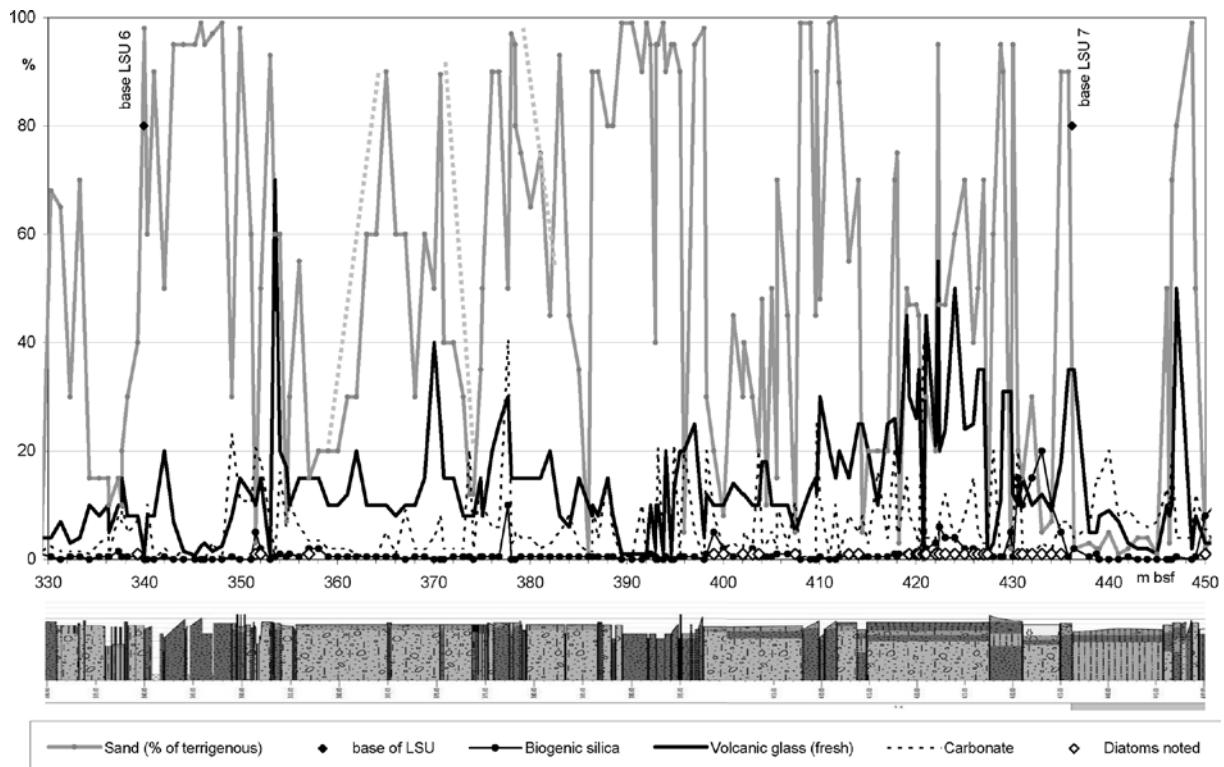


Fig. 11 – Core compositional features in LSU 7 based on smear slides. Dotted grey lines highlight trend in sand data.

one more geochemical subunit boundary could have been set at 398.25 mbsf. The highest Ba content in the core is noted in weakly-consolidated pebbly sand from 353.07 to 353.14 mbsf (Fig. 3).

(f) One centimetric lava clast from the diamictite (AND-2A 374.05 mbsf) shows trachyte composition after XRF major element analysis (Fig. 2).

### **Lithostratigraphic Unit 8.1**

(436.18–502.69 mbsf)

LSU 8.1 consists of volcanic-bearing mudstone with or without dispersed clasts, sandstone and diamictite.

(a) This subunit has an average content of 68 clasts per metre and is characterised by the largest variability in clast dimension, with diffused cobbles of dolerites and intrusive rocks and some dolerite boulders present within diamictite lithofacies (including the biggest clast, 41.86 cm). The gravel fraction consists of volcanic rocks, dolerites and intrusive rocks dominating over metamorphic rocks, quartz, intraformational clasts and sedimentary rocks. The total number of clasts increases down-core. All clast lithology contents are characterised by fluctuating trends coincident with the alternation of different lithofacies within the lithostratigraphic subunit; moreover, both quartz and metamorphic rocks are discontinuously present.

(a) Similar to overlying lithostratigraphic units, intrusive igneous rocks are dominated by grey and pink biotite monzogranites (foliated and not), with minor occurrences of probable felsic to intermediate porphyry, gabbro/diorite and foliated granodiorite/tonalite (to be sampled). Metamorphic rocks include biotite monzogranitic orthogneisses (sometimes with mylonitic textures), biotite ± Ca-amphibole gneiss, biotite or Ca-amphibole-clinopyroxene schist, clinopyroxene granofels, marble and low-grade metasediment (biotite metasandstone).

(b) The sedimentary clast sampled from LSU 8.1 (AND-2A 484.77 mbsf) is a well-rounded and non-spherical clast, of mud-supported marly biomicrite (wackestone), rich in microfossils. The texture is characterised by a light orientation of the fossils, which make faint lamination. Scattered siliciclastic angular grains of non-undulatory monocrystalline quartz, so as feldspar and mica, are present. These are very small in grain size (max coarse silt). Rare and small green grains, resembling glauconite, are also present.

(c) Volcanic clasts in LSU 8.1 include lava and scoria and minor pumice. This subunit contains less scoria relative to LSU 7 but more than LSU 6. The scoria lapilli and ash are concentrated (c. 8 clasts per metre) in the sandy mudstone towards the base of the unit (interval 490–494 mbsf). The scoria was deposited in finer-grained sediment relative to the scoria concentrations in LSU 7, which are associated with sandy diamictite. The scoria clasts are mostly small (<3 mm) but several are >1 cm long (major axis). In thin section, scoria clasts show transparent vesiculated glass with occasionally microlites of

feldspar (AND-2A 491.08 and 493.81 mbsf). Eight small (<3 mm) pumice clasts occur within the same interval. The diversity of lava compositions in LSU 8.1 is similar to LSU 7 in that mafic, intermediate and felsic varieties are identified. Individual lava clasts are up to 6.5 cm in longest dimension but most are less than 2 cm. Texturally the lavas range from non-vesicular to highly vesicular and from aphanitic to moderately porphyritic (feldspar- and pyroxene-phyric). Petrographic analyses of a mafic lava clast show the presence of large phenocrysts of plagioclase and olivine (up to 0.5 mm), clinopyroxene and oxides (AND-2A 486.40 mbsf) in a mafic lava clast, whereas felsic lavas (e.g., AND-2A 440.83 mbsf) show pilotaxitic texture and rare phenocrysts of K-feldspar and altered amphibole.

(d) This unit marks the highest occurrence of black pyrite cement, which appears to coat grains where not pervasively filling all pore space. It is often associated with blocky calcite cement. Where sandstone is very white, feldspars are completely replaced by calcite, otherwise they alter to clay. Sand varies between quartz (7–33%) to feldspar (18–76%) enriched with moderate to low percentage of lithics (2–30%). Lithics are dominated by either biotite granite and metasandstone or basalt altered to opaque-chlorite. Schist, dolerite, dolostone and glass altered to zeolite or opaques make up the rest. Other minerals (2–10%) include biotite, chlorite, amphibole, two types of pyroxene and abundant opaque minerals. Blocky brown and vesicular white glass is present in low amounts (trace to 5%). Bioclasts (trace) include sponge spicules, foraminifera and bryozoans.

(c) Biogenic silica is present in smear slides throughout most of this unit, with a peak around 460 mbsf, followed by a decrease, then a gradual rise through a sandstone unit up into a mudstone around 450 mbsf (Fig. 12). There is little biogenic silica in the thick mudstone centred on 440 mbsf, though there is a possible increase near the top. There is a clearer increase up-section in biogenic silica in the lower mudstone centred at 493 mbsf. No clear trends in percent sand within units within this LSU are apparent from the smear slide data. Volcanic glass is present at low levels throughout but is perhaps more abundant near the base and top of the LSU and there is a spike around 447 mbsf.

(e) **Geochemical Unit 8.1** (436.18–489.66 mbsf): (see LSU 8.4 for Geochemical Unit description).

### **Lithostratigraphic Unit 8.2**

(502.69 - 544.47 mbsf)

LSU 8.2 is composed of volcanic-bearing diamictite, mudstone with/without dispersed clasts and sandstone.

(a) In LSU 8.2 the average clast content is 95 per metre, increasing down-core. Volcanic rock dominates over intrusive rock, dolerite, metamorphic rock, intraformational clasts and quartz, the sedimentary rocks being only a minor occurrence. Quartz and metamorphic rocks discontinuously occur throughout

the core, whereas volcanic rock content increases down-core. Intrusive rocks and dolerite show smoothly decreasing trends down-core. The gravel fraction is mostly represented by granules and pebbles, with minor cobbles of metamorphic rock and dolerite.

(a) Both clasts of igneous intrusive and metamorphic rocks are similar to those present in LSU 8.1. Porphyry is more diffuse, including also mylonitic metamorphic varieties. Orthogneiss also includes syenogranitic and granodioritic composition. Gneiss is sometimes characterised by layering and mylonitic textures and marbles are usually impure. Low-grade metasediment include phyllite. Quartzite is present.

(b) Sedimentary clasts include quartz arenite and subarkose (e.g., Fig. 5), with similar features to those of LSU 7.1. They are subangular- to- sub-rounded. Subarkose (AND-2A 511.47 mbsf) is medium in grain size, and its texture is clast-supported without matrix and moderate to well sorting. Internal clasts are subangular- to- sub-rounded. Grain assemblages essentially consist of monocrystalline quartz (rarely polycrystalline) with quartz overgrowths, with the adding of subordinate plagioclase and K-feldspar. The contacts among quartz clasts are tangential or interpenetrated, to outline a high grade of packing and orientation. Cement is mainly quartz with subordinate blocky/micrite calcite and phyllosilicate. Quartz arenite clast (AND-2A 530.31 mbsf), coarse in grain size, differs from the above subarkose, for the composition (only quartz grains) and for the well-sorting. Moreover, the internal clasts are rimmed by quartz overgrowths and contacts are linear, tangential and interpenetrated. Interstitial spaces are filled by

microcrystalline/sparry calcite cement. Quartz grains are mainly monocrystalline with undulose extinction, subordinately polycrystalline; very rare feldspar grains are present.

(c) Volcanic clasts in LSU 8.2 include lava and scoria and minor pumice. In this subunit ash- and lapilli-sized scoria are concentrated (c. 20 per metre) in finer-grained lithologies (clayey siltstone, sandy mudstone and muddy diamictite) over a broad interval at the base of the unit (538-544 mbsf). The largest scoria clasts reach 8 to 9 mm (long axis). They have similar petrographic features to some previous scoria samples (AND-2A 529.12 and 530.47 mbsf) and are variably altered, having vesicles filled by secondary minerals such as chlorite. Five small (<4 mm) pumice clasts occur within a 5 cm interval between 530 and 531 mbsf. Dark-cored, white-rimmed lava clasts (Fig. 6A), each ≤1 cm in dimension, occur between 531 and 534 mbsf and are similar in appearance to the 'armored lapilli' described in LSU 5. Lava compositions in LSU 8.2 range from mafic to intermediate to felsic. Clasts are on average smaller than those in LSU 8.1 with most having a long axis of less than 1 cm but reaching a maximum of 2.8 cm. Texturally, the lava ranges from non-vesicular to highly vesicular and from aphanitic to moderately porphyritic (feldspar- and pyroxene-phyric).

(d) Diamictites groundmass (42-68%) contains clays and microspar but little blocky calcite cement except as infill in vesicles in scoria grains. Bioclasts (tr) include serpulid tubes, sponge spicules, foraminifera and shell fragments. There is a very high percent of unaltered glass (20-25%) composed of three different colours as proxies for composition: brown

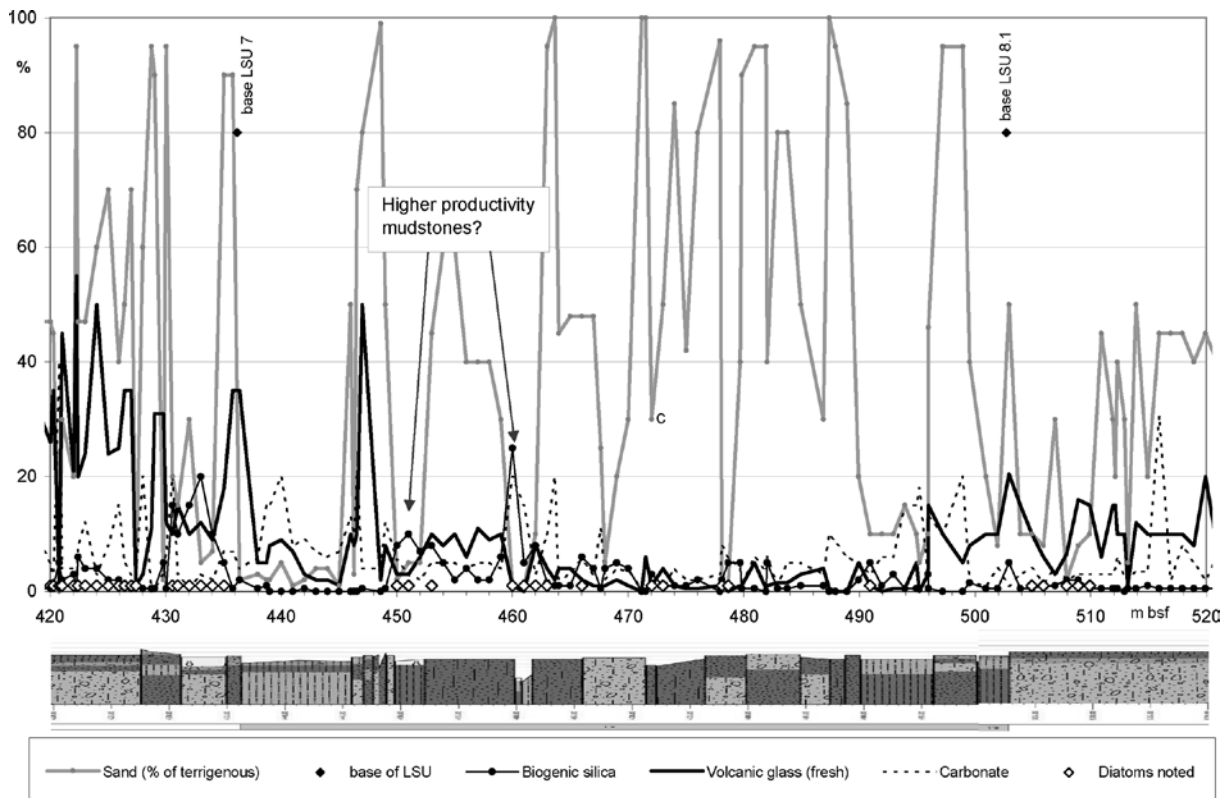


Fig. 12 – Core compositional features in LSU 8.1 based on smear slides.

(vesicular, blocky, with plagioclase crystals), white (vesicular, tubular) and green (vesicular, tubular). Quartz (5-25%) is monocrystalline, subangular-to-well-rounded; feldspars (3-10%) are both K-feldspar and plagioclase generally altered to sericite. Lithics (10-15%) are dominated by basalts altered to opaques-chlorite or glass altered to opaques, zeolites or calcite depending on chemical composition. Dolerite, metasandstone, schist, marble and granite are also present. Other minerals (2-4%) include two types of pyroxene, biotite, muscovite, chlorite and opaques.

(d) Smear slide estimates indicate low percentages of matrix sand in the lower diamictites (Fig. 13). There is four times the sand content in the matrix of the top diamictite and the proportion of sand appears to decrease up-section within it. Biogenic silica is present in parts of each of the three main units of diamictite. The amount of fresh volcanic glass is less in the sandy interval near the middle of this LSU.

(e) Geochemical Unit 8.2 (489.66 – 530.13 mbsf): (see LSU 8.4 for Geochemical Unit description).

### **Lithostratigraphic Unit 8.3** (544.47 - 579.33 mbsf)

LSU 8.3 consists of volcanic-bearing sandstone, conglomerate, mudstone with dispersed clasts and diamictite.

(a) The average clast content in LSU 8.3 is 162 per metre and is characterised by a fluctuating trend, with a maximum of c. 1 000 clasts per metre within sandy conglomerate lithofacies (563.88 - 566.45 mbsf). The gravel fraction consists mostly of volcanic rocks, largely dominating over intrusive rocks, with discontinuous

occurrences of dolerite, quartz, metamorphic rocks, intraformational clasts and sedimentary rocks. Clast dimensions usually range from granule to pebble size, with minor cobbles of dolerite, intrusive and volcanic rocks. Intrusive and metamorphic rocks are similar to those present in LSU 8.1, except for the absence of granodiorite/tonalite and granofels and the occurrence of a tonalitic orthogneiss.

(b) Sedimentary clasts, enclosed in non-diamictite facies, consist of arkose (e.g., Fig. 5) and volcanoclastic rudite/conglomerates. Volcanoclastic rudite/conglomerate (AND-2A 556.56 mbsf) is mainly composed of well-rounded lithic volcanic fragments, granule-fine pebble in size. They are altered and characterised by glassy groundmass with plagioclase phenocrysts. Clasts may be totally altered or unaltered, sometimes with groundmass and subrounded vesicles. Subordinately, minor smaller grains of basalt, plagioclase, pyroxene, quartz and K-feldspar are present. Arkose (AND-2A 557.89 mbsf) is medium-coarse in grain size, the texture is clast-supported lacking of matrix, and a light orientation and grading of the clasts are observable. The cement is formed by quartz overgrowths, clay minerals and calcite also as patches. The grain assemblage consists of quartz, plagioclase, K-feldspar and rare mica. Quartz grains are monocrystalline with both light and strong undulose extinction, and polycrystalline. K-feldspar is present as orthoclase and microcline with evident alteration. Rare small white mica is also present.

(c) Volcanic clasts in LSU 8.3 include lava and scoria. In LSU 8.3 ash and lapilli-sized scoria are concentrated (c. 17 per metre) within sandy diamictite and sandy mudstone over a short interval in the lower

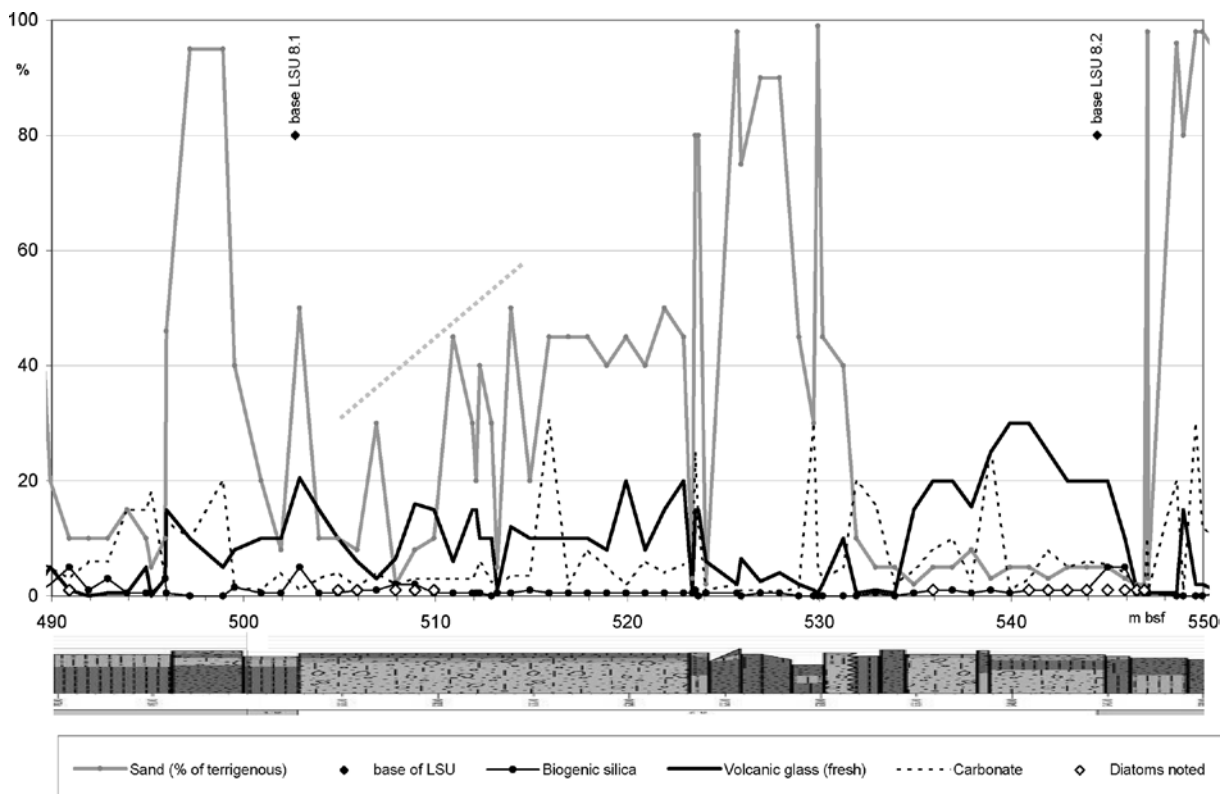


Fig. 13 – Core compositional features in LSU 8.2 based on smear slides. Dotted grey line highlights trend in sand data.

third of the unit (566 – 568 mbsf). This subunit has less scoria than LSU 8.2 but more than LSU 8.1. The scoria clasts are subrounded to very angular and have a maximum dimension of 1cm but most are less than 3mm. Several small (<6 mm) fragments of black glass occur around 570 mbsf and one small (<3 mm), altered pumice clast is found at 546.24 mbsf. Lava clasts are similar in composition and texture to those in LSU 8.1 and 8.2, ranging from mafic to felsic, aphanitic to porphyritic and non-vesicular to vesicular. Mafic lavas are porphyritic with plagioclase and clinopyroxene phenocrysts in a glassy interstitial groundmass (e.g., AND-2A 555.81 mbsf). Felsic lavas show pilotaxitic texture and rare K-feldspar and clinopyroxene phenocrysts (e.g., AND-2A 564.87 and 564.92 mbsf).

(d) The pebbly mudstone and siltstone have 42 to 76% matrix of clays with microspar and opaque/pyrite(?) cement. Bioclast component (1%) is varied with serpulid tubes, bryozoans, foraminifera, sponge spicules and bivalve fragments represented. Quartz is the dominant mineral (7-30%) followed by unaltered volcanic glass (2-10%). Feldspar (3-5%) includes plagioclase and K-feldspar. Lithics (2-7%) are dominated by basalt altered to opaques-chlorite-hematite and lesser glass altered to zeolite and glauconite. Minor amounts of metasandstone, chert, dolerite and granite are present. Unaltered glass (2-10%) includes brown, green, white and mingled brown-white and green-white varieties. All are variably blocky, vesicular or tubular. Coarser sandstone is enriched in quartz (<60%) or lithics (<73%) compared to the other components but are otherwise similar in composition. The sandstone enriched in quartz also contains more dolerite and granite clasts relative to altered basalt.

(d) Smear slide data show a rapid increase in fresh volcanic glass near the base of this LSU, tailing off to low levels until near the top of the unit (Fig. 14). There are increases in the amount of biosilica and ?non-biogenic carbonate near the base and top of the unit (though these components do not track together near the top of the unit).

(e) Geochemical Unit 8.3 (530.13 – 551.46mbsf): (see LSU 8.4 for Geochemical Unit description).

#### **Lithostratigraphic Unit 8.4** (579.33-607.35 mbsf)

LSU 8.4 is composed of volcanic-bearing diamictite, siltstone, sandstone and conglomerate.

(a) The average clast content in this subunit is 114 per metre. Clasts are mainly represented by volcanic rocks, with minor intrusive rock, dolerite, metamorphic rocks, quartz and intraformational clasts; sedimentary rocks can be considered almost insignificant. Volcanic rock content increases down-core, whereas intrusive rock content decreases. Both intrusive and metamorphic rocks are similar to those present in LSU 8.1. Quartzite is present, sometimes characterised by a textural layering and by the presence of Ca-amphibole and biotite sub-

idioblasts.

(b) The only sedimentary clast sampled in LSU 8.4 is represented by medium-fine arkose (AND-2A 592.52 mbsf). The clast is not well rounded, with non-spherical shape. The arkose is well-sorted, clast-supported in texture, with moderate orientation of the clasts and moderate packing. Internal grains are from subrounded to subangular. Quartz overgrowths, clay minerals and sparry calcite constitute the cement. Grain assemblage of the rock is represented by monocrystalline and subordinate polycrystalline quartz, plagioclase and altered K-feldspar.

(c) Volcanic clasts in LSU 8.4 include lava, scoria and pumice. Subrounded to very angular ash and lapilli-sized (up to 1.5 cm) scoria occur throughout this subunit but are more abundant (c. 13 per metre) within mudstone near the base (597 – 602 mbsf). Several black non-vesicular glassy fragments occur within the same interval. Pumice is found as dispersed clasts between 597 and 598 mbsf ( $n = 8$ , maximum size = 1.2 cm) and as one minor accumulation at 605.29 mbsf ( $n = 5$ , max = 1.2 cm). The lava clasts are similar in composition and texture to other LSU 8 subunits, ranging from mafic to felsic (e.g., AND-2A 587.19), aphanitic to porphyritic and non-vesicular to vesicular.

(d) Diamictites contain 65-85% matrix composed of clays and very fine volcanic glass altered to zeolite. Unaltered glass (tr-5%) is variable in composition including brown (blocky, vesicular, plagioclase crystals), white (blocky, vesicular) and green (blocky to tubular). Bioclasts (tr-1%) include sponge spicules, diatoms and serpulid tubes. Quartz (6-15%) is monocrystalline and mostly subangular with a few well rounded grains. Feldspar makes up 2-5% of the matrix. K-feldspar is generally altered to sericite, whereas the plagioclase varies between altered and unaltered. Three types of pyroxene are present along with biotite, muscovite, chlorite and possibly tourmaline. Lithics (2-10%) include the usual basalt altered to opaque, brown glass altered to zeolite, dolerite, marble, metasandstone, metalimestone and granite.

(d) Smear slide data for the diamictite unit that comprises most of this LSU might provide clues to its mode of accumulation. Biogenic silica occurs nearly throughout the diamictite and the percentage of sand in the matrix of the central part of the diamictite appears to increase up-section (Fig. 15). The percentage of fresh volcanic glass decreases near the top of the diamictite.

(e) On the basis of the XRF measurements LSU 8 can be divided into 5 GUs:

Geochemical Unit 8.1 (436.18 - 489.66 mbsf), Geochemical Unit 8.2 (489.66 - 530.13 mbsf), and Geochemical Unit 8.3 (530.13 - 551.46 mbsf): these three Geochemical Units have a similar pattern from base to top, with increasing values for Fe, Si, Ca and K. Whilst Si, Ca and K values increase steadily, the Fe values slowly increase in the diamictites and have a minimal value in the sandstone beds above

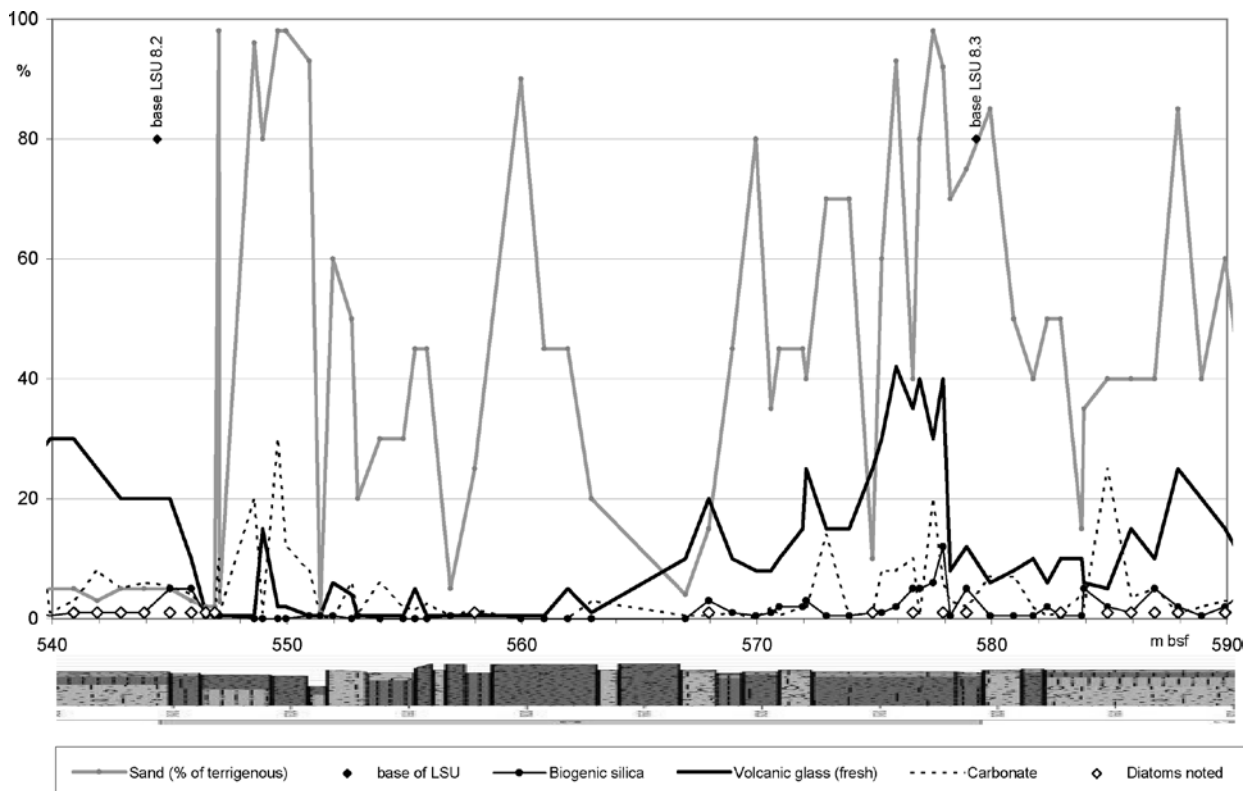


Fig. 14 – Core compositional features in LSU 8.3 based on smear slides.

before reaching maximum levels in the siltstones and mudstones. Chlorine (Cl) and Ba show opposite curve pattern to Fe.

**Geochemical Unit 8.4** (551.46 - 579.33 mbsf): the Fe values increase from the base to a broad plateau of high Fe values between 567 mbsf and the top of this unit (Fig. 3). Potassium has a corresponding pattern, but values scatter as in Ca and Si without such a clear mean trend. Chlorine and Ba, as in the upper units, have an opposite curve pattern to Fe, but with more scattering.

**Geochemical Unit 8.5** (579.33 - 607.35 mbsf): this GU corresponds to LSU 8.4. The general trend of element concentrations in this GU differs from the upper four subunits. Iron (Fe) and Cl decrease slightly from base to top, whereas Si, Ca, K and Ba increase very gradually and show a peak in concentration at the top of this GU.

#### **Lithostratigraphic Unit 9** (607.35-648.74 mbsf)

LSU 9 includes volcanic-bearing sandstone, siltstone and minor diamictite.

(a) The average clast content in this unit is 52 clasts per metre. The gravel fraction largely comprises volcanic rock, with minor intraformational clasts, intrusive rock and discontinuously present dolerite, metamorphic rock, quartz and sedimentary rock. Diamictite and mudstone intraclasts are concentrated within the siltstone with dispersed clasts and volcanic bearing clast-poor sandy diamictite lithofacies (634.79 - 636.91 mbsf). Both the total number of clasts and volcanic and intrusive rock contents are characterised by fluctuating trends. Clasts range from granule to pebble grain size, with only one cobble of dolerite

occurring at the bottom of the unit.

(a) Clasts of igneous intrusive rocks mostly consist of biotite  $\pm$  hornblende monzogranite, with minor hornblende-biotite granodiorite (Fig. 4a) and diorites/quartz-diorite. Monzogranite shows a large variety of textures, ranging from hypidiomorphic (undeformed) to mylonitic (strongly deformed); colours vary from leucocratic/grey to pink/reddish, with the progressive increase of alteration. Metamorphic rocks include biotite orthogneiss and gneiss (sometimes with mylonitic textures), biotite schist, quartzite, Ca-amphibole-biotite-clinopyroxene granofels, impure marble and low-grade metasediment (biotite metasandstone and metasiltstone, metalimestone, phyllite).

(b) Sedimentary clasts are represented by quartz arenite (e.g., Fig. 5) and lithic arkose, dispersed in fine sandstone and mudstone beds. Lithic arkose (AND-2A 612.75 mbsf) is fine in grain size, with moderate-to well-sorting; matrix is very scarce and quartz overgrowths, calcareous and clay minerals cements are present. Internal clasts are subangular to angular, composed (in decreasing order of amount) of quartz, lithic fragments, plagioclase, K-feldspar, muscovite, calcite and opaque minerals. Quartz grains are mainly monocrystalline with slightly undulose extinction and inclusions, rarely are they composite. Feldspar grains are angular, with considerable grade of alteration (sericitization and vacuolization). Fine-texture lithic fragments are comprehensive of metamorphic rocks and very deeply altered volcanic grains. Muscovite grains are small and rare. Calcite occurs as clastic recrystallized grains, but also as patches. Quartz arenite (AND-2A 615.08 mbsf) is medium-coarse

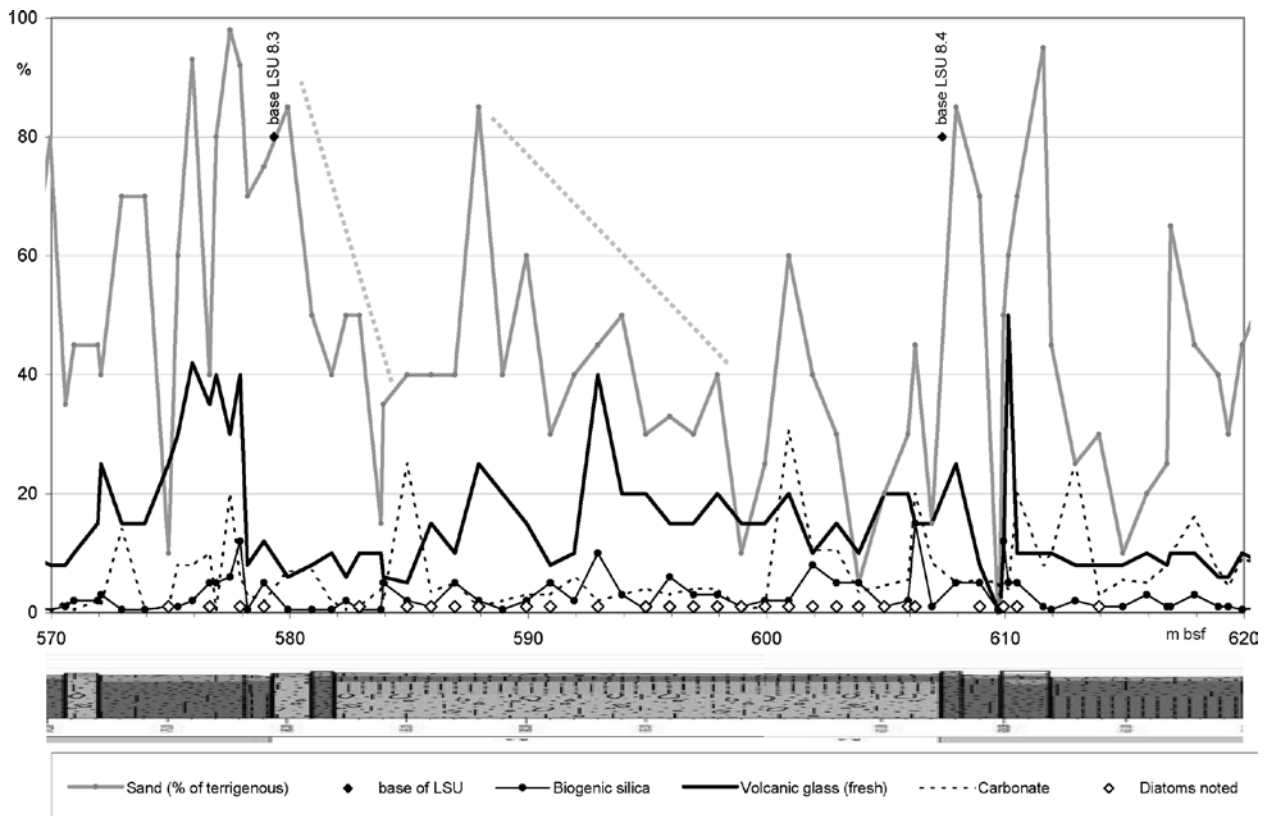


Fig. 15 – Core compositional features in LSU 8.4 based on smear slides. Dotted grey lines highlight trend in sand data.

in grain-size, with well- to moderate-sorting. Matrix is not present, so the rock is clast-supported with quartz cement overgrowths. Internal clasts include well-rounded quartz and very subordinate subrounded feldspar. Quartz grains are almost exclusively monocrystalline, with slightly undulose extinction and diffuse inclusions. Feldspar grains are affected by a high grade of alteration (sericitization).

(c) Volcanic clasts in LSU 9 include lavas, scoria and pumice. The pyroclastic material in this unit occurs as dispersed clasts as well as in concentrated layers. Three thin (<3 cm), closely spaced, volcanic sands occur between 636.17 and 636.26 mbsf, and they are composed of reddish-brown scoriaceous sand- to pebble-sized angular to subrounded clasts. Crystals include plagioclase and pyroxene, suggesting that the volcanic material is mafic in composition. Based on their close spacing, texture and composition it is likely that the volcanic sands were originally part of a single pyroclastic deposit. A six cm-thick pyroclastic deposit occurs at 640 mbsf within a sandstone interval and is a dark green pumaceous coarse ash to lapilli tuff. The primary pyroclastic layer is normally graded with a gradational top and a loaded base. Pumices are angular with elongate vesicles (Fig. 6F). Crystals of potassium feldspar separated from this layer suggest that it is intermediate to felsic in composition and datable by the  $^{40}\text{Ar}/^{39}\text{Ar}$  method (see Acton et al., this volume). Other more dispersed accumulations of reworked volcanic pyroclasts (subrounded to very angular, sand to pebble size) occur between 619.67 and 619.74 mbsf (green-grey pumice and black scoria, e.g. AND-2A 619.72 mbsf), at 622.6 mbsf

(black to reddish brown scoria) and between 621.24 and 621.42 mbsf (light-grey to tan pumice). Clasts of lava are similar in composition and texture to previous units, ranging from mafic to felsic (e.g., AND-2A 619.72), aphanitic to porphyritic and non-vesicular to vesicular.

(d) Siltstones range from bioclastic (c. 15%) to volcanic ash bearing (c. 15%). Bioclasts, often recrystallized and filled with blocky spar, include serpulid tubes, bryozoans, bivalves, sponge spicules (especially in the glass-rich layers) and foraminifera. Unaltered volcanic glass types include mafic(?) brown (rounded, blocky, vesicular, some with plagioclase crystals), felsic/silicic(?) white or clear (cusped, vesicular, tubular) and alkaline(?) green (blocky). Altered glass is primarily brown glass altered to hematite/opaque or zeolite and it is included in the lithic component (tr-20%). Other lithics include basalt, both unaltered and altered to opaques/chlorite, dolerite, biotite granite, metasandstone and marble. Quartz is mostly monocrystalline and subangular with a few well rounded clasts. Feldspar is a mixture of altered K-feldspar and unaltered to altered plagioclase. Other detrital minerals include three types of pyroxene, biotite, amphibole, muscovite and opaques. The groundmass is composed of clays, microspar and blocky calcite cement.

(d) Sandstones range from grain- to matrix-supported (3-25% matrix), with the matrix composed of clays, with cements of micro- to blocky spar and opaques. Bioclasts (tr-1%) include diatoms, bryozoans, foraminifera and serpulid tubes. Unaltered glass (3-20%) includes brown (blocky, vesicular,

plagioclase crystals), white (vesicular, tubular, blocky) and green (blocky, mingled with white). Altered glass is included in the lithic component (15-40%) and is primarily brown glass altered to zeolite and rarely opaques or calcite. Lithics are dominated by basalts altered to opaques and chlorite and rarely calcite or unaltered. Other common lithics are metasandstones and schists. Less common lithics include biotite granite, dolerite and marble. Quartz (25-30%) is generally monocrystalline and subangular with some well-rounded. Feldspars are a mixture of sericite altered K-feldspar and unaltered to altered plagioclase.

(d) Biogenic silica is present within most of this LSU, though marine diatoms were noted in smear slides only near the top and in the lower half (Fig. 16). Fresh volcanic glass occurs commonly and reaches 20% or more in six places. There appear to be four up-section increases in abundance of fresh volcanic glass (peaks around 643, 636, 628 and 608mbsf). Carbonate comprises about 5-20% of most smear slides. Some peaks in sand abundance coincide with peaks in interval velocity (as do some peaks in carbonate).

(e) Geochemical Unit 9 (607.35 - 648.74 mbsf): this LSU shows two cycles of comparable geochemical pattern. The first cycle reaches from the top of the LSU to 625.60 mbsf. A second cycle follows to the bottom of this LSU. From bottom to top the cyclic pattern starts with a drop in Fe and Ca content to narrow minima at 643 and 622 mbsf, respectively (Fig. 17). Above here, the values of both elements increase gradually with some scattering up to the top of the cycle. Si and K show higher values in the

lower cycle combined with a stronger scattering. Both elements have peaks at the top of this LSU. Cl shows an increase with high scattering across the whole LSU. Ba decreases in several steps from the bottom to the top of this LSU (Fig. 17).

(f) A porphyritic lava clast (ruditic grain size) from a sandstone was analysed by XRF (AND-2A 619.68 mbsf). Its major element composition plots in the basalt field in the TAS diagram (Fig. 2). It should be noted that this is the only sample plotting so far outside the known compositional field of the McMurdo Volcanic Group, having normative-Q and unusual low alkali/silica ratio.

### **Lithostratigraphic Unit 10**

(648.74–778.34 mbsf)

LSU 10 consists of volcanic-bearing diamictite, sandstone and sandy mudstone.

(a) The average clast content of this unit is 102 per metre. Volcanic rocks still dominate over intrusive rocks, with minor occurrences of metamorphic rocks, dolerites, quartz and intraformational clasts; sedimentary rock content is very low. Intraclasts are mostly restricted within the intraformational clast breccia lithofacies (721.87 - 722.10 mbsf) and within disturbed zones characterised by soft-sediment deformation (*i.e.* 691.00 - 692.08 mbsf). In contrast with dolerites, metamorphic rock content shows a down-core increasing trend, whereas all other lithological contents are characterised by fluctuations. Gravel fraction includes granule to pebble grain size, with only minor cobbles of dolerites and intrusive, volcanic and metamorphic rocks.

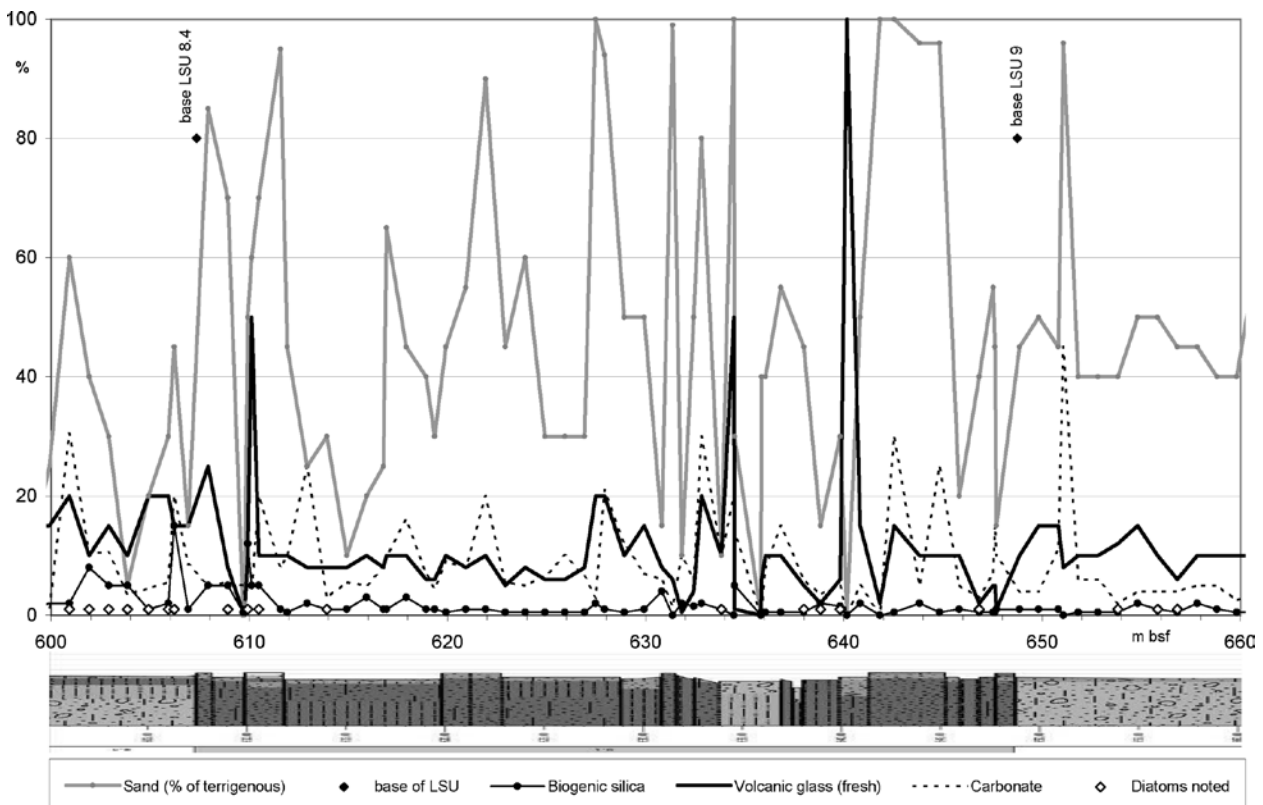


Fig. 16 – Core compositional features in LSU 9 based on smear slides.

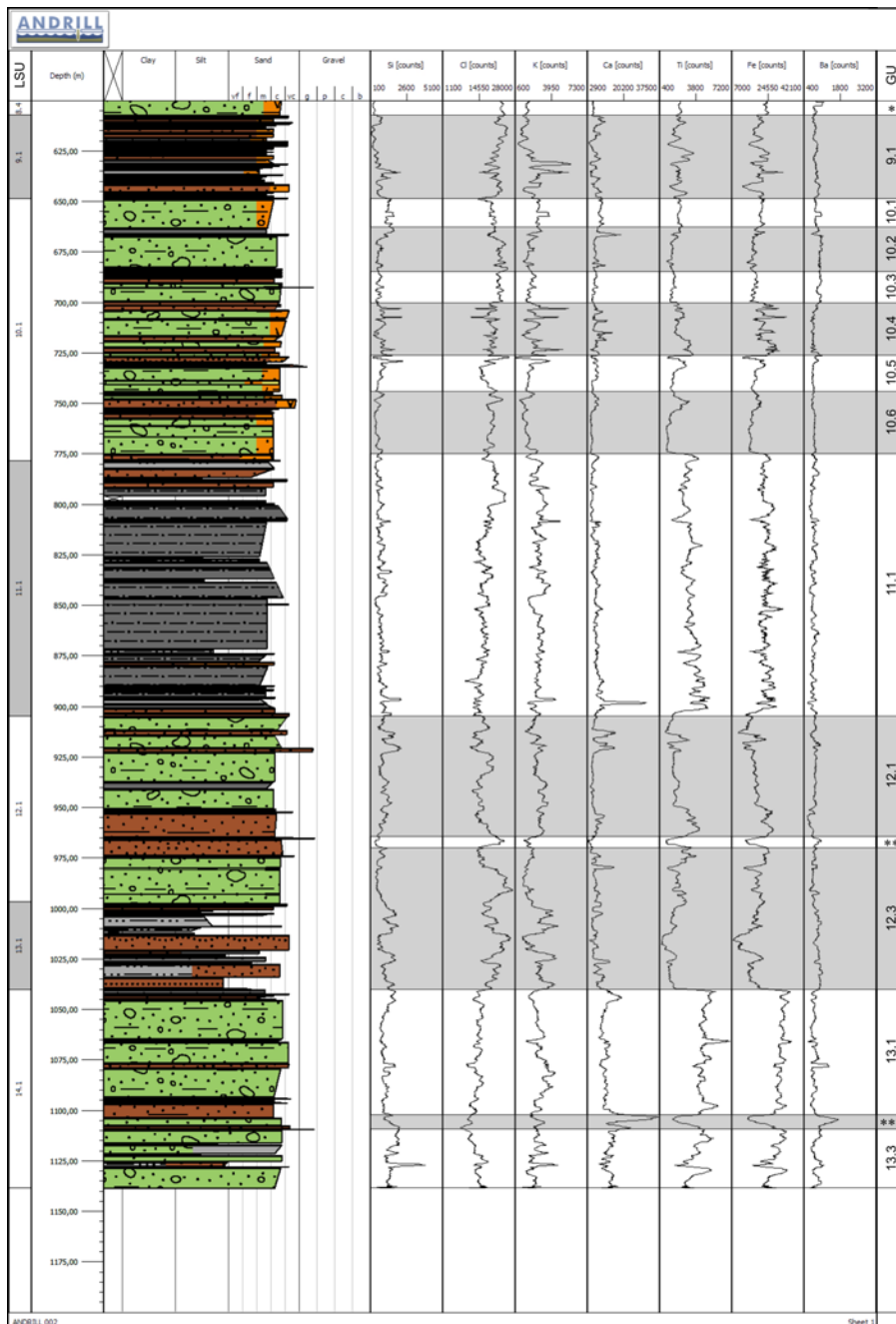


Fig. 17 – Lithostratigraphic Units (LSU; left margin), lithologic log and Geochemical Units (GU; right margin) with selected element counts from the XRF Core scanner for the interval 600.00 – 1138.54 mbsf of the AND-2A core (\* GSU 8.5; \*\* GSU 12.2; \*\*\* GSU 13.2).

(a) Clasts of igneous intrusive rocks include a large variety of lithotypes, consisting of biotite ± hornblende monzogranites (leucocratic to pink in colour, undeformed to mylonitic in texture) associated with granodiorites/tonalites, quartz-diorites/gabbrodiorites and minor syenogranites and minor felsic to intermediate porphyries. Metamorphic rocks consist of biotite ± Ca-amphibole syenitic to tonalitic orthogneisses (sometimes with mylonitic texture, Fig. 4b), biotite ± Ca-amphibole gneisses, biotite ± Ca-amphibole ± clinopyroxene schists, quartzites, impure marbles, clinopyroxene or Ca-amphibole granofels and a significant variety of low-grade metasediments (phyllites, biotite or biotite-spotted metasiltstones, biotite ± white mica ± calcite metasandstones,

metalmestones and metaconglomerates; Fig. 4c). Minor occurrences of felsic metaporphyries and a clast of biotite meta-tonalite are also present.

(b) The LSU 10 contains sedimentary clasts belonging to a great variety of lithological groups, as quartz arenites, subarkoses, feldspatic litharenites, volcanic arenites, diamictites and conglomerate/sandstone intraclasts. They are enclosed in stratified diamictite beds and in sandstone and mudstone beds. All the intrabasinal clasts (diamictite and conglomerate) come from the lower part of the LSU 10, whereas the other extrabasinal clasts come from the upper part. Feldspatic litharenite (AND-2A 649.38 mbsf) is fine-medium in grain size, with a poor to moderate sorting, with presence of matrix, so to get close a greywacke. Matrix is partially recrystallized, so to be confused with pseudomatrix, whereas the cement is formed of calcite and clay minerals. Internal grains, mainly subangular, are composed of quartz, lithic fragments, plagioclase, K-feldspar and few white mica. Lithic fragments prevail on feldspar grains. Quartz grains are mainly monocrystalline, with slightly undulose extinction and inclusions. Feldspar grains are often sericitized and vacuolized. Lithic fragments,

of metamorphic type, are often deeply altered, so to simulate a matrix. Subarkose (AND-2A 663.47 mbsf) shows very well-sorting and medium-coarse grain size. Internal grains are rounded to well rounded, in absence of matrix, whereas the cement is present as quartz overgrowths, and subordinately as phyllosilicate rims and sparry calcite. The grain assemblage includes quartz (mainly monocrystalline with light undulose extinction) and minor lithic fragments of metamorphic rock, plagioclase and K-feldspar (orthoclase and microcline) with strong sericitization. Quartz arenite (AND-2A 678.55 mbsf) is medium in grain size, with clast-supported texture and well-rounded clasts. Matrix is absent, whereas the cement occurs as

quartz overgrowths and few clay minerals. Grain assemblage includes essentially quartz, with very minor altered feldspar (plagioclase and K-feldspar) and altered lithic fragments. Quartz grains are generally monocrystalline, with slightly undulose extinction. Volcaniclastic arenite (AND-2A 721.95 mbsf) has oriented texture, formed by clasts enclosed within an altered groundmass or matrix, with fluidal look, similar to pyroclastic rock. Dominant grains are of volcanic origin, as basalt and plagioclase; these last minerals are zoned and deeply altered. Rarely, quartz grains are present, with well rounded to subangular roundness, and with undulose extinction. Diamictite intraclast (AND-2A 711.29 mbsf) is texturally quite similar to those described for the LSU 4, from which it differs for the lesser amount of basalt lithic fragments. In fact, it includes grains of quartz, plagioclase, K-feldspar, basalt, metamorphic rock, intrusive rock, pyroxene and calcite. Likewise to diamictite intraclasts, the conglomerate/coarse sandstone intraclasts (AND-2A 680.61, 687.35, 746.72 mbsf) represent the intrabasinal reworking clasts from conglomerate or sandstone beds. Clasts are subprismoidal in shape and rounded to subangular in roundness. They are formed by grains ranging in size from 0.2 to 1 mm (coarse to very coarse sandstone), with rare grains of coarser size up to 6.5-7 mm (pebble), or a finer grain-size from 0.05 to 1.25 mm (coarse siltstone to coarse sandstone). Generally grains are not in contact, but they are separated by a dark-brown clay-marl matrix, or by microcrystalline calcite, probably due to replacement processes. Grains are well-rounded- to- angular and the samples may be texturally divisible in portions, rich in muddy matrix, or rich in clasts even if matrix-supported. Grain assemblage includes (in decreasing order of abundance) lithic fragments, quartz, feldspar, pyroxene. Quartz grains are mainly monocrystalline with slightly undulose extinction and few inclusions. Subordinate composite quartz is also present. Rounding of quartz grains range from well rounded- to- subangular. The rounded grains have quartz overgrowths which emphasize the sedimentary recycling. Feldspar grains are plagioclase with euhedral shape and high grade of sericitization, and highly altered K-feldspar (orthoclase and microcline). Lithic grains are sedimentary as arkose, subarkose and quartz arenite, metamorphic as micaschists, metasandstones and gneiss, volcanic as basalt/dolerite, and much altered vitrophiric rock, intrusive as granitoids. Patchy calcite and substitutions of other altered minerals are also present. Basalt grains may be absolutely dominant, as for the sample AND-2A 746.72 mbsf.

(c) Volcanic clasts in LSU 10 include lavas, scoria and pumice. Significant clast supported accumulations of pumice, up to 3.5 cm thick, occur in ripple cross laminated sands between 709.00 and 709.30 mbsf. The pumice is subrounded- to- rounded, sand to pebble grain size and concentrated along ripple foresets. More diffuse (c. 11 per metre) occurrences of subrounded to very angular ash and lapilli size

(up to 1.0 cm) scoriaceous to pumiceous clasts occur within sandy diamictite near the top of the unit (648 to 659 mbsf) and in the lower third of the unit between 734 and 742 mbsf, and between 759 and 767 mbsf. These highly vesicular clasts within the lower third show a variety of colours that range from black to dark greenish-grey, to purplish-brown. Clasts of lava have the same range in composition and textures as previous units (mafic AND-2A-700.52; intermediate AND-2A 710.82 and 712.28; and felsic AND-2A 666.02, 675.20 and 741.96 mbsf). However, relative to LSU 9, there is a higher proportion of a dark purplish-grey to black, finely porphyritic, sparsely vesicular lava, which from 317 mbsf (LSU 6) has been a persistent clast type. Sample AND-2A 675.20 mbsf is a vitrophyre that displays abundant devitrification textures. Some of the volcanic clasts are altered with calcite and chlorite being the main secondary phases in vesicles (*i.e.* amygdaloidal) and as pseudomorphs.

(d) Diamictites are mainly matrix-dominated with the matrix ranging from 28% to 70% and are composed of clay and microspar. Bioclasts (shell fragments, serpulid tubes, sponge spicules) are usually present but in low quantities (trace to 1%). Unaltered glass is also usually present ranging from 1 to 30% and is highly variable in composition and texture. Brown, possibly mafic, glass is rounded to blocky to vesicular and often contains plagioclase laths. Clear or white, possibly felsic, glass ranges from ragged highly vesicular to long tube textures. Vesicles may be filled and grains may be rimmed by calcite cement. Green, possibly alkaline, glass is usually blocky to slightly vesicular and may be mingled with white glass. Altered glass is included in the lithic category (5-10%) since it may have been altered at source rather than diagenetically and includes brown glass altered to zeolite or opaques or rarely chlorite and white glass altered to calcite. Other lithics include basalt ranging from unaltered to highly altered to opaques and chlorite, some with feldspars altering to sericite; granite (biotite and microcline); metamorphic sediments (schists, marble, metasandstone); and dolerites (some heavily weathered with feldspars altering to sericite). Three types of pyroxenes have been identified, along with biotite, amphibole and chlorite. Feldspars are a mixture of altered K-feldspar and unaltered to altered plagioclase. Quartz is generally monocrystalline, mostly subangular with some well rounded grains.

(d) Intercalated sandstones are grain-supported litharenites ranging from 35 to 78% lithics. Lithic composition is dominantly volcanic, including basalt (unaltered to highly altered to opaques and chlorite), brown glass altered to zeolite, palagonite and rarely glauconite, white glass altered to calcite and dolerite. Other lithics include siltstone, metasandstone, schist, marble and granite (biotite, microcline, myrmekitic). Quartz is generally monocrystalline, mostly subangular with some well rounded grains with remnant overgrowths. Feldspars are mixed

altered K-feldspar and altered to unaltered plagioclase. Other single crystal minerals include three types of pyroxene, amphibole, chlorite, biotite and muscovite. Shell fragments are present in trace amounts. The groundmass is composed of clays, microspar and some blocky cement, often rimming glass grains or infilling vesicles. There are a few examples of possible zeolite alteration of the matrix clays around volcanic grains.

(d) Fresh volcanic glass is more common in the lower half of this unit and in several instances appears abruptly before tailing off up-section (Fig. 18). Carbonate occurs more as discrete spikes in this LSU. Biogenic silica occurs in three main zones in the lower half of this LSU. The lowest zone shows an up-section decrease in abundance within a thick unit of diamictite. There is a well-defined increase in percent sand within a diamictite around 690 mbsf and perhaps another around 735 mbsf.

(e) This LSU can be divided into 6 Geochemical Units with a sharp lower boundary at 774.94 mbsf (Fig. 17):

Geochemical Unit 10.1 (648.74 - 662.69 mbsf). Fe increases only slightly on a high level plateau and Ca values increase from bottom to top. K and Si values are high and show some scattering. Cl values are on a lower, and Ba values are on a medium level.

Geochemical Unit 10.2 (662.69 - 684.90 mbsf). Fe values increase from bottom to top with moderate scattering. Ca values have a weak, increasing trend on a medium high plateau. K and Si values are low, and Cl values are high. Barium values are high as can be seen in GU 10.3 (see below).

Geochemical Unit 10.3 (684.90 - 700.31 mbsf).

Fe, K and Ca values increase from bottom to top at medium high levels. They all have some scattering. Silica is lower, but scatters with higher values. Chlorine is medium to high.

Geochemical Unit 10.4 (700.31 - 726.31 mbsf).

This GU consists of five to six small subunits with high variations in elemental concentrations. All elements therefore show small maxima and minima. Fe and Si base levels are at a high, Cl and Ca at a medium and Ba is at a lower level.

Geochemical Unit 10.5 (726.31 - 744.12 mbsf). Fe, Si and Ca show a small general increase towards the top. Above this increase, Fe has a small maximum and drops to a small minimum. K increases moderately with a narrow peak at the top. Cl values decrease from the bottom to the top of this GU.

Geochemical Unit 10.6 (744.12 - 774.94 mbsf). Values of Fe, Si and Ca are low with a sharp increase and maximum further above. K decreases with several minor maxima and a more pronounced one at the top. Ba remains, as in GU 10.5, at a lower to moderate level with some scattering, but shows no general trend. Cl scatters at a medium high level without a trend.

Please note that XRF data for the LSU 10 core interval between 774.94 and 778.34 mbsf will be described below in LSU 11, since this interval is assigned to GU 11 which includes both the lowermost section of LSU 10 and the entire LSU 11.

(f) A porphyritic poorly vesiculated mafic clast from the diamictite (AND-2A 764.40 mbsf) with phenocrysts of olivine, Ti-rich clinopyroxene (based on colour and pleochroism) and plagioclase, and microphenocrysts of magnetite was analyzed by XRF. The major element composition plots in the trachybasalt field (Fig. 2).

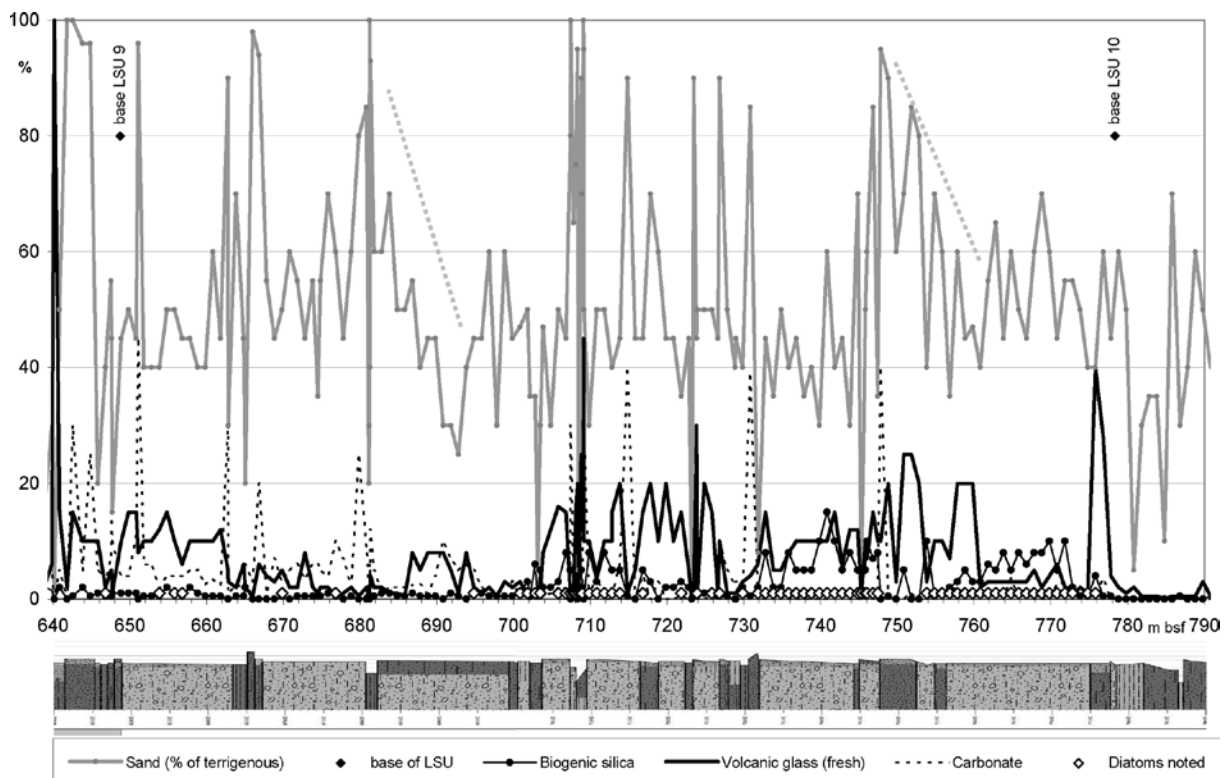


Fig. 18 – Core compositional features in LSU 10 based on smear slides. Dotted grey lines highlight trend in sand data.

**Lithostratigraphic Unit 11**

(778.34 – 904.66 mbsf)

LSU 11 includes sandy siltstone with dispersed clasts and sandstone with/without dispersed clasts.

(a) The average clast content is 20 per metre. The gravel fraction is almost entirely represented by volcanic rocks, with only minor occurrences of intrusive rocks and scattered appearances of sedimentary rocks, metamorphic rocks, dolerites, intraformational clasts and quartz. Sedimentary rocks include coal granules, particularly diffused within the 786.02 - 786.44 and 799.47 - 800.32 mbsf intervals. Both total clast and intrusive rock contents are characterised by fluctuating trends, whereas volcanic rock content is more or less constant throughout the unit. Clasts consist of granule to pebble grain class, with very minor occurrences of cobbles of dolerites and volcanic and intrusive rocks.

(a) Clasts of igneous intrusive rocks are mostly represented by leucocratic to pink biotite±hornblende or white mica monzogranites, including both foliated and unfoliated varieties and sometimes characterised by the presence of K-feldspar megacrysts. Only minor occurrences of syenogranites and granodiorites/tonalites are present. Metamorphic rock clasts include biotite orthogneisses and gneisses (sometimes with mylonitic textures), Ca-amphibole±clinopyroxene or biotite schists, impure marbles, quartzites and low-grade metasediments (white mica-chlorite metasandstones, white mica-biotite phyllites; Fig. 4d).

(c) Volcanic clasts in LSU 11 include lavas and pumice. The absence of scoria makes this unit distinctive from previous units (LSU 7-10). Small

(<4 mm) pumice clasts are concentrated in three intervals (831, 873 and 878 mbsf). The pumice accumulation at 831 mbsf is the thickest (c. 1 cm thick) and most concentrated of the accumulations. The pumice is clast-supported and has gradational top and bottom contacts with silty sandstone, which indicates moderate reworking. Volcanic lava clasts, once again, show a range in compositional and textural diversity. The dark purplish-grey to black, finely porphyritic, sparsely vesicular lava described in LSU 10 is also an abundant clast within this unit. It is also noted that macroscopic indicators of weathering (e.g., thick weathering rinds) and alteration (e.g., discoloration and vesicle/vug fillings) of volcanic clasts are more apparent in this unit relative to LSU 9 and 10.

(d) Biogenic silica generally occurs in only trace amounts though there are peaks in the middle of the thickest mudstone unit and around its top (Fig. 19). Fresh volcanic glass is present in small amounts through most of this LSU, with small peaks around 901, 879, 849 and 823 mbsf. Sand is generally less abundant in the lower half of the LSU whereas carbonate is more common.

(e) Geochemical Unit 11 (774.94 - 904.66 mbsf): the XRF data indicate that LSU 11 and the lowermost part of LSU 10 can be distinguished as GU 11 (774.94 - 904.66 mbsf). This GU is mainly defined by the Fe and lesser by the Ca contents. The lower boundary is a transition that reaches from about 913.70 to 900.20 mbsf. In this interval the Fe content increases significantly (Fig. 17). Further above it remains at a high level, but varies very much with high amplitude maxima and minima. About 27 of these phases are visible in a smoothed raw data

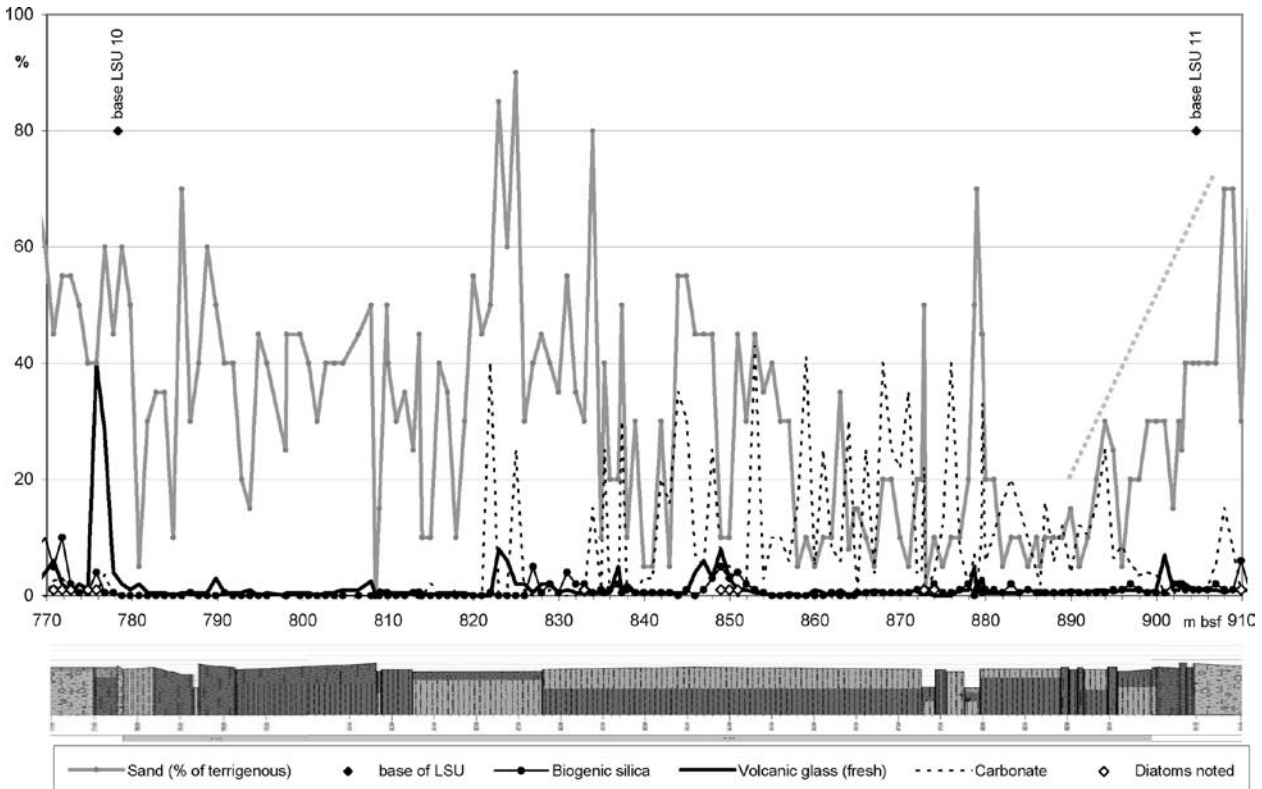


Fig. 19 – Core compositional features in LSU 11 based on smear slides. Dotted grey line highlights trend in sand data.

set and in the variations of other elements as well. Ca increases with large fluctuations to high levels at about 898.30 mbsf (Fig. 17). Up core it then decreases with high amplitude variations. Ba shows a trend of increasing values from 807 mbsf to the top of this GU. K values are higher in this finer-grained unit. Both elements have large variations, but increasing mean values from 912 to 850 mbsf. There is a minimum at 847 mbsf that is also visible in the Si values. At 842 mbsf, K is on a high level again and then varies with large amplitudes on the same level up to 792 mbsf and decreases gradually towards the top of GU 11. Chlorine values decrease from the top to the bottom with large variability.

### **Lithostratigraphic Unit 12**

(904.66 – 996.69 mbsf)

LSU 12 consists of clast-rich and clast-poor diamictite, muddy sandstone with dispersed clasts and minor mudstone with dispersed clasts.

(a) The average clast content of this unit is 76 per metre. Volcanic rocks dominate over intrusive rocks and minor dolerites and metamorphic rocks, whereas quartz, sedimentary rocks and intraformational clasts are only rare. The total number of clasts is higher within the sandstone with abundant clasts in the sandy conglomerate lithofacies (919.45 - 922.38 mbsf). The intrusive rock content has a down-core decreasing trend, with the maximum values located within the 917.70 - 935.70 mbsf interval, where intrusive rocks dominate over volcanic rocks. Both dolerites and metamorphic rocks abundances are relatively diffused from the top of the unit to 950.70 mbsf; below that depth, their content decreases down-core. The gravel fraction includes granules, pebbles and rare cobbles of dolerites and intrusive, metamorphic and volcanic rocks.

(a) Clasts of igneous intrusive rocks are largely dominated by biotite ± hornblende monzogranites (leucocratic to pink in colour, undeformed to foliated in texture), with minor occurrences of tonalites, quartz-diorites and felsic to intermediate porphyries (sometimes characterised by foliation). Metamorphic rocks include biotite-white mica orthogneisses, biotite ± Ca-amphibole gneisses (sometimes migmatitic) and schists, clinopyroxene-biotite granofels, actinolite-biotite amphibolites, quartzites, low-grade metasediments (biotite ± white mica or Ca-amphibole metasandstones, biotite-white mica phyllites and metalimestones) and minor white mica-biotite felsic metaporphyries.

(b) Sedimentary clasts are represented by subarkoses (AND-2A 910.45 and 985.83 mbsf), enclosed in stratified diamictites. Subarkoses are medium-fine in grain size, with well rounded to subangular grains and moderate sorting with about 5% or less of matrix. Cement is constituted by quartz overgrowths, calcite and clay minerals. Grain assemblage includes abundant quartz and minor feldspar. Quartz grains are mainly monocrystalline with slightly undulose extinction and quartz

overgrowths. Feldspar grains as K-feldspar (orthoclase and microcline) and plagioclase show high grade of alteration to sericite. Few grains of muscovite may occur.

(c) Volcanic clasts in LSU 12 include lavas, pumice and rare scoria. Between 953 and 964 mbsf there are six accumulations of mixed yellow-grey pumice and dark green highly angular clasts in muddy fine sandstone (Fig. 6C). The dark green clasts (up to 7mm in long dimension) represent altered pumice that has been replaced by zeolite, calcite, Fe-oxides (Fig. 6D). The accumulations are dispersed and matrix-supported and range from 2 to 10 cm in thickness. The diversity of lava clast compositions appears to be more restricted in this unit, dominated by intermediate to felsic types, including the dark purplish grey type noted in LSU 10 and 11.

(d) Biogenic silica is present in trace amounts in most smear slides, increasing slightly in abundance in diamictite units compared to other lithologies. The amount of biogenic silica increases up-section in two diamictites near the top of the LSU (Fig. 20). Fresh volcanic glass is generally low throughout though there is a spike within a thick unit of sandstone around 953 mbsf. Carbonate occurs more commonly and in greater amounts up-section in LSU 12 and in places coincides with increases in interval velocity.

(e) XRF core scanning results for this LSU are reported below in LSU 13 description, since both LSU 12 and LSU 13 are part of the GU 12.

### **Lithostratigraphic Unit 13**

(996.69 – 1040.28 mbsf)

LSU 13 is composed of fine siltstone, coarse siltstone, and very fine-grained sandstone, with very fine- to fine-grained sandstone with dispersed clasts, and rare diamictite.

(a) This unit is characterised by the lowest average clast content (10 per metre) of all LSUs. Volcanic rocks still dominate over minor intraformational clasts and intrusive rocks, with only scattered occurrences of dolerites, quartz and metamorphic and sedimentary rocks. The total number of clasts at first decreases and then increases down-core. Intraclasts are more abundant within lithofacies affected by soft-sediment deformation (*i.e.* 1 000.48 - 1 001.01, 1 027.05 - 1 030.87, 1 035.87 - 1 037.87 mbsf intervals). The gravel fraction includes granule- to- pebble-sized clasts.

(a) Clasts of igneous intrusive rocks consist of biotite ± hornblende monzogranites (leucocratic to pink in colour, undeformed to foliated in texture), with only rare occurrences of possible granodiorites. Metamorphic rocks are represented only by biotite gneisses/orthogneisses.

(c) The abundance of volcanic clasts in LSU 13 is low relative to all other lithostratigraphic units. Volcanic clasts include lava and scoria. No pumice was identified. Very small (*c.* 1-2 mm) purplish black vesiculated clasts are concentrated along ripple foresets in fine grained sandstones between 1 015.46 and 1 017.56 mbsf. Brownish grey vesicular to

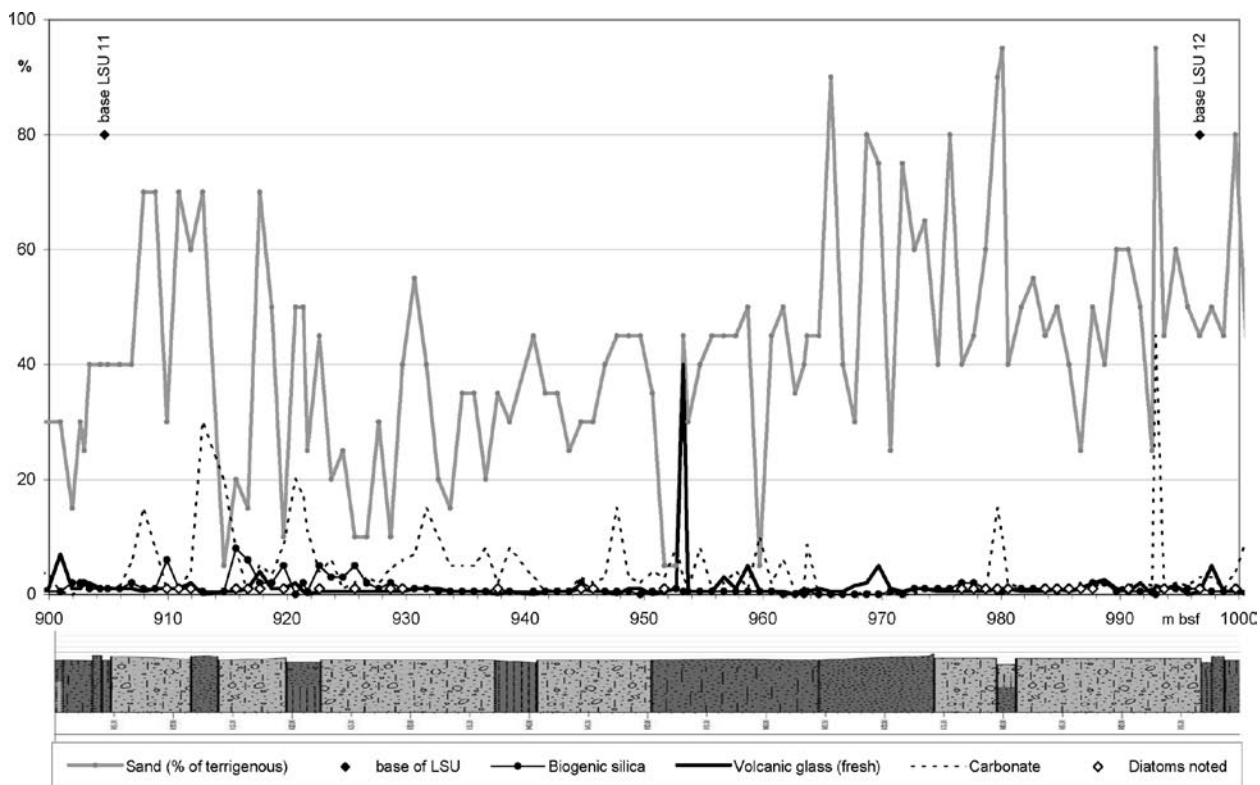


Fig. 20 – Core compositional features in LSU 12 based on smear slides.

scoriaceous clasts, ranging in size from 1cm to 3mm are dispersed between 1 029.77 to 1 035.10 mbsf in sandy mudstone. Lava clasts include the purplish grey variety several black aphanitic mafic clasts.

(d) Biogenic silica occurs both sparsely and in low abundances in LSU 13 though diatoms were recognisable in places, even below 1 000 mbsf. Fresh volcanic glass is present in most units and reaches a maximum of 10% (Fig. 21). Carbonate content varies greatly and does not show a clear relationship to lithotype.

(e) The two LSU 12 and 13 do not have unique geochemical patterns. They are unified in Geochemical Unit 12 (904.66 - 1 040.28 mbsf). This unit was separated into:

Geochemical Unit 12.1 (904.66 - 964.38 mbsf). This geochemical subunit coincides with the finer grained upper sequence of LSU 12. Fe decreases from high values at the bottom of this GU with two peaks at 961 and 552 mbsf to low values at the top (Fig. 17). Ca at the bottom increases in high amplitude variations to a peak at 954 mbsf. At this point Ba has a minimum. Further upwards Ca values decrease again and show low levels between 949 and 923 mbsf. In this section the variation of all elements is low. The values show a decrease for Fe, a plateau of low levels for Ca, and of higher levels for Ba. K and Si have high values and variations from base to about 934 mbsf. From 934 to 923 mbsf both elements have minima that correspond with high Cl concentrations. This could be a masking effect from ion absorption of the X-ray fluorescence of the light elements Si and Ca. Between 923 and 911 mbsf all elements show high amplitude variations and reach high peak values. Ca

and Fe are anti-correlated.

Geochemical Unit 12.2 (964.38 - 970.10 mbsf). This GU is characterised by a minimum anomaly in the high Fe values above and below and separates the general up core decreasing trend of mean Fe values in the GU above and its increasing trend in the GU below. Most of the other elements show anomalies, with minimums for Fe, Ca, Si and K. Barium and Cl have maximum values in this GU. Perhaps sedimentation in this GU was influenced by volcanic activity close by, as indicated by the abundance of pumice in this portion of the core (see Fielding et al., this volume)

Geochemical Unit 12.3 (970.10 - 1 040.28 mbsf). In this GU Cl values reach total core maximum levels and decrease below and above. Besides the peak in GU 12.2, two broad peaks with maximum Cl concentrations occur at 990 and 1 014 mbsf (Fig. 17). Silica and K have minima at these depths and clear maxima at 1 003, 1 009, 1 024 and 1 038 mbsf. Calcium has three very narrow but high peaks at 980, 1 002 and 1 026 mbsf and several lower ones. Otherwise the background level is low. Barium values gradually decrease up-core from medium high values at the bottom to the top. Iron values show an opposite trend. Generally Fe increases upwards, with the exception of a maximum at 1 025 mbsf followed by a minimum at 1 015 mbsf. Another narrow Fe minimum is at 980 mbsf and maximum values are reached at 972 mbsf.

#### **Lithostratigraphic Unit 14**

(1 040.28 – 1 138.54 mbsf, total core depth)

LSU 14 consists of sandy diamictite and sandstone with dispersed clasts.

(a) The average clast content is 80 per metre.

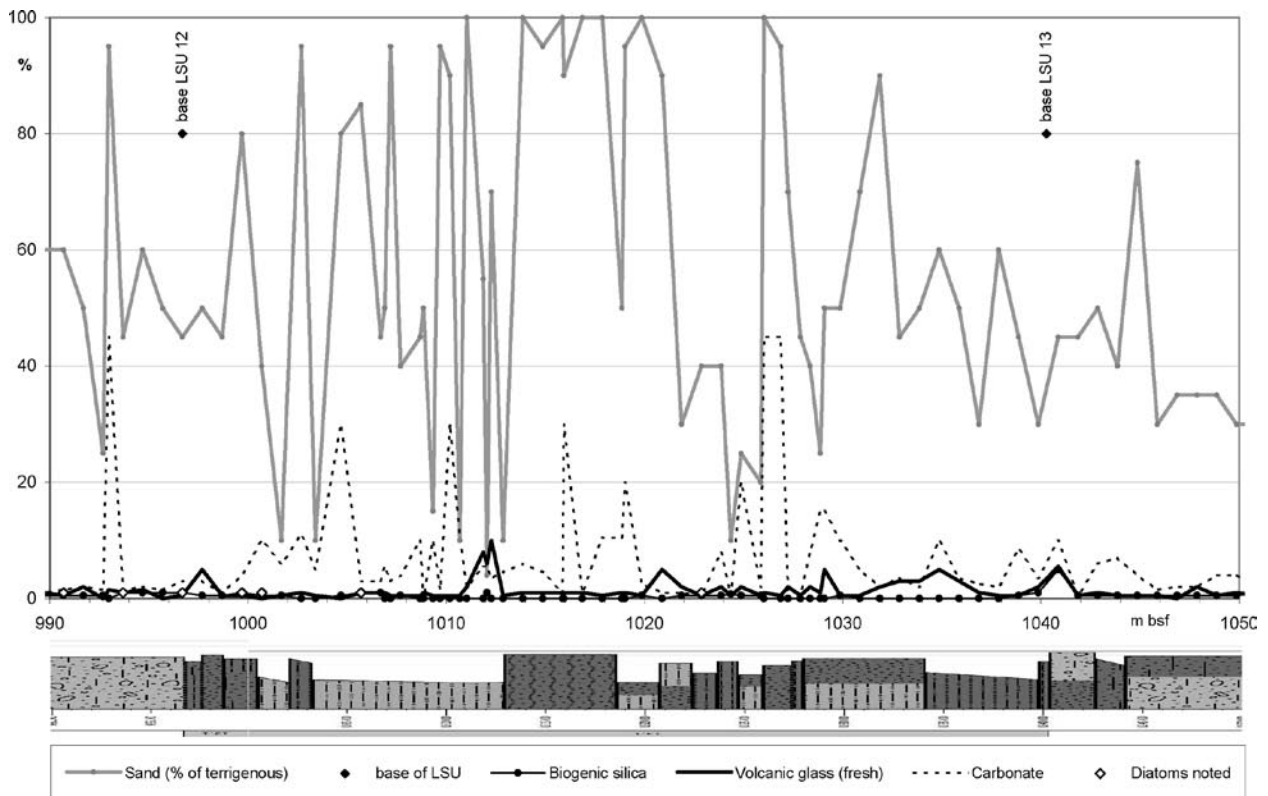


Fig. 21 – Core compositional features in LSU 13 based on smear slides.

Clasts are mainly represented by volcanic rocks dominating over intrusive rocks, minor metamorphic rocks, and only discontinuous occurrences of quartz, intraformational clasts, sedimentary rocks and dolerites. The total number of clasts is characterised by a fluctuating trend. Both intrusive and metamorphic rocks have a down-core increasing trend, whereas volcanic rocks decrease slightly down-core. The gravel fraction mostly includes granules and pebbles, with minor cobbles of volcanic, intrusive and metamorphic rocks and dolerites.

(a) Igneous clasts include biotite  $\pm$ hornblende monzogranites (leucocratic to pink in colour, undeformed to mylonitic in texture, coarse to fine grained), foliated or unfoliated granodiorites/tonalites, quartz-diorites/diorites-gabbros and intermediate to felsic porphyries. Metamorphic rocks comprise biotite  $\pm$ white mica gneisses or orthogneisses (sometimes characterised by compositional layering or mylonitic texture), biotite  $\pm$ Ca-amphibole schists, quartzites, marbles and low-grade metasediments (biotite metasiltstones and metasandstones).

(c) Volcanic clasts in LSU 14 include lavas and scoria. In addition, dense non-vesicular glassy lense-shaped clasts, similar to those identified in LSU 12, occur between 1 092.75 and 1 095.11 mbsf. Minor occurrences of small (generally <5 mm) variably altered, black and red scoria are scattered throughout LSU 14. The overall range in lava clast composition varies from mafic to felsic, and texturally from aphanitic to porphyritic and non-vesicular to vesicular. The dark purplish-grey to black, finely porphyritic, sparsely vesicular lava identified in LSU 10-12 is a common clast type. Black aphanitic to poorly porphyritic,

angular to subrounded clasts of mafic volcanics are dispersed between 1 047.90 and 1 050.96 mbsf and in several other intervals.

(d) Biogenic silica is still present near the base of the hole but occurs only in trace amounts (Fig. 22). Fresh volcanic glass is present at most levels but barely surpasses trace amounts. Carbonate content is generally low and variable but is higher near the base of the hole.

(e) This LSU has been divided into three GUs. At the Top of GSU 13 Rh values that were stable throughout the rest of the core decrease to a lower level then stabilises (Fig. 23). There is a small transition between 1 039.50 to 1 040.50 mbsf from high to lower values that exactly mirrors also the other steep gradients of chemical elements at the GU boundary.

Geochemical Unit 13.1 (1 040.28 - 1 102.20 mbsf). Geochemically the top boundary of this GU is the sharpest boundary of the whole core. Below it Fe values are almost as high as in LSU 1. They increase gradually upwards from high to very high values (max. at 1 041.45 mbsf) with low amplitude but clear cycles (c. 11). Calcium, with a peak at 1 044.33 mbsf, is also very high at the top of this GU and has a high mean level below. At the boundary to GU 12.3 this mean level in Ca drops significantly (Fig. 17). Ba has an anti-correlated pattern and its mean value levels are lower in GU 13.1 than above. Potassium and Cl have minima at the top of this GU at 1 043.70 and 1 045.30 mbsf, respectively. At the upper GU boundary they have a strong gradient and maxima values above. From base of the GU to 1 082 mbsf, K values increase with strong amplitude variations. Towards the top of this GU mean K values

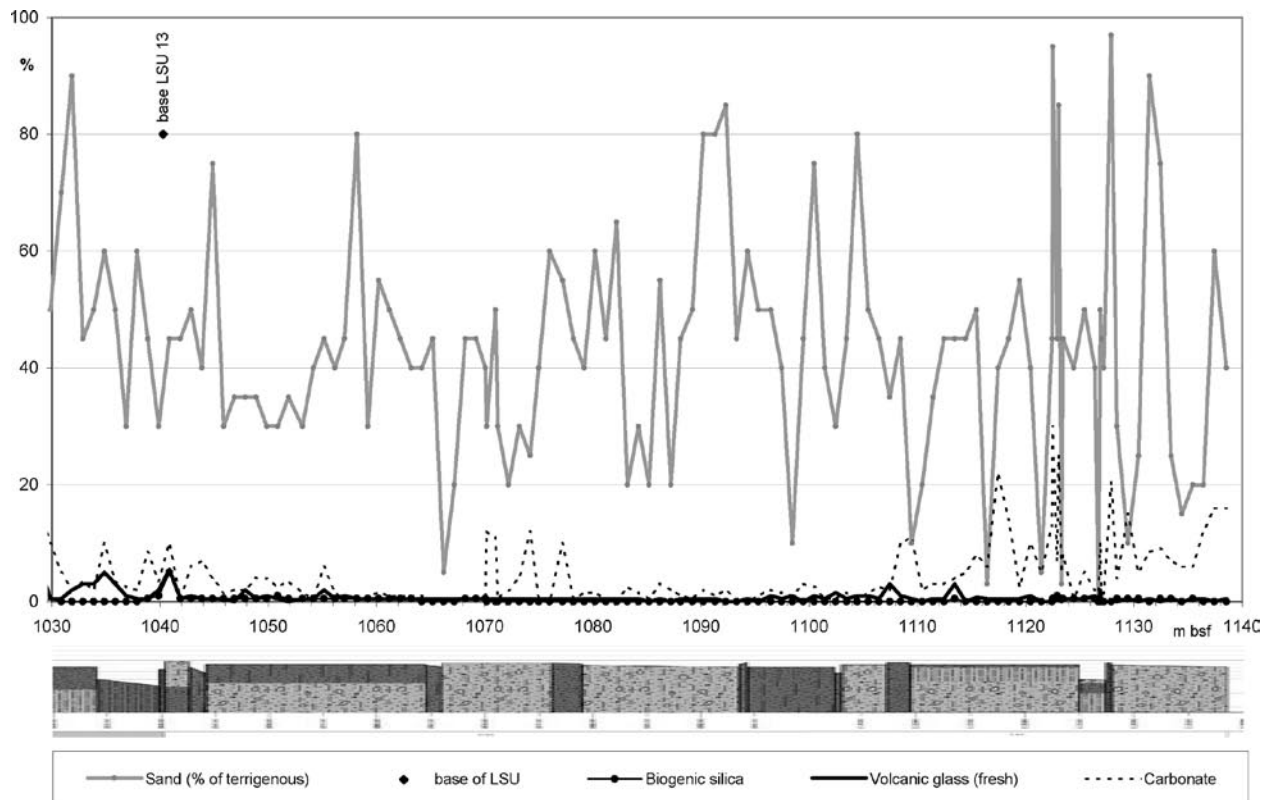


Fig. 22 – Core compositional features in LSU 14 based on smear slides

decrease again. Si values are low from bottom to 1 057 mbsf and increase to medium high values towards the top of the GU.

**Geochemical Unit 13.2** (1 102.20 - 1 109.47 mbsf). The highest mean Ca values in the whole core were measured at 1 103.57 mbsf (Fig. 17). A vein filled with calcite runs down the centre of the core from 1102.75 to 1 105.44 mbsf. A second maximum is at 1 108.69 mbsf where calcite-filled fractures were described between 1 108.44 and 1 109.12 mbsf (see Fielding et al., this volume). Barium has a high peak at 1 104.46 mbsf about one metre below the upper Ca peak. Iron has a broad minimum in this GU and shows the lowest values where Ca is the highest. The Cl values are the lowest of the lower part of the core. This can indicate low pore water content due to cementation.

**Geochemical Unit 13.3** (1 109.47 - 1 138.54 mbsf). The mean Fe values increase up core in this GU (Fig. 17). The variations in Fe have high amplitudes and maxima are at 1 130.07, and close to the top at 1113.82 and 1110.48 mbsf. Two narrow minima are visible around 1 126 mbsf. Calcium has no general trend. The variations are moderate and anti-correlated to the Fe variations. Both K and Si increase slightly up-core and have sharp peaks. Three maxima with decreasing peak values are at 1 127.08, 1 121.36 and 1 116.78 mbsf. Cl values increase again downcore.

#### DISCUSSION OF CLAST AND SAND PETROLOGY, VOLCANOLOGY AND GEOCHEMISTRY OF LSU

(a) *Clasts*. A total of 103 696 clasts (including both intra- and extra-formational types) were logged in

the AND-2A core. Relative abundance data of major clast lithologies and average number of clasts per metre within lithostratigraphic units are shown in figure 24.

Preliminary investigations of basement clasts indicate the Granite Harbour Intrusive Complex as the most likely source for the intrusive rock and orthogneiss clasts. The medium-grade metasediments are common rock types in the Koettlitz Group and in the Horney Formation (sourced from the region between Darwin and Byrd glaciers), whereas the low-grade metasediments are likely derived from the Skelton Group. Koettlitz Group is exposed in the area between Ferrar and Koettlitz glaciers, in the on-shore area close to the AND-2A drill site, whereas the Skelton Group crops out further south, in the Skelton Glacier area. The Granite Harbour Intrusive Complex is extensively exposed throughout the entire region. Nevertheless the most extensive outcrops of strongly deformed granitoids (showing fabrics closely similar to those of AND-2A clasts) appear to be restricted to the area between Darwin and Skelton glaciers.

The results provide direct information about the potential source regions and evidence of an evolving provenance, most likely controlled by variable ice volume conditions and ice-flow directions during the deposition of most clast-rich intervals. Two main basement clast assemblages, diagnostic of specific source regions, have been identified: (i) including marble, garnet micaschist and diopside schists, suggesting oscillation of "local" glaciers of the Ferrar Glacier - Koettlitz Glacier area; and (ii) including low-grade metasediments and mylonitic granitoids,

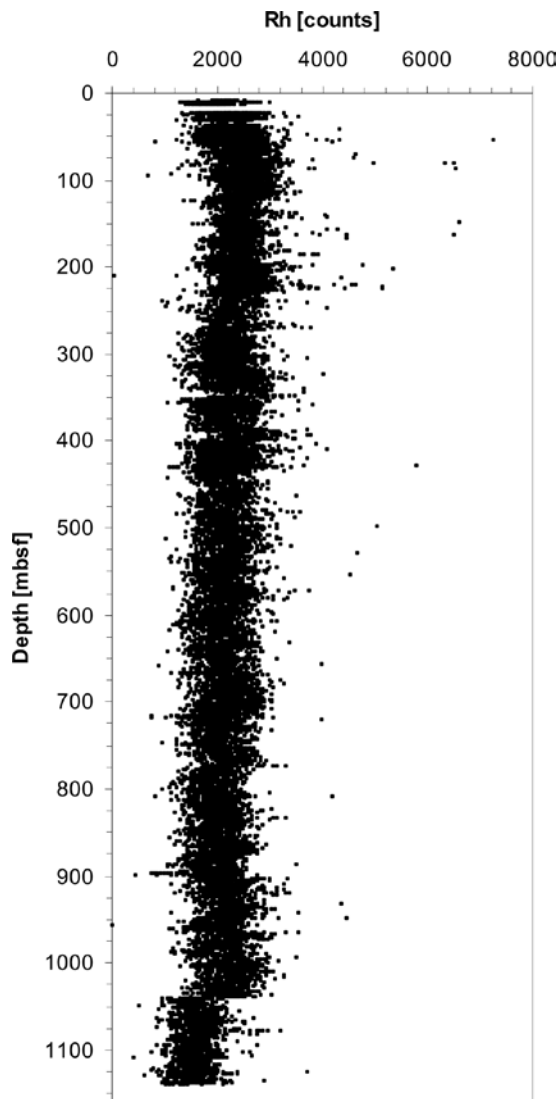


Fig. 23 – Rh counts down-core. A clear drop of about 30% is obvious at 1 040.38 mbsf.

indicating oscillations of a most extensive ice sheet/shelf with a clear provenance from the Skelton Glacier - Darwin Glacier area.

Mineral chemistry analyses of sampled lithologies and work on the requested additional samples during the science documentation phase will help to constrain further these preliminary interpretations. Major targets for future studies will also include 1) the assessment of the implications for sedimentological and paleoclimate models (including tectonics versus climate change interactions) and 2), through the integration of different provenance data sets, the comparison with other Pleistocene to Miocene sedimentary records in the southern McMurdo Sound area (CRP, CIROS, AND-1B drillcores).

(b) *Sedimentary clasts*. The detected lithological groups or petrofacies for the coarse sedimentary clasts are as follow: petrofacies A and A' – arkose, lithic arkose and arkosic litharenite; petrofacies B – quartz arenite; petrofacies D – subarkose; petrofacies Q – volcanic litharenite; petrofacies E – biomicrite/wackestone; petrofacies K and K' characterised by intrabasinal clasts, respectively as diamictite and conglomerate

or coarse sandstone (Appendix 1, Tab. A1.2 and Fig. 5). The down-core distribution of the petrofacies and the relationships between intraclasts and sedimentary extrabasinal clasts (these last data worked by the on-ice clast logging), joined with the distribution of erosional surfaces, allowed the subdivision of the cored sedimentary succession in some preliminary sedimentary clast petrographic units (SPUs). It is worth noting that the ratio intraclasts/sedimentary extrabasinal clasts is not steady downcore, but it is variable, with LSUs marked by high concentration of the former (*i.e.* from LSU 1.1 to 4.1), alternate with LSUs characterised by relative dominance of the latter (*i.e.* from LSU 5.1 to the upper half of LSU 10.1). Most of the examined sedimentary clasts are included in diamictite facies beds (facies Dm and Ds for a total percentage of 67%), subordinately in more organized facies beds like conglomerates, sandstones and mudstones (facies Gs, Sm, Fs, Fb, Fisd, Bif for a total percentage of 33%); for these latter the presence of extrabasinal clasts generally prevails.

The low total number of sedimentary clasts, particularly if compared with clasts of other origin (magmatic and metamorphic), highlights the reduced involvement of sedimentary covers in the erosional-depositional history of the drilled succession. It is also emphasized by the occurrence among them of several samples of diamictite clasts, which testify a prominent intrabasinal reworking. Regarding provenance, based on the comparison with on-shore rock units in the present-day outcrops of the Transantarctic Mountains, the petrofacies A, B and D consistently indicate a provenance from the Beacon Supergroup. Differently, the petrofacies E apparently does not match any rock type belonging to the Beacon Supergroup, for which, at the moment, an extrabasinal or intrabasinal origin could be inferred.

(c, d) *Volcanic clasts and tephra*. Volcanic material is persistent throughout the AND-2A core and includes, in order of relative abundance, volcanic sediment, juvenile magmatic clasts (*i.e.* pyroclasts) and lava. Apart from the *in-situ* volcanic deposits recovered at the top of the core (LSU 1, *c.* 37 to 10 mbsf), which are considered to be from a previously unknown proximal volcanic vent, the specific point sources of the volcanic material are not known. Volcanic clasts range from <1 cm to >13 cm (long axis) and consist of lava, volcanic breccia, and rounded scoria and pumice granules and pebbles. Clasts of lava vary in texture from glassy aphanitic to fine-grained pilotaxitic to coarsely porphyritic, and in composition from mafic [clinopyroxene (Mg-rich), olivine, plagioclase] to intermediate [plagioclase, clinopyroxene (Fe-rich) ± amphibole] to felsic [K-feldspar, clinopyroxene (aegirine) ± amphibole]. Most lithostratigraphic units contain all three compositional types. Exceptions include LSU 1, 5, 6 and 13 which contain predominately mafic to intermediate clasts and LSU 12, which contains mostly intermediate to felsic clasts.

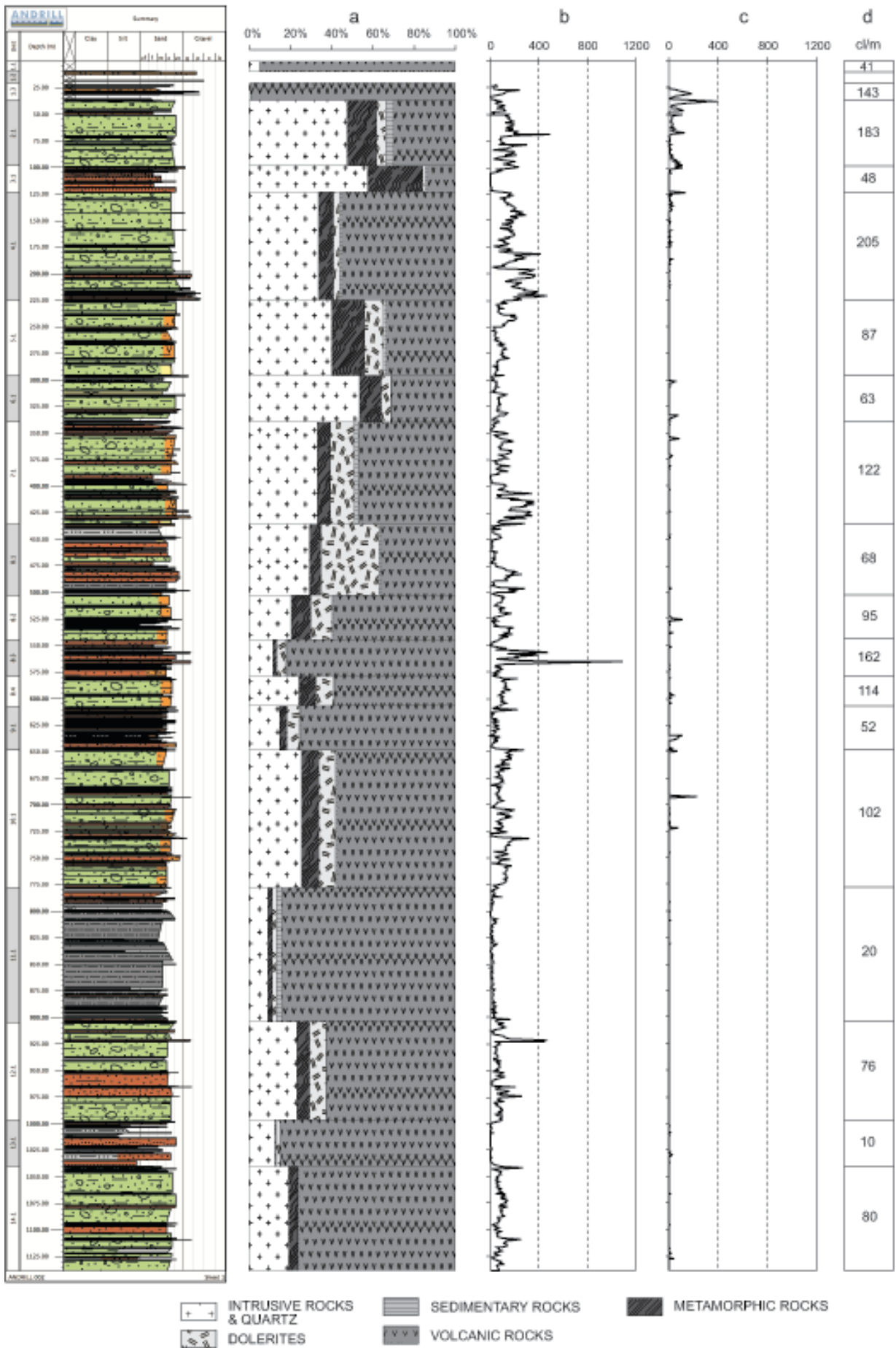


Fig. 24 – Relative average proportions of major extraformational clast types within AND-2A lithostratigraphic units (a), distribution patterns of total number of extraformational (b) and intraformational (c) clasts, and average number of clasts per metre (c/m) within AND-2A lithostratigraphic units (d).

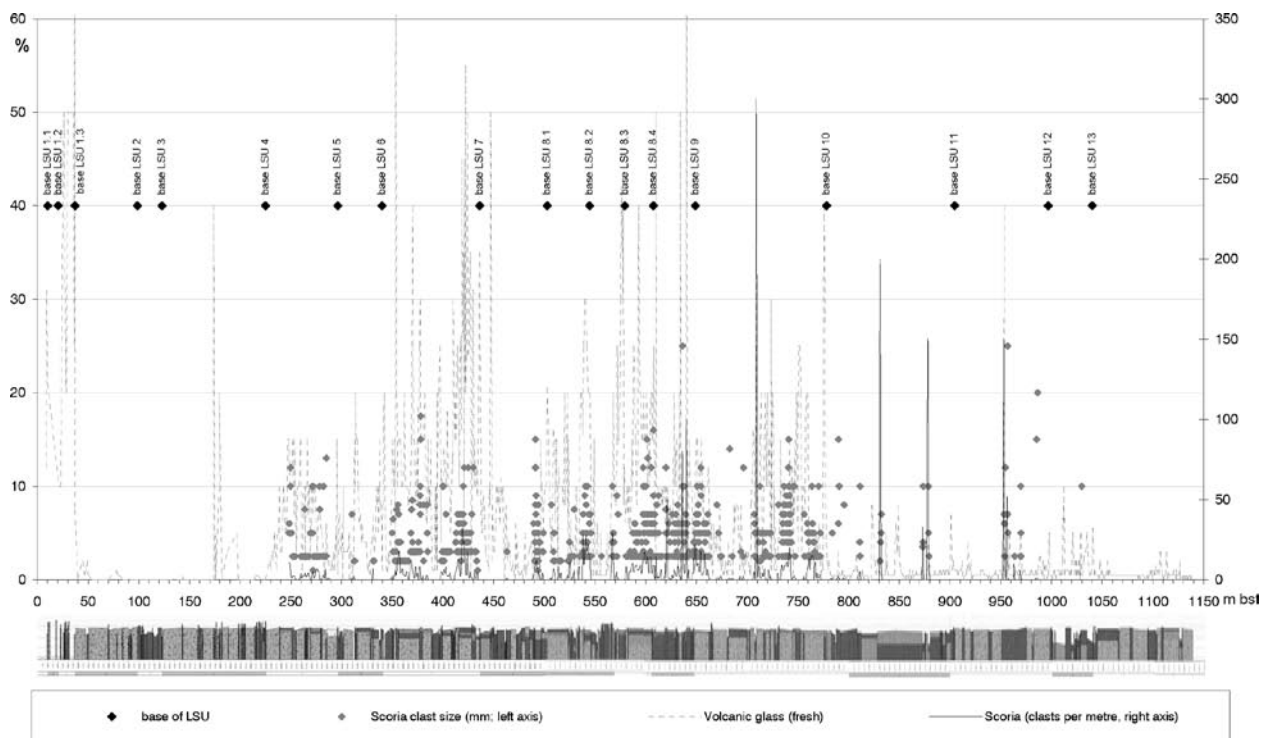


Fig. 25 – Plot of fresh volcanic glass recorded in smear slides, scoria and pumice clasts per metre recorded in the core and scoria clast size.

In the AND-2A core, highly vesiculated vitriclasts (scoria and pumice) are considered to be either primary (fallout tephra) or minimally reworked; wind blown and/or transported atop or within ice. Primary to gently reworked tephra layers are found within sandstone and siltstone at depths within the Early and Middle Miocene interval (1 093 to 640 mbsf; LSU 14-9). A 6 cm-thick layer of lapilli tuff occurs at 640 mbsf (LSU 9) and several clast supported accumulations of pumice, up to 3.5 cm thick, occur in ripple cross-laminated sands at 709 mbsf (LSU 10). Additional evidence for input from explosive activity include five, 2 to 7 metre-thick intervals between 355 and 765 mbsf (LSU 7-10) which contain accumulations of angular scoria and pumice dispersed (c. 20/m) within fine-grained glass-rich (up to 30 vol.%) sediments (Fig. 25). Volcanic glass and minerals from tephra horizons at c. 640, 709 and 831 mbsf were analysed by electron microprobe. Pumice consists of highly vesiculated colourless glass showing tubular vesicles with delicate bubble walls, which in most cases are filled by secondary minerals (e.g., dolomite, calcite, chlorite, zeolites, pyrite) or have been completely replaced. The pumice clasts are aphyric but in rare instances contain phenocrysts of K-feldspar (anorthoclase). Euhedral crystals of volcanic-derived alkali feldspar are found scattered within the tephra horizons. Analyses of the pumice glass show that they are highly altered, having very low alkali, magnesium and iron contents. Pumice from the lapilli tuff at 640 mbsf (Fig. 6F) are set in a fine grained matrix of volcanic ash of the same composition along with very small amounts of foreign detritus (e.g., rounded quartz and feldspar grains, rock fragments). These observations, along with the layer's normally graded gradational top and loaded

base, suggest that it was formed by direct sinking of subaerial pyroclastic fallout. Reworked tephra contain higher amounts of foreign detritus and have gradational tops and bases. Brown glass shards within the pumice-rich cross-laminated sands at c. 709 mbsf range in composition from basanite to hawaiite to mugearite (Fig. 2).

(d) *Sand petrology and smear slides.* Preliminary provenance analysis, based on petrography of sandstones and diamictites in the SMS core, indicates that sediment is dominated by the local McMurdo Volcanics for the duration of the core (c. 20 m.y.). Much is derived from erosion of the volcanic edifices which provide epiclastic material ranging from basaltic to intermediate, generally vesicular scoria and altered to unaltered clasts of intrusives and lava flows. Volcanic glass is a prominent component and ranges from blocky and cusped brown shards (mafic?), long tube white pumice (rhyolitic?), and blocky green shards (alkaline?) (Fig. 26). Glass composition changes down core (Fig. 27). Brown mafic glass is present in all of the samples examined down core (0 to c. 750 mbsf). White pumice glass comes in at LSU 4 at c. 125 mbsf. Alkaline green glass gets added c. 450 m down the core in LSU 8.1. The change in glass composition may indicate a change in the volcanic eruptive history in the region. A large component of the ash is fresh unaltered glass indicating ashfall onto ice sheets then transported to distal marine diamictites. However, much of the glass is variably altered to Fe-oxides, three types of zeolites, calcite, pyrite(?), chlorite and possibly glauconite depending on primary composition and depth in the core (Fig. 28). The change with depth of the alteration minerals is typical of a diffuse hydrothermal ore complex indicating

proximity to active volcanism. This interpretation is also supported by primary subaerial lava flows in the top 40 m of the core and a high geothermal gradient (inferred from high downhole temperatures, see Wonik et al., this volume)

Other framework grains in the core include quartz, feldspar, pyroxene, biotite and basement lithics including dolerites, granitoids, metasediments, and schists and gneisses. The metamorphic clasts were likely derived from the Koettlitz Group and the granitoids and many of the feldspars and quartz from the Granite Harbour Intrusives that form the local basement in the adjacent Transantarctic Mountains. Many of the quartz grains are well rounded and show remnant Si-cement preservation (Fig. 29). These were probably derived from the Beacon Supergroup quartz arenites. The well rounded grains are generally associated with an abundance of three different types of pyroxenes, probably derived from the Ferrar Dolerites that intruded the Beacon quartz arenites. The basement granitoid contribution increases up section whereas the Beacon/Ferrar contribution decreases indicating a general unroofing trend from the Transantarctic Mountains. Changes in the metamorphic basement clasts and the presence of

other minerals such as biotite, muscovite, amphiboles and pyroxenes may mirror the patterns seen in the clast counts and may reflect changes in ice transport from local Koettlitz Glacier area to further south in the Skelton Glacier area.

The sedimentary fill within the Ross Sea Embayment provides a unique record of the interaction of volcanism, glacial sedimentation and the formation of the West Antarctic rift system during the Cenozoic. The SMS drill site is at the southern end of the Victoria Land Basin in a complex structural half graben along the Transantarctic Mountain front. The location of large volcanic edifices is possibly fault controlled and has affected both the geometry of the basin and the diagenesis of the sedimentary deposits. Since sedimentary fill records the advance and retreat of local glaciers draining off the Transantarctic Mountains into the Victoria Land Basin and the interaction with the West Antarctic Ice Sheet it is important to correctly interpret the tectonic control on glacier flow. Provenance analysis of the deposits will reveal the unroofing history of the Transantarctic Mountains, activity on basin bounding faults, and the timing of the onset of nearby volcanism and local impedance of flow.

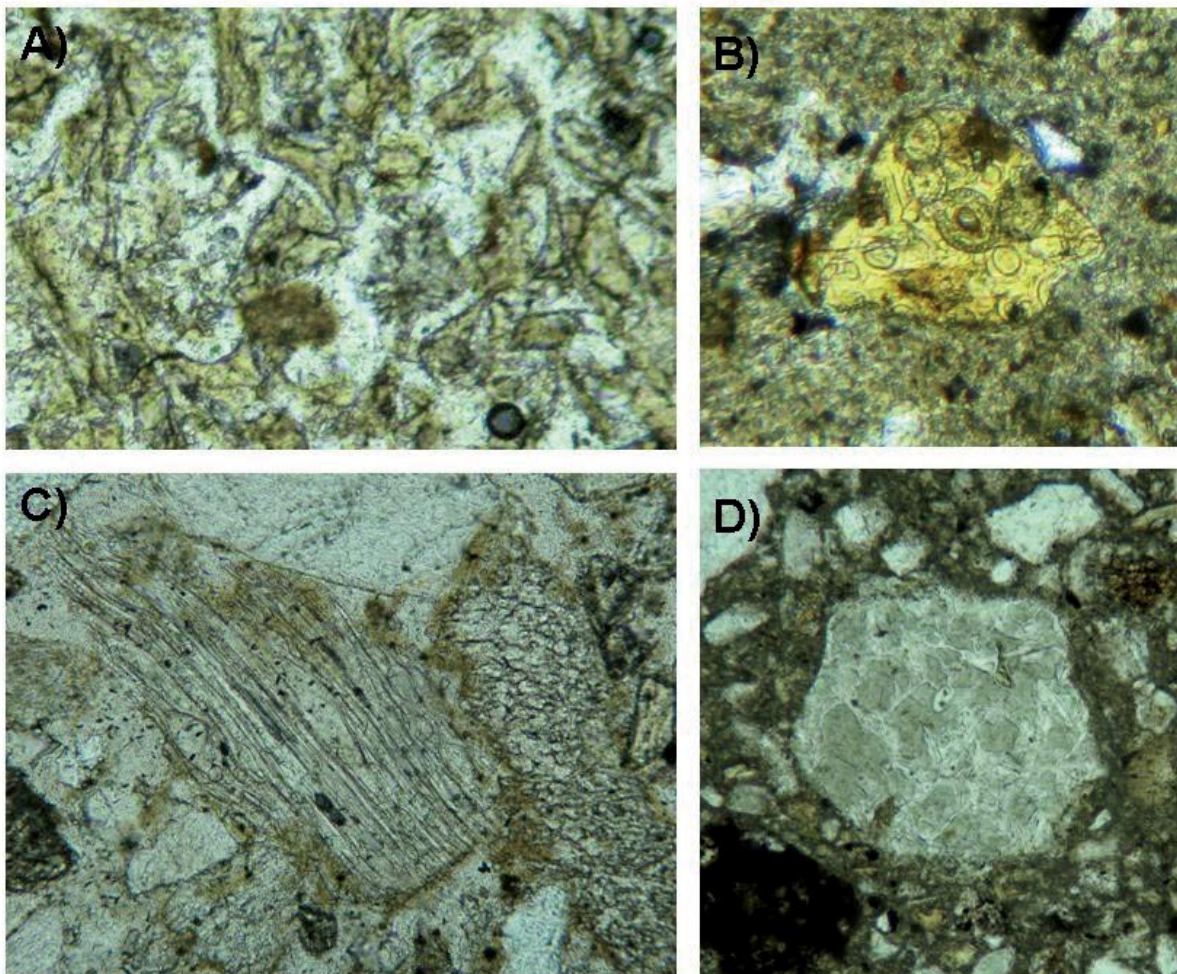


Fig. 26 – Glass types change down core. Brown possibly mafic glass is present throughout the core but changes from cusped shards in LSU 1 (a), example 136.32 mbsf, to blocky or rounded in all other occurrences (b), example from LSU 1 29.95 mbsf. Clear possibly rhyolitic pumice comes in at LSU 4 (c), example 173.52 mbsf. Green possibly alkaline glass, generally blocky to rounded, occurs from LSU 8 to 10 (d), example from LSU 10 714.01mbsf.

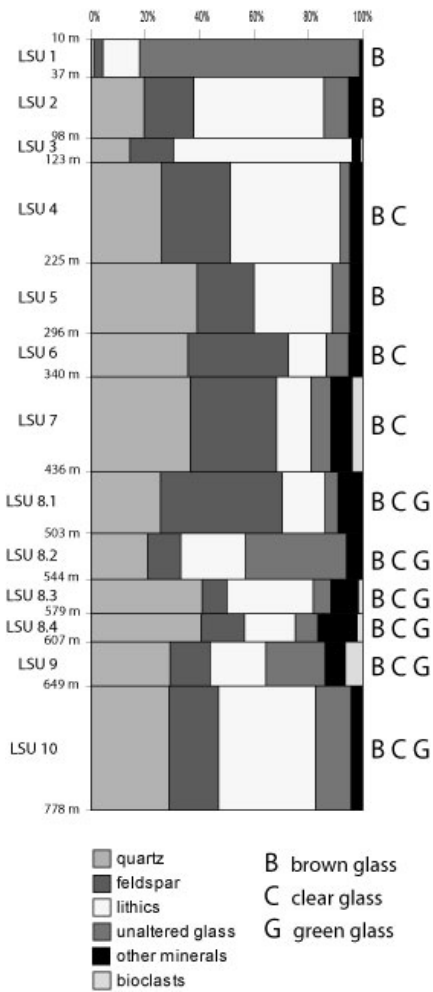


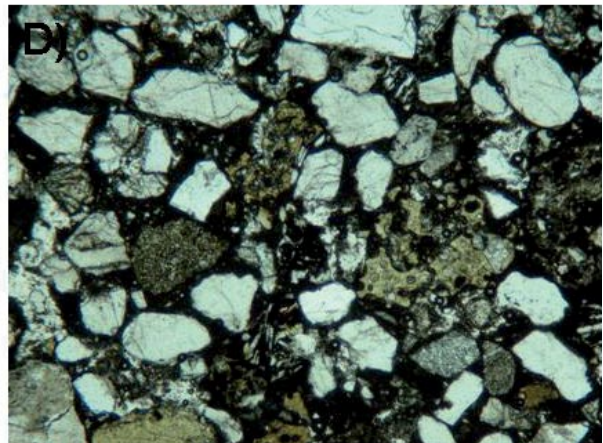
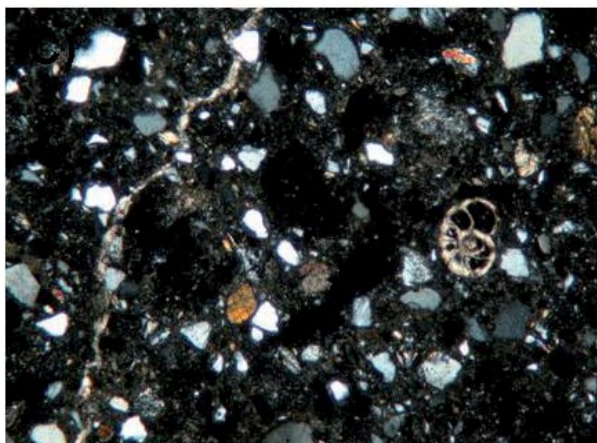
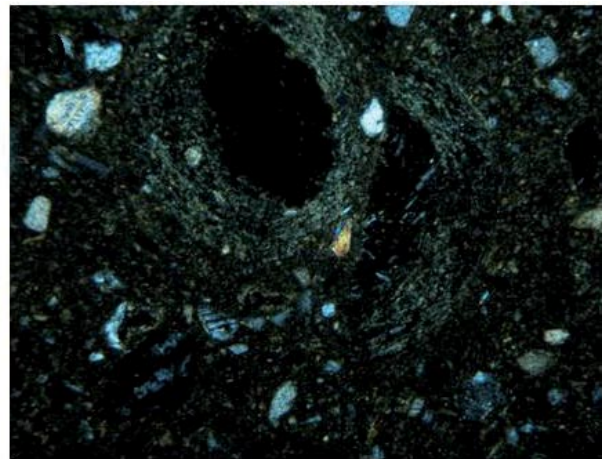
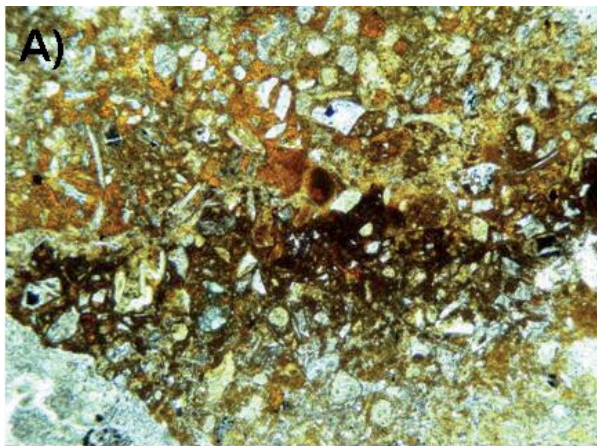
Fig. 27 (left) – The bar graph shows estimates of percentages of framework minerals divided by LSU. Glass types are identified along the side and include both altered and unaltered grains.

Features apparent from a compilation of smear slide data over the entire drillhole indicate: 1) an increase in both biogenic silica and fresh volcanic glass from c. 230 to 780 mbsf. Biogenic silica, fresh volcanic glass and non-biogenic carbonate each occur in pulses, commonly showing ramping up or down trends rather than occurring as single spikes; 2) high sand proportions in the “terrigenous” component occur from c. 350 to 750 mbsf and below 970 mbsf.

The abundance of scoria clasts in the core approximately matches that of fresh volcanic glass (Fig. 25), suggesting variations in fresh glass content record variations in volcanic activity and are not controlled entirely by diagenesis. Crossplots indicate that high biogenic silica does not correlate with high fresh volcanic glass, suggesting abundances of the two components are not linked directly.

Biogenic silica is present in most of the diamictites in LSUs 5 to 14 at background levels and this

Fig. 28 (below) – Examples of various diagenetic features. (a) Brown glass altering to Fe-oxide at shallow depths in the core. Example from LSU 1 29.95 mbsf. (b) Chlorite rims around volcanic grains. Example from LSU 2 68.91 mbsf. (c) Calcite veins and microspar. Example from LSU 5 256.40 mbsf. (d) Black opaque, possibly pyrite, cement. Example from LSU 9 648.45 mbsf.



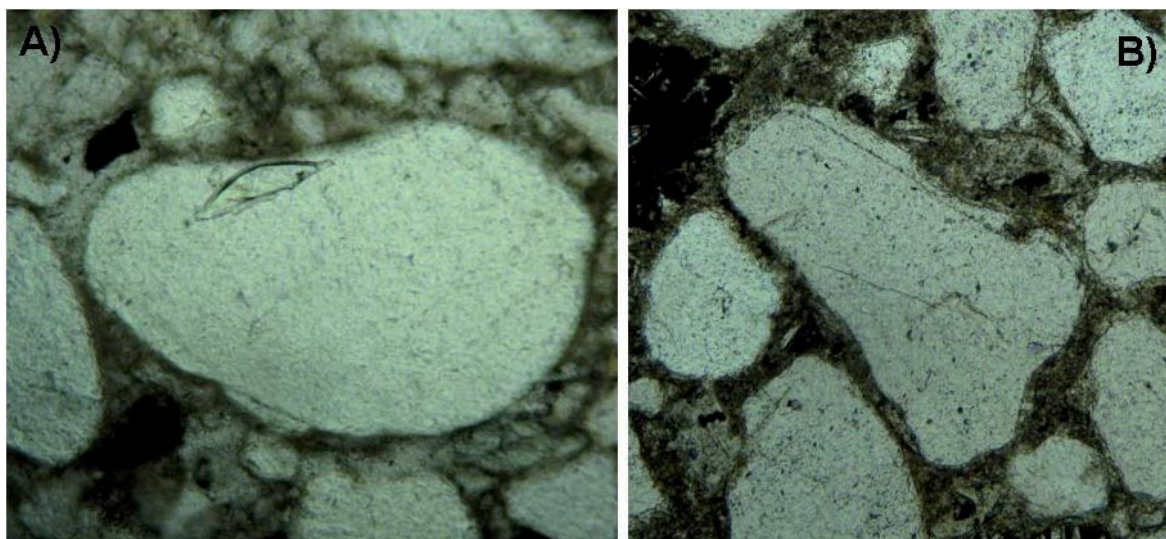


Fig. 29 – Well rounded quartz grains with preserved quartz overgrowths become more common down core. Examples from LSU 6 (A) 313.59 mbsf, FoV= 2 mm. (B) 327.04 mbsf, FoV= 0.5 mm.

suggests the diamictites were deposited as rain-out from non-grounded ice (though some could have been reworked). Variations in the abundance of biogenic silica between LSUs might record changes in productivity or watermass turbidity, perhaps related to changes in climate and types of glacial activity. The percentage of sand in the matrix of some diamictites appears to increase (or decrease) up-section. This might be related to ice advance or retreat.

Initial crossplots show few clear relationships, though high spar content seems to correlate with high sand content, with most spar in units with 40-60% sand. Micrite-sized carbonate occurs widely in silty lithologies and also occurs in highly sandy lithologies though it should be noted that the size range of carbonate particles might have been altered during the sampling process. Some mutual exclusions appear to hold:

- High micrite does not occur with high clay
- High spar does not occur with high clay
- High biogenic silica does not occur with high carbonate
- High spar does not occur with high micrite
- High micrite does not occur with high biogenic silica
- High spar does not occur with high biogenic silica
- High carbonate occurs rarely with high fresh volcanic glass

(e) *Continuous XRF scanning.* The first extracted element counts of the raw data from Si, Cl, K, Ca, Ti, Fe and Ba were used to divide the AND-2A core into 13 Geochemical Units (GUs) and several subunits (Tab. 1 and Figs. 3 & 17). Each of these elements can be used to improve the identification of variations in the sedimentary environment that could be correlated with palaeoclimatic changes in the Antarctic cryosphere.

Iron typically reflects a terrigenous or volcanic source. In the AND-2A core Fe increase in sandstones and diamictites with a high volcanic component.

Correspondingly the Fe counts drop in better sorted sandstones. Furthermore the Ti in the core shows the same geochemical pattern as Fe and can be also interpreted as terrigenous and volcanic signal. Only between 700 and 720 mbsf the Ti and Fe peaks are anti-correlated (Fig. 17). This could be related to a diagenetically reduced Fe content. The measured Ca values can probably be associated with  $\text{CaCO}_3$  from a biogenic or diagenetic source. In addition, the observed marble clasts from the basement rocks and calcite veins can affect the Ca counts. K is usually a terrigenous-derived element and is often related to finer-grained sediments in the core. High values of K can be found in diamictite above 224.82 mbsf, and in the sand and siltstones below (Fig. 3). In the AND-2A core the XRF measurements of Ba have to be investigated with care. The drilling fluid contains  $\text{BaSO}_4$ , which could have contaminated the core. Particularly the observed high peak of Ba at 353 mbsf can be an indicator for penetration of drilling fluid throughout the core (Fig. 3).

The high-resolution geochemical data set of the AND-2A core provides an outstanding opportunity to obtain information about rapid paleoclimatic changes in the Antarctic realm by compositional changes that are reflected in elemental variations down-core. These variations show a rhythmically stacked pattern in parts and will be tested for a relationship to orbital changes. Sharp gradients will be interpreted as glacial surfaces of erosion generated during glacial advances, or surfaces of transgressions during rising sea levels in warmer periods or enhanced tectonic subsidence. To ensure the quality of the data collected on-ice, diverse corrections will be carried out on all core sections (see Ar correction in Appendix 3 and *Explanatory Notes*, this volume). XRF core scanning measurements on open cracks, filled veins and on the clasts are still within the data set and have to be removed manually.

(f) *Geochemistry of clasts and glasses.* The first 20 samples analysed by XRF for whole-rock major

Tab. 1 - Geochemical Units (GU) for AND-2A core.

| Geochemical Unit | Top [mbsf] | Bottom [mbsf] |
|------------------|------------|---------------|
| 1.1              | 0.00       | 10.22         |
| 1.2              | 10.22      | 20.57         |
| 1.3              | 20.57      | 37.07         |
| 2.1              | 37.07      | 98.47         |
| 3.1              | 98.47      | 122.86        |
| 4.1              | 122.86     | 224.82        |
| 5.1              | 224.82     | 296.34        |
| 6.1              | 296.34     | 339.92        |
| 7.1              | 339.92     | 389.03        |
| 7.2              | 389.03     | 436.18        |
| 8.1              | 436.18     | 489.66        |
| 8.2              | 489.66     | 530.13        |
| 8.3              | 530.13     | 551.46        |
| 8.4              | 551.46     | 579.33        |
| 8.5              | 579.33     | 607.35        |
| 9.1              | 607.35     | 648.74        |
| 10.1             | 648.74     | 662.69        |
| 10.2             | 662.69     | 684.90        |
| 10.3             | 684.90     | 700.31        |
| 10.4             | 700.31     | 726.31        |
| 10.5             | 726.31     | 744.12        |
| 10.6             | 744.12     | 774.94        |
| 11.1             | 774.94     | 904.66        |
| 12.1             | 904.66     | 964.38        |
| 12.2             | 964.38     | 970.10        |
| 12.3             | 970.10     | 1040.28       |
| 13.1             | 1040.28    | 1102.20       |
| 13.2             | 1102.20    | 1109.47       |
| 13.3             | 1109.47    | 1138.54       |

elements are from LSU 1.1, 1.2, 2, 4, 5, 7, 9 and 10. As a general observation, all the samples have alkaline affinity, plotting inside the known compositional fields of the McMurdo Volcanic Group (Fig. 2). Yet, significant compositional differences are observed. According to the relationships between silica and alkali contents, an overall strongly alkaline affinity is highlighted for samples from LSU 1.1 and 1.2. In contrast, samples from LSU 2, 4, 5, 7, 9 and 10 are characterised by a moderately alkaline affinity.

In terms of evolutionary degree, both affinity lineages include primitive to poorly evolved samples along with strongly evolved ones. It is noteworthy that the most evolved samples (trachyte and rhyolite) from the moderately alkaline lineage have a peralkaline chemical signature.

The preliminary glass shard analyses from AND-2A core, when compared to the major element XRF whole-rock data of the volcanic clasts, show overall more basic compositions and partial overlap with the basic-intermediate clast samples.

Finally, the whole rock clast and glass shard

compositions from AND-2A core display a very limited overlap with the volcanic glasses from AND-1B core (Pompilio et al., 2007, Fig. 6). This distinction might indicate an important spatial and temporal change in the chemical evolution of the volcanic activity in the region.

## PORE WATER GEOCHEMISTRY AND DIAGENESIS

Thirty-five 5- to 10-cm-long whole-round core samples were collected from the AND-2A core for extraction and analysis of interstitial water. The sampling protocol called for obtaining 5 cm sections from the PQ core (0 - 229.12 mbsf) and 10 cm sections from the narrower gauge HQ core (229.12 - 1011.04 mbsf). These samples were taken at c. 10 m intervals to 100 mbsf, and then every c. 20 m to the bottom of the HQ hole. The shallowest sample was taken from 9.67 mbsf and the deepest from 963.44 mbsf, ensuring coverage of diagenetic processes throughout the PQ and HQ holes. Because of its relatively narrow diameter, the NQ core was not sampled for pore water analysis. Methods employed in the pore water geochemistry and diagenesis study is presented in the section *Explanatory Notes* (this volume).

## RESULTS

Analytical results are provided in table 2 and figure 30. The two shallowest samples (AND-2A 9.67 and 25.17 mbsf) were frozen during transit, and resulting data should be treated with caution. Of the samples collected, 21 yielded enough pore water for analysis. The remaining samples were either dry (no yield) or deemed too lithified to squeeze and returned to the curator for replacement into the core. Splits of the pore water samples were analysed for conductivity, pH and, when more than c. 8 ml of water was collected, alkalinity. Additional splits were stored for off-ice determinations of oxygen, hydrogen, carbon and strontium isotopic compositions.

Alkalinity increases downcore, from 2.4 mM at 9.67 mbsf to a maximum of 54.9 mM at 293.30 mbsf. Two samples analysed below this depth yielded progressively lower values: 46.0mM at 336.18 mbsf and 13.5 mM at 545.0 mbsf. Salinity, determined from chloride measurements (salinity, *psu* = *Cl*, *ppt* x 1.80655), increases downcore. Within the upper 100 mbsf, values remain within the range of normal to highly saline seawater. At greater depths, salinity crosses the brine threshold of 50 *psu* and increases gradually downcore to a maximum of 198 *psu* at 963.44 mbsf. The pH drops from 7.8 at 9.67 mbsf, a value close to that of seawater, to 6.4 at 30.09 mbsf. The pH then shows little variation ( $6.5 \pm 0.2$ ) downcore to 619.35 mbsf. The pH values below this point are relatively high, reaching a maximum of 7.5 at 779.69 mbsf.

Concentrations of Na, K, Mg, Ca and Li were determined down to 619.35 mbsf (Fig. 30). For each element, concentrations increase from near seawater values at the top of the core to concentrations that are several times higher at depth. Sodium concentrations increase linearly from c. 12 000 parts per million (ppm) to a maximum of c. 49 000 ppm. The potassium content also increases with depth, from c. 550 ppm near the top of the core to c. 3 000 ppm at 619.35 mbsf. Although Mg and Li concentrations also increase downcore, their profiles are more variable (Fig. 30). Both elements increase from near-seawater concentrations at the top of the core to higher concentrations (Mg = 5 134 ppm; Li = 4.73 ppm) at 293.30 mbsf. Concentrations then decrease through LSU 6 and into the upper c. 50m of LSU 7. The maximum concentrations of these elements occur at 545.01 mbsf (Mg = 6 700 ppm; Li = 5.16 ppm), below a sampling gap of approximately 200 m. The deepest samples at 619.35 mbsf have lower concentrations. Although Ca was also measured, the results are considered unreliable due to a high Ca<sup>2+</sup> content in the blank (Crary Lab Milli-Q water) that was used to prepare sample and standard dilutions.

Concentrations of the major anions Cl<sup>-</sup>, Br<sup>-</sup> and SO<sub>4</sub><sup>2-</sup> were determined down to 963.44 mbsf (Fig. 30). As with the major cations, the Cl and Br contents

increase from near seawater values at the top of the core to concentrations several times higher at depth. In the upper part of the core, chloride and bromide concentrations increase linearly to a depth of 155.76 mbsf to 39 582 ppm and 125 ppm, respectively. Between 155.76 and 235.66 mbsf, the concentrations of both concentrations nearly double, to 69 990 ppm Cl and 240 ppm Br. Concentrations increase linearly below this point, to maxima of 109 950 ppm and 417 ppm for Cl and Br, respectively (Fig. 30). Unlike the other major ions, sulfate shows little variation from average seawater values of with depth, averaging 2600 ± 154 ppm.

#### DISCUSSION OF PORE WATER CHEMISTRY

The alkalinities and salinities reach values that are exceptionally high for marine sediments. Salinity crosses the threshold (50 psu) from saline water to brine between c. 150 and 225 mbsf and reaches values that exceed 5x seawater salinity at 963.44 mbsf. The most plausible explanation for the presence of a high-alkalinity brine involves exchange between pore fluids and reactive volcanogenic particles, in particular volcanic glass, that make up a large proportion of the host sediment. Water-rock exchange in volcanoclastic sediments has been shown

Tab. 2 - Salinity, pH, alkalinity and major ion concentrations in AND-2A core pore water.

| Top (mbsf)           | Bottom (mbsf) | Salinity (psu) | pH  | Alkalinity (mM) | Li (ppm) | Na (ppm) | K (ppm) | Mg (ppm) | Cl (ppm) | Br (ppm) | Sulfate (ppm) |
|----------------------|---------------|----------------|-----|-----------------|----------|----------|---------|----------|----------|----------|---------------|
| 9.67                 | 9.72          | 41.9           | 7.8 | 2.38            | 0.48     | 12809    | 1198    | 1427     | 23192    | 80       | 2841          |
| 30.09                | 30.15         | 36.9           | 6.4 | 17.39           | 1.19     | 11275    | 547     | 1373     | 20432    | 81       | 2682          |
| 37.41                | 37.46         | 39.2           | 6.5 | 30.93           | 1.70     | 12026    | 559     | 1631     | 21700    | 87       | 2561          |
| 43.72                | 43.77         | 42.2           | 6.6 | 44.14           | 1.99     | 12945    | 673     | 1866     | 23362    | 89       | 2430          |
| 51.30                | 51.35         | 44.4           | 6.8 | 40.81           | 2.16     | 13740    | 676     | 1984     | 24576    | 92       | 2519          |
| 57.21                | 57.26         | 44.3           | 6.6 | 42.00           | 2.14     | 13752    | 668     | 1971     | 24524    | 92       | 2485          |
| 62.66                | 62.71         | 44.2           | 6.6 | 38.34           | 1.98     | 13756    | 705     | 1905     | 24494    | 96       | 2421          |
| 73.15                | 73.20         | 52.6           | 6.6 | 41.64           | 2.26     | 16591    | 825     | 2413     | 29098    | 113      | 2917          |
| 81.03                | 81.08         | 46.2           | 6.4 | 38.80           | 2.00     | 14286    | 765     | 1987     | 25586    | 93       | 2441          |
| 92.97                | 93.02         | 47.4           | 6.4 | 44.51           | 2.01     | 14723    | 692     | 2141     | 26222    | 94       | 2499          |
| 116.22               | 116.27        | 51.5           | 6.6 | 35.76           | 1.77     | 15931    | 696     | 2311     | 28492    | 106      | 2821          |
| 155.76               | 155.81        | 71.5           | 6.4 | 53.02           | 2.97     | 20330    | 1021    | 2646     | 39582    | 125      | 2853          |
| 235.66               | 235.76        | 126.4          | 6.3 | 51.00           | 4.07     | 34437    | 1832    | 4589     | 69990    | 241      | 2589          |
| 293.30               | 293.40        | 134.5          | 6.5 | 54.92           | 4.73     | 36904    | 1667    | 5134     | 74451    | 260      | 2376          |
| 336.18               | 336.28        | 147.5          | 6.0 | 46.04           | 4.13     | 39603    | 1857    | 5170     | 81653    | 261      | 2598          |
| 353.53               | 353.63        | 144.3          | 6.7 | -               | 3.74     | 38995    | 2093    | 4961     | 79854    | 267      | 2556          |
| 545.01               | 545.11        | 177.5          | 6.4 | 13.48           | 5.16     | 49179    | 2597    | 6700     | 98244    | 339      | 2817          |
| 619.35               | 619.45        | 174.7          | 6.1 | -               | 4.12     | 47057    | 2970    | 5802     | 96704    | 333      | 2481          |
| 779.69               | 779.79        | 185.4          | 7.5 | -               | -        | -        | -       | -        | 102630   | 361      | 2520          |
| 809.84               | 809.94        | 174.3          | -   | -               | -        | -        | -       | -        | 96491    | 329      | 2307          |
| 963.44               | 963.54        | 198.0          | 7.0 | -               | -        | -        | -       | -        | 109590   | 418      | 2874          |
|                      |               |                |     |                 |          |          |         |          |          |          |               |
| Crary seawater       |               | 35.8           | -   | -               | 0.39     | 11098    | 424     | 1249     | 19820    | 69       | 2864          |
| Fm water (~360 mbsf) |               | 133.6          | -   | -               | 3.54     | 35782    | 2072    | 4522     | 73926    | 230      | 2744          |

to produce brines at relatively low temperatures and over geologically short time intervals (Egeberg, et al., 1990; Egeberg, 1992; Martin, 1994; Martin, et al., 1995). The major processes involve uptake of H<sub>2</sub>O by hydration of volcanic glass and the formation of hydrous secondary minerals such as zeolites, layered

silicates, and chlorite (Gifkins, et al., 2005). These phases are present throughout much of the section, as replacement phases and as cement in intra- and inter-granular pore space (see Fielding, et al., this volume). As H<sub>2</sub>O is taken up into hydrous phases, ions that do not readily go into other minerals (*i.e.* Cl<sup>-</sup>)

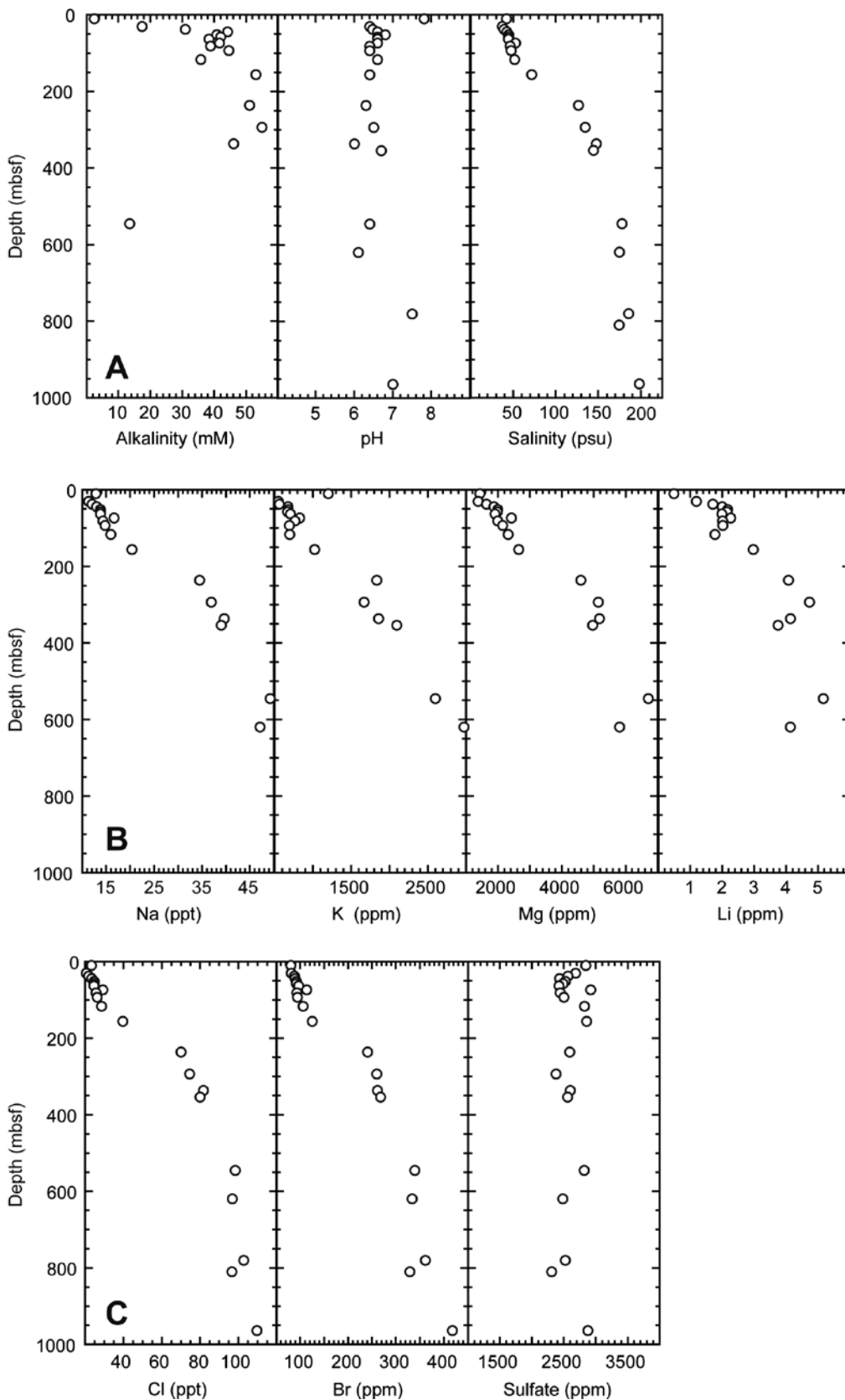
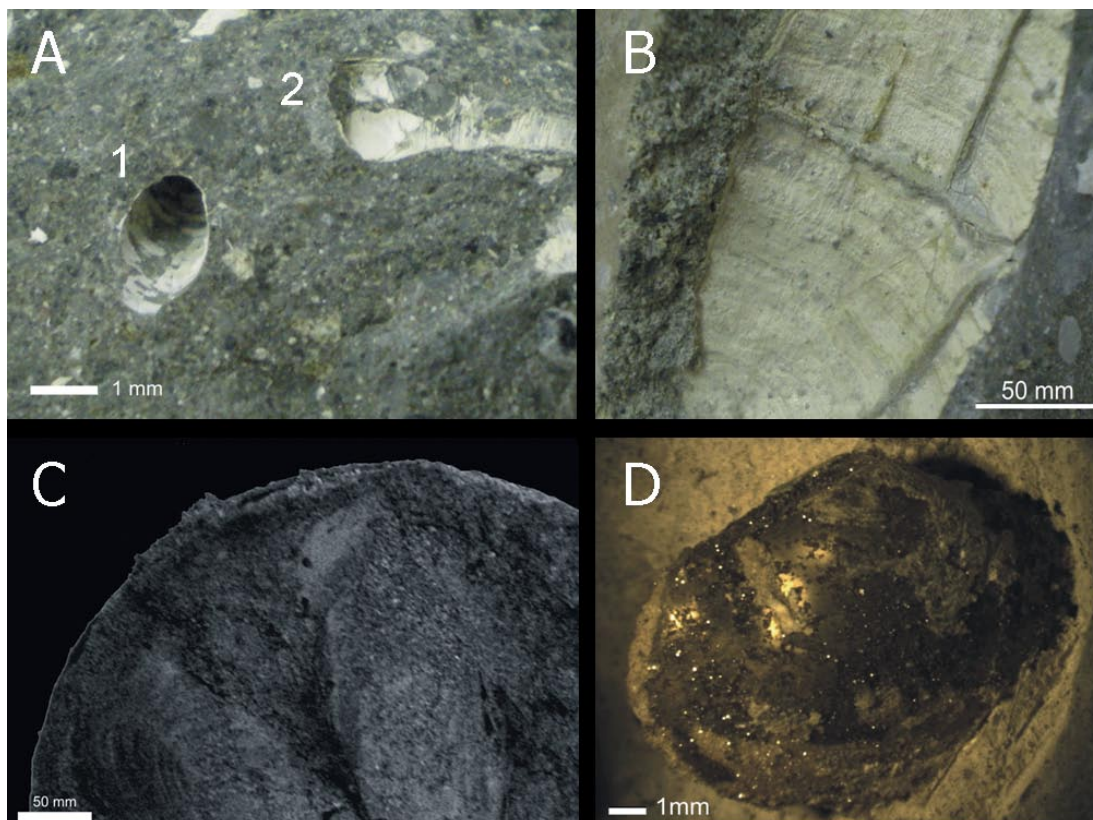
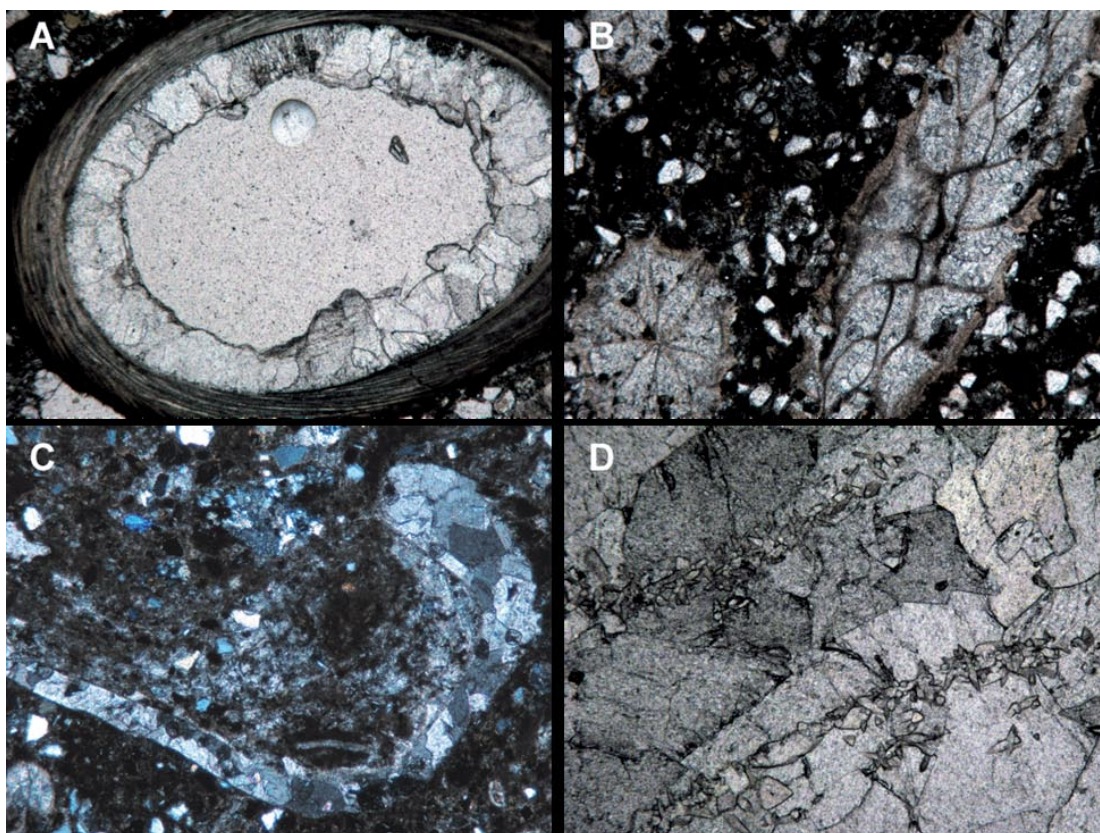


Fig. 30 – Pore water geochemical profiles for AND-2A. (A) Salinity, pH and alkalinity. (B) Major cations: Na, K, Mg and Li. (C) Major anions: Cl, Br and sulfate.



*Fig. 31* – Photographs of allochems showing various types of carbonate skeletal preservation in AND-2A. (A) Serpulid tubes displaying almost complete dissolution of original shell resulting in (1) vugs and (2) chalky texture (367.54 mbsf). (B) Chalky, almost sugar-like texture of a large barnacle plate (159.02 mbsf). (C) Mold of a completely dissolved shell of an articulated hiatellid bivalve (377.19 mbsf). (D) Pyritised mold of an articulated protobranchiate bivalve (543.15 mbsf).



*Fig. 32* – Photomicrographs of carbonate allochems in AND-2A. FoV = 4 mm. (A) Serpulid tube showing preservation of foliated microstructure. Intraparticle space is partially infilled with bladed calcite cement. (B) Bryozoan fragments showing well-preserved skeletal microstructure. Intraparticle space is completely filled with bladed to blocky calcite cement. (C) Mold of a bivalve shell that has been completely infilled with blocky calcite cement. (D) Gastropod mold. Shell walls have been replaced by bladed calcite cement, shown stretching from lower left to upper right across the lower third and upper third of the photograph. Intraparticle pore space is filled with coarse, blocky calcite cement.

are expelled and build up in the pore water system. Reaction rates in the AND-2A core may have also been enhanced by the relatively high geothermal gradient in the area (45 K/km), based downhole logging results (see Wonik, et al., this volume).

#### DIAGENESIS OF CARBONATE ALLOCHEMS

Calcareous allochems are consistently distributed throughout the core and represented by marine invertebrate skeletal parts which were originally calcitic, namely serpulids, bryozoans, cirripeds (barnacles), foraminifers, brachiopods, ostracods, echinoderms, bivalves (*pro-parte*), aragonitic (gastropods, bivalves *pro-parte*) and perhaps mixed (bivalves *pro-parte*). Preservation of the calcareous allochems ranges from excellent to poor. Various types of allochem preservation have been observed, which grade from partial to complete dissolution of skeletal carbonate and/or mineral replacement in response to a variety of taphonomic processes (Fig. 31). As for many other Cenozoic drillcores records (e.g., Aghib, et al., 2003; Bellanca, et al., 2005), these *post-mortem* diagenetic skeletal alterations may significantly affect the original biological legacy introducing a potential bias in the assessment of past environmental attributes (Cape Roberts Science Team, 1998, 1999, 2000; Taviani et al., 2000). Many partially altered specimens have a chalky appearance in the core (Fig. 31A, B). In thin section, the remains of calcitic organisms appear relatively well preserved (Fig. 32A, B), with primary microstructures clearly visible. Despite preservation of shells and tests, however, the intragranular pore space in these grains is often partially- to completely-filled with blocky calcite and, below 430 mbsf, pyrite cement. With the exception of a few samples, in particular those that lie between c. 430 and 431 mbsf and possibly at 1 063.71 mbsf, the aragonitic mollusc shells are altered. In the most extreme cases, shells (mainly gastropods and bivalves) have been removed by dissolution, leaving molds behind (Fig. 31C). Some molds, including the original shell interior, have been filled with coarse blocky calcite cement, a relatively common case affecting serpulid tubes and gastropods (Fig. 32D). In some specimens of serpulids and bivalves, both original shell and its infilling have been replaced by pyrite (Fig. 31D).

*Acknowledgements* - We are all indebted to the curatorial staff and to Steven Petrushak (Florida State University) for his daily thin-sectioning hard (and excellent) work. We thank ARISE team members Joanna Hubbard and Rainer Lehmann for taking photomicrographs of the smear slides, and Ken Mankoff for help with *ViewPoints* software. Cross plots were made using *ViewPoint* (Levit & Gazis, [http://astrophysics.arc.nasa.gov/~pgazis/viewpoints/vp\\_download\\_page.htm](http://astrophysics.arc.nasa.gov/~pgazis/viewpoints/vp_download_page.htm)). Tracy Frank would like to thank Chieh Peng (IODP) for advice on lab preparation in the lead-up to the field season. She is also grateful to Kathy Welch (Byrd Polar Research Center, The Ohio State University) for providing

access to the Ion Chromatograph overseen by the Long Term Ecological Research (LTER) group in the Cray Science and Engineering Centre at McMurdo Station. The assistance of the drill-site team in the selection and preservation of whole-round samples is also appreciated. The ANDRILL Programme is a multinational collaboration between the Antarctic programmes of Germany, Italy, New Zealand and the United States. Antarctica New Zealand is the project operator and developed the drilling system in collaboration with Alex Pyne at Victoria University of Wellington and Webster Drilling and Exploration Ltd. Antarctica New Zealand supported the drilling team at Scott Base; Raytheon Polar Services Corporation supported the science team at McMurdo Station and the Cray Science and Engineering Laboratory. The ANDRILL Science Management Office at the University of Nebraska-Lincoln provided science planning and operational support. Scientific studies are jointly supported by the US National Science Foundation (NSF), NZ Foundation for Research, Science and Technology (FRST), the Italian Antarctic Research Programme (PNRA), the German Research Foundation (DFG) and the Alfred Wegener Institute for Polar and Marine Research (AWI).

#### REFERENCES

- Acton G., Florindo F., Jovane L., Lum B., Ohneiser C., Sagnotti L., Strada E., Verosub K.L., Wilson G.S., & the ANDRILL-SMS Science Team, 2008. Preliminary Integrated Chronostratigraphy of the AND-2A Core, ANDRILL Southern McMurdo Sound Project, Antarctica. *Terra Antarctica*, this volume
- Adegbie A.T., Schneider R.R., Röhl U. & Wefer G., 2003. Glacial millennial-scale fluctuations in central African precipitation recorded in terrigenous sediment supply and freshwater signals offshore Cameroon. *Palaeogeography, Palaeoclimatology, Palaeoecology*, **197**, 323-333.
- Aghib F.S., Fielding C.R. & Frank T.D., 2003. Carbonate diagenesis of the Cenozoic sedimentary succession from the CRP-3 core, Ross Sea, Antarctica. *Terra Antarctica*, **10**, 27-37.
- Armienti P., Civetta L., Innocenti F., Manetti P., Tripodo A., Villari L. & Vita G., 1991. New petrological and geochemical data on Mt. Melbourne volcanic field, Northern Victoria Land, Antarctica. (II Italian Antarctic Expedition). *Memorie della Società Geologica Italiana*, **46**, 397-424.
- Balsam W.L., Deaton B.C. & Damuth J.E., 1998. The effects of water content on diffuse reflectance spectrophotometry studies of deep-sea sediment cores. *Marine Geology*, **149**, 177-189.
- Bellanca A., Aghib F., Neri R. & Sabatino N., 2005. Bulk carbonate isotope stratigraphy from CRP-3 core (Victoria Land Basin, Antarctica): evidence for Eocene-Oligocene palaeoclimatic evolution. *Global and Planetary Change*, **45**, 237-247.
- Cape Roberts Science Team, 1998. Initial Report on CRP-1, Cape Roberts Project, Antarctica. *Terra Antarctica*, **5**, 1-187.
- Cape Roberts Science Team, 1999. Studies from Cape Roberts Project. Initial Report on CRP-2/2A, Ross Sea, Antarctica. *Terra Antarctica*, **6**, 1-173.
- Cape Roberts Science Team, 2000. Studies from the Cape Roberts Project, Ross Sea, Antarctica. Initial Report on CRP-3. *Terra Antarctica*, **7**, 1-209.
- Egeberg P.K. & Leg 126 Shipboard Scientific Party, 1990. Unusual composition of pore waters found in the Izu-Bonin fore-arc sedimentary basin. *Nature*, **344**, 215-218.
- Egeberg P.K., 1992. Thermodynamic aspects of Leg 126 Interstitial Waters. *Proceedings of the Ocean Drilling Program, Scientific Results*, **126**, 519-529.
- Fielding C.R., Atkins C.B., Bassett K.N., Browne G.H., Dunbar G.B., Field B.D., Frank T.D., Krissek L.A., Panter K.S., Passchier S., Pekar S.F., Sandroni S., Talarico F., & the ANDRILL-SMS Science Team, 2008. Sedimentology and Stratigraphy of the AND-2A Core. ANDRILL Southern McMurdo Sound Project, Antarctica. *Terra Antarctica*, this volume.

- Gieskes J.M., Gamo T. & Brumsack H., 1991. Chemical methods for interstitial water analysis aboard JOIDES Resolution. *Ocean Drilling Program, Technical Note* **15**, 60 pp.
- Giffkins C., Hermann W. & Large R., 2005. Altered Volcanic Rocks: A Guide to Description and Interpretation. Centre for Ore Deposit Research (CODES), University of Tasmania, Australia, 275 pp.
- Grützner J., Hillenbrand C.D. & Rebesco M., 2005. Terrigenous flux and biogenic silica deposition at the Antarctic continental rise during the late Miocene to early Pliocene: implications for ice sheet stability and sea ice coverage. *Global and Planetary Change*, **45**, 131-149.
- Haug G. H., Hughen K.A., Sigman D.M., Peterson L.C. & Röhl U., 2001. Southward migration of the intertropical convergence zone through the Holocene. *Science*, **293**, 1304-1308.
- Helmke J.P., Bauch H.A., Röhl U. & Mazaud A., 2005. Changes in sedimentation patterns of the Nordic seas region across the mid-Pleistocene. *Marine Geology*, **215**, 107-122.
- Kyle P.R., Moore J.A. & Thirlwall M.F., 1992. Petrologic evolution of anorthoclase phonolite lavas at Mount Erebus, Ross Island, Antarctica. *Journal of Petrology*, **33**, 849-875.
- Kretz R., 1983. Symbols for rock forming minerals. *Am. Mineral.*, **68**, 277-279.
- LeMasurier, W.E. & Thomson, J.W. (Eds.), 1990. Volcanoes of the Antarctic Plate and Southern Oceans. *Antarctic Research Series*, **48**, American Geophysical Union, Washington, D.C., 487 pp.
- Manheim F.T. & Sayles F.L., 1974. Composition and origin of interstitial waters of marine sediments, based on deep sea drill cores. In: Goldberg E.D. (Ed.), *The Sea: Marine Chemistry*, (Vol. 5). The Sedimentary Cycle. New York (Wiley), 527-568.
- Martin J.B., 1994. Diagenesis and hydrology at the New Hebrides forearc and intra-arc basin. *Proceedings of the Ocean Drilling Program, Scientific Results*, **134**, 109-130.
- Martin J.B., Kastner M. & Egeberg P.K., 1995. Origins of saline fluids at convergent margins, In: Taylor B. & Natland J. (Eds.), *Active Margins and Marginal Basins of the Western Pacific. AGU Geophysical Monograph Series*, **88**, 219-239.
- Minolta Camera Co. L., 1991. *Spektrophotometer CM-2002 Bedienerhandbuch*. In: L. Minolta Camera Co. (Ed.), Minolta GmbH, Ahrensburg.
- Pompilio M., Dunbar N., Gebhardt A.C., Helling D., Kuhn G., Kyle P., McKay R., Talarico F., Tulaczyk S., Vogel S., Wilch T. & the ANDRILL-MIS Science Team, 2007. Petrology and geochemistry of the AND-1B Core, ANDRILL McMurdo Ice Shelf Project, Antarctica. *Terra Antarctica*, **14**, 255-288.
- Richter T.O., van der Gaast S., Koster B., Vaars A., Gieles R., de Stigter H.C., de Haas H. & van Weering T.C.E., 2006. The Avaatech XRF Core Scanner: technical description and applications to NE Atlantic sediments. In: Rothwell G. (Ed.), *New Techniques in Sediment Core Analysis, Geol. Soc. London Spec. Publ.*, **267**, 39-50.
- Rocchi S., Armienti P., D'Orazio M., Tonarini S., Wijbrans J.R. & Di Vincenzo G., 2002. Cenozoic magmatism in the western Ross Embayment: role of mantle plume vs. plate dynamics in the development of the West Antarctic Rift System. *Journal of Geophysical Research*, **107**(B9), 2195.
- Rocchi S., LeMasurier W.E. & Di Vincenzo G., 2006. Oligocene to Holocene erosion and glacial history in Marie Byrd Land, West Antarctica, inferred from exhumation of the Dorrel Rock intrusive complex and from volcano morphologies. *Geological Society of America Bulletin*, **118**, 991-1005.
- Settimi D., Cornamusini G. & Talarico F., 2005. Petrography and provenance of sedimentary coarse clasts in CRP-2/2A and CRP-3 cores, Tertiary Victoria Land Basin, Antarctica. In: *East Antarctic Workshop, Cenozoic onshore and offshore stratigraphic record from the East Antarctic Margin: recent results and future directions, GeoItalia 2005*, Spoleto, Italy.
- Tamponi M., Bertoli F., Innocenti F. & Leoni L., 2003. X-ray fluorescence analysis of major elements in silicate rocks using fused glass discs. *Atti della Società Toscana di Scienze Naturali, Memorie Serie A*, **CVII**, 73-80.
- Taviani M., Beu A. & Jonkers H.A., 2000. Macrofossils from CRP-2/2A, Victoria Land Basin, Antarctica. *Terra Antarctica*, **7**, 513-526.
- Westerhold T., Bickert T. & Röhl U., 2005. Middle to late Miocene oxygen isotope stratigraphy of ODP site 1085 (SE Atlantic): new constraints on Miocene climate variability and sea-level fluctuations. *Palaeogeography, Palaeoclimatology, Palaeoecology*, **217**, 205-222.
- Wonik T., Grelle T., Handwerker D., Jarrar, R.D., McKee A., Patterson T., Paulsen T., Pierdominici S., Schmitt D.R., Schroder H., Speece M., Wilson T. & the SMS Science Team, 2008. Downhole Measurements in the AND-2A Borehole, ANDRILL Southern McMurdo Sound Project, Antarctica. *Terra Antarctica*, this volume.

### Supplementary Information

The following supplementary information in tables and figures for this contribution are available on-line at the Terra Antarctica website [www.mna.it/english/Publications/TAP/terranta.html](http://www.mna.it/english/Publications/TAP/terranta.html) and at the ANDRILL data site [www.andrill.org/data](http://www.andrill.org/data).

#### Appendix 1

- Supplementary SMS 9 Table A1.1 - Basement clast samples in AND-2A core.
- Supplementary SMS 9 Table A1.2 - Distribution of the sedimentary clasts and their relationships with the Lithostratigraphic Units and the encasing facies beds.
- Supplementary SMS 9 Table A1.3 - Preliminary petrographic description of volcanics and dolerites in the AND-2A core.

#### Appendix 2

- Supplementary SMS 9 Table A2.1 - Technical details of the Avaatech XRF core scanner.
- Supplementary SMS 9 Table A2.2 - Instrumental measurement settings.
- Supplementary SMS 9 Fig. A2.1 - Geometry of the main components inside the Avaatech XRF core scanner.

#### Appendix 3

- Supplementary SMS 9 Fig. A3.1 - Standard material measurements from 16 October until 2 December 2007.
- Supplementary SMS 9 Fig. A3.2 - Ar measurements in the atmosphere plotted against Al, Si, Fe and Ti counts.